

Regulation of the Basic Transcriptional Machinery by the Interacting Proteins TIPT and Geminin

Dissertation

zur Erlangung des Doktorgrades
der Mathematisch-Naturwissenschaftlichen Fakultäten
der Georg-August-Universität zu Göttingen

vorgelegt von

Mara-Elena Pitulescu, geborene Manescu

aus Resita, Rumänien

Göttingen 2006

D 7

Referent: Herr Prof. Dr. Michael Kessel

Korreferent: Herr Prof. Dr. Ernst Wimmer

Tag der mündlichen Prüfung: 17.01.2007

*To Marian, with all my love,
and to my Family*

Table of contents

Summary	1
Introduction	2
1. The General Transcription Machinery in Eukaryotes	2
2. RNA Polymerase I-Dependent Transcription	2
3. RNA Polymerase II-Dependent Transcription	3
3.1. RNA Polymerase II-Dependent Transcriptional Initiation	3
3.2. The TATA Element	4
3.3. The TATA Binding Protein	6
3.4. The TATA Binding Protein-Like Factor	7
3.4.1. The Role of TBPL1 in Transcription	7
3.4.2. The Role of TBPL1 in Animal Development	8
4. Chromatin Remodeling Activities	9
4.1. Spermatogenesis	9
4.2. Polycomb Group Proteins	10
4.3. Geminin	11
5. Aim of the Thesis	13
Results	14
1. TIPT DNA, RNA and Protein	14
1.1. TIPT Identification in a Yeast Two-Hybrid Screen	14
1.2. TIPT is Conserved in Mammalian Vertebrates	14
1.3. TIPT RNA and Protein Expression	17
1.3.1. TIPT RNA Expression	17
1.3.2. Anti-TIPT Antibodies	19
1.3.3. TIPT Phosphorylation	20
1.3.4. TIPT Expression in Embryonic Brain and Neurons	23
1.3.5. TIPT Expression in Testis	25
1.3.6. TIPT Subcellular Expression	29
2. The TIPT Interactome	31
2.1. Candidates Testing Approach	31
2.1.1. Geminin	31
2.1.2. Polycomb Group Proteins	32
2.1.3. TATA Binding Protein and TATA Binding Protein-Like Factor	32
2.2. Yeast Two-Hybrid Screen	34
2.3. Co-Immunoprecipitation Assay	35
3. TIPT and Cell Cycle	36
3.1. Transient Overexpression of HA-TIPT Affects Cell Cycle Phases	36
3.2. Stable Overexpression of HA-TIPT Does not Affect Cell Proliferation	37
3.3. TIPT Cannot be Down-Regulated	39
4. TIPT and Pol I	40
4.1. Evidence for a Role of TIPT in rRNA Synthesis	40
4.2. TIPT Activates Pol I Transcription	40
4.3. TIPT Interacts neither with Pol I and TIF-IA Proteins, nor with rDNA Promoter and Coding Regions	42
4.4. TIPT Has no Role in Ribosomal RNA Processing	43
5. TIPT and Pol II	45
5.1. TBPL1 Protein Model is Similar to TBP's	45
5.2. TIPT Activates Pol II Transcription from TATA box Promoter	46

5.2.1. TIPT Binds the Adenovirus Major Late Promoter	46
5.2.1.1. TIPT Binds the BRE ^u Element of the Adenovirus Major Late Promoter	48
5.2.1.2. TIPT, TBP and AdMLP Form a Ternary Complex	49
5.2.1.3. TIPT, TBP and Geminin Activate Synergistically the AdML promoter	49
5.2.2. TIPT, TBP and Geminin Activate Synergistically the Herpes Virus Thymidine Kinase Promoter	52
5.2.3. Geminin Decreases the Binding of TBP to the Adenovirus E4 Promoter	52
5.3. TIPT Activates Pol II Transcription from TATA-less Promoter	53
5.3.1. TIPT, TBPL1 and Neurofibromin Promoter DNA Form a Ternary Complex	53
5.3.2. TIPT, Geminin and TBPL1 Activate Synergistically the NF1 Promoter	55
Discussion	57
1. TIPT Expression	57
1.1. The Embryonic and Postnatal TIPT Expression	57
1.2. The Subcellular Expression Domains of TIPT	57
2. The TIPT Interactome	59
2.1. TIPT Interaction with Geminin	59
2.2. TIPT Interaction with Polycomb Group Proteins	59
2.3. TIPT Interaction with AF10	60
2.4. TIPT Interaction with TBP and TBPL1	60
3. TIPT and Cell Cycle	61
4. TIPT and Pol I Transcription	62
5. TIPT and Pol II Transcription	63
5.1. TIPT and Geminin Effect on TATA-containing Promoters	63
5.2. TIPT and Geminin Effect on TATA-less Promoter	65
5.3. TIPT May be a Common Factor for TBP- and TBPL1-Dependent Transcriptional Activation	67
6. Conclusion	68
Materials and Methods	70
1. Isolation of Nucleic Acids	70
1.1. Plasmid DNA Isolation from <i>E. coli</i>	70
1.2. Genomic DNA Extraction from Mammalian Cells	70
1.3. DNA Electrophoresis and Purification from Agarose Gel	70
1.4. Total RNA Isolation from Eukaryotic Cells, Embryos, or Mouse Testis	71
1.5. Purification of Linearized DNA or PCR Products	71
2. Modifications and Manipulations of Nucleic Acids	72
2.1. DIG Labeled RNA Probe Preparation	72
2.2. Random Radioactively Labeled RNA Probe Preparation	72
2.3. Purification of Labeled Nucleic Acids and Double Stranded DNA Oligos	72
2.4. DNA Digestion with Restriction Enzymes	73
2.5. Dephosphorylation of DNA Fragment	73
2.6. Annealing of Complementary Single-Stranded DNAs	73
2.7. Ligation	74
3. Polymerase Chain Reaction (PCR)	74
3.1. Standard and Genomic PCRs	74
3.2. RT-PCR	74
4. Transformation of <i>E. coli</i>	75
4.1. Preparation of Electrocompetent Cells	75
4.2. Preparation of Competent Cells for Heat Shock Transformation	75
4.3. Transformation of <i>E. coli</i> by Electroporation	76

4.4. Transformation of <i>E. coli</i> by Heat Shock.....	76
5. Protein Purification and Analysis.....	77
5.1. Protein Purification.....	77
5.2. Protein Extraction.....	79
5.3. <i>In vitro</i> Transcription/Translation.....	82
5.4. Protein Analysis.....	82
5.5. Casein Kinase II Assay.....	84
6. Yeast Two-Hybrid Screen.....	85
7. Analysis of Protein-Protein Interactions.....	86
7.1. GST Pull-Down Assay.....	86
7.2. Immunoprecipitation.....	87
7.3. Peptide Array Analysis.....	88
8. Analysis of Protein-Nucleic Acids Associations.....	89
8.1. Gel Mobility Shift Assays.....	89
8.2. Chromatin Immunoprecipitation (ChIP) Assay.....	90
9. Cell Culture and Immunocytochemistry.....	91
9.1. Cell Revival.....	91
9.2. Cell Passage and Freeze.....	91
9.3. HA-TIPT Human U2OS Stable Cell Line.....	92
9.4. Cells Synchronization with Aphidicolin.....	93
9.5. FACS Analysis of Human U2OS Cells.....	93
9.6. Immunocytochemistry.....	94
9.7. Cell Transfections with Plasmids or siRNAs.....	96
9.8. Luciferase Assay.....	97
References	98
Appendices	109
Abbreviations	111
Acknowledgements	115
Curriculum Vitae	117

Summary

Geminin functions in the regulation and possibly coordination of replication and embryonic development. It interacts with the licensing factor Cdt1, with several homeodomain proteins and with members of chromatin modifying complexes, in particular the polycomb and the SWI/SNF complexes. In a two-hybrid screen a so far undescribed protein “TIPT” (TBPL1 Interacting Protein) was identified. TIPT is widely expressed in embryonic and adult tissues, and as well in normal and cancer cell lines. The protein is enriched in the cytoplasm, the centrosome and the nucleolus. The nucleolar localization suggests that TIPT is either involved in Pol I transcription or is only stored there. TIPT interacts strongly not only with geminin, but also with the Polycomb group members, the transcription factor AF10, nucleolar and centrosomal proteins (nucleolin, nucleophosmin), and components of the basic transcription machinery (TBP and TBP-like factor).

Transient overexpression of TIPT in culture cells elongates S phase and shortens G2/M phase during one cell cycle, suggesting an activation of an intra-S phase checkpoint. However, proliferation in general is not affected by TIPT as judged in stably overexpressing cells. Inhibition of Pol I transcription by actinomycin D, or RNA depletion by RNase A in tissue culture cells abolished the nucleolar localization of TIPT. Overexpression of TIPT activates both endogenous and reporter Pol I transcription in a dose dependent manner. However, TIPT was not found associated *in vivo* neither with the Pol I preinitiation complex, nor with the ribosomal DNA promoter, therefore its direct role on Pol I transcription needs further clarifications.

TIPT binds *in vitro* the adenovirus major late promoter on its upstream BRE (TFIIB binding site) element forming a ternary complex with TBP. It forms a similar complex by binding to the G/C rich region of the neurofibromin promoter and TBPL1. Reporter gene assays indicate a positive influence of TIPT on TATA box-containing and TATA-less Pol II dependent transcription, which is significantly enhanced by the co-expression of geminin. However, the binding of TIPT to DNA seems not to be necessary in order to produce this effect. Geminin's activatory role reveals a novel function of this multifaceted protein, different from its previously described repressive role. *In vitro*, geminin mostly inhibits the binding of TBP or TBPL1 to DNA, and its interaction with TIPT reduces the effect.

In conclusion, this study presents TIPT as a ubiquitous, highly expressed factor interacting with the basic transcription machinery and with chromatin associated factors.

Introduction

1. The General Transcription Machinery in Eukaryotes

One of the central mechanisms of life is how to turn the genes “on” and “off”. Precise spatial and temporal control of gene expression is essential for the normal growth and development of all organisms. The predominant mechanism for controlling the complex process of gene expression is at the level of RNA synthesis. Transcription occurs in the cell nucleus, allowing the translation of genetic information held in the DNA into RNA, mediated by RNA polymerase (Pol), the first time postulated by Crick in the central dogma of molecular biology [1]. The basic transcription reaction is similar in all organisms. In prokaryotes, one enzyme catalyzes the synthesis of three types of RNA, messenger RNA (mRNA), ribosomal RNA (rRNA) and transfer RNA (tRNA), whereas three distinct RNA polymerases I, II and III exist in eukaryotes [2]. RNA Pol I synthesizes rRNA precursors, RNA Pol II catalyzes the synthesis of mRNAs, microRNAs (miRs), and most small nuclear (snRNA), and the RNA Pol III synthesizes tRNAs, 5S rRNA and other small RNAs found in the nucleus and cytosol.

Eukaryotic gene transcription is a process tightly regulated at many levels, which requires the assembly of a complex molecular machinery that includes general transcription factors, gene specific transcription factors, cofactor complexes and chromatin remodeling factors [3].

A first decision is taken at the chromatin level, by covalent modifications of histone tail and DNA. An accessible DNA template is prepared from nucleosomes by chromatin remodeling complexes. Next, regulatory factors bind DNA to regulate the formation or function of the preinitiation complex [4].

As the organisms evolved, an increasing complexity of the mechanisms regulating gene expression was necessary to sustain an increased flexibility and capacity to adapt to any change.

2. RNA Polymerase I-Dependent Transcription

Nucleolus is the place where rDNA transcription, pre-rRNA processing and modifications, and initial steps of pre-ribosome assembly occur [5]. All cellular organisms synthesize large amount of rRNA necessary to produce several millions of ribosomes per cell. A cell normally contains hundreds of *rRNA* genes organized in tandem head-to-tail repeats that cluster

together [6]. However, only a small subset of the total rDNA is active, the rest being silenced. The *rRNA* gene promoter contains an essential core element essential for proper transcription initiation, and an upstream control element (UCE) [7]. The mouse TIF-IB complex, containing the TATA box binding protein (TBP) together with the upstream binding factor (UBF) and TIF-IA, recruit Pol I and assemble on the *rRNA* gene promoter into the preinitiation complex to start the rRNA synthesis [8].

The primary 45/47S rRNA transcript synthesized by Pol I is processed into the mature 18S, 5.8S and 28S rRNAs, which together with the 5S rRNA transcribed by the Pol III make part of the ribosome [8]. rRNA processing, 2'-*O*-ribose methylation and pseudouridylation of the precursor rRNA take place with the help of numerous small nuclear ribonucleoprotein particles (snoRNPs) which contain small nucleolar RNAs (snoRNAs) [9]. Recently, it was confirmed that not only in yeast and plants, but also in mammals rRNA synthesis is coordinated with rRNA processing [10, 11]. The assembly of ribosomal proteins begins in the nucleolus on the primary pre-rRNA transcript, leading to the formation of a 90S pre-ribosomal particle [9]. This undergoes a series of processing steps resulting a pre-60S large subunit, which contains 28S and 5.8S rRNAs, and a 43S small subunit precursor, with 20S rRNA included. Both subunits are separately exported to the cytosol where other processing steps are necessary to form the mature ribosomal subunits.

Pol I transcription has a major impact on the life and destiny of a cell, mediating the level of rRNA production which affects the protein synthesis machinery of the cell.

3. RNA Polymerase II-Dependent Transcription

3.1. RNA Polymerase II-Dependent Transcriptional Initiation

In eukaryotes, RNA polymerase II transcribes all the protein coding genes. The protein coding sequences represent only a small fraction of a typical metazoan genome and only 5-10% of the total coding capacity is dedicated to proteins that regulate transcription, in humans estimated 3000 transcription factors [12, 13]. The core promoter of a gene is the minimal region of DNA highly conserved between genes where RNA Polymerase II can initiate basal transcription. The core promoter is compact, and typically extends approximately 35 base pairs (bp) upstream and/or downstream of the transcription start site, and can contain several distinct core promoter sequence elements such as the TATA box, located -25 to -30 bp

upstream of the transcription start site, the initiator element (INR) located at -3 to +5 around the transcription start site, and the downstream promoter element (DPE) located at +10 to +35 downstream from the transcription start site [14]. Core promoters present a structural and functional diversity very important for the combinatorial regulation of gene expression, each core promoter sequence element being found only in a subset of genes [15]. So far, only the TATA box and the INR element have been shown to be capable of directing accurate Pol II transcription initiation independent of other core promoter elements.

The basal transcription machinery was defined as the sum of factors, including RNA polymerase II itself, which is minimally required to direct the transcription *in vitro* from an isolated core promoter. The formation of the preinitiation complex containing the basal transcription factors (TFIIA, TFIIB, TFIID, TFIIE, TFIIIF, TFIIF) and RNA polymerase II, at the right time and at the right promoter is the first step of transcription. This process was intensively studied and two different assembly pathways are in debate: the sequential pathway, and the holoenzyme pathway [16]. It is believed that both pathways assemble *in vivo*, depending on the promoter. In the sequential assembly pathway TFIID, containing TBP and TBP-associated factors (TAFs), nucleates the complex through binding to the TATA element, followed by TFIIA and TFIIB that stabilize the binding of TFIID, and TFIIIF that associates with unphosphorylated Pol II (Figure 1A). Afterwards, TFIIE is recruited, and finally TFIIF binds. TFIIF phosphorylates the C-terminal domain (CTD) of Pol II and has a helicase activity, unwinding the DNA around the transcription initiation site. The Pol II holoenzyme pathway was described *in vitro* by purification of a Pol II complex containing TFIIB, TFIIE, TFIIIF, TFIIF, GCN5 acetyltransferase, SWI/SNF chromatin remodeling complex and SRBs, however lacking TFIID and TFIIA. Many class II promoters do not have a TATA box, therefore the initiation of transcription must involve alternative pathways excluding the presence of TBP [16].

3.2. The TATA Element

The TATA box, an A/T rich sequence, is the first core promoter element identified in the eukaryotic genome and the most studied. Recent database analysis showed that the prevalence of the TATA box was overestimated, and in humans only 32% from the analyzed promoters contain a TATA element [17]. A TATA box associates with TBP, the subunit of TFIID [18, 19]. Its consensus sequence was determined from the alignment of different promoters to be

T-A-T-A-A/T-A-A/T-A/G (http://www.epd.isb-sib.ch/promoter_elements) [20]. The TATA element is highly conserved, being found in ancient eukaryotes and even in archaea. The upstream sequences are not as well conserved as the TATA box, and play frequently important roles in determining the efficiency of transcription initiation [21]. Wolner and Gralla showed that the sequences flanking the core TATA box influence the basal level of transcription and the response to activators [15].

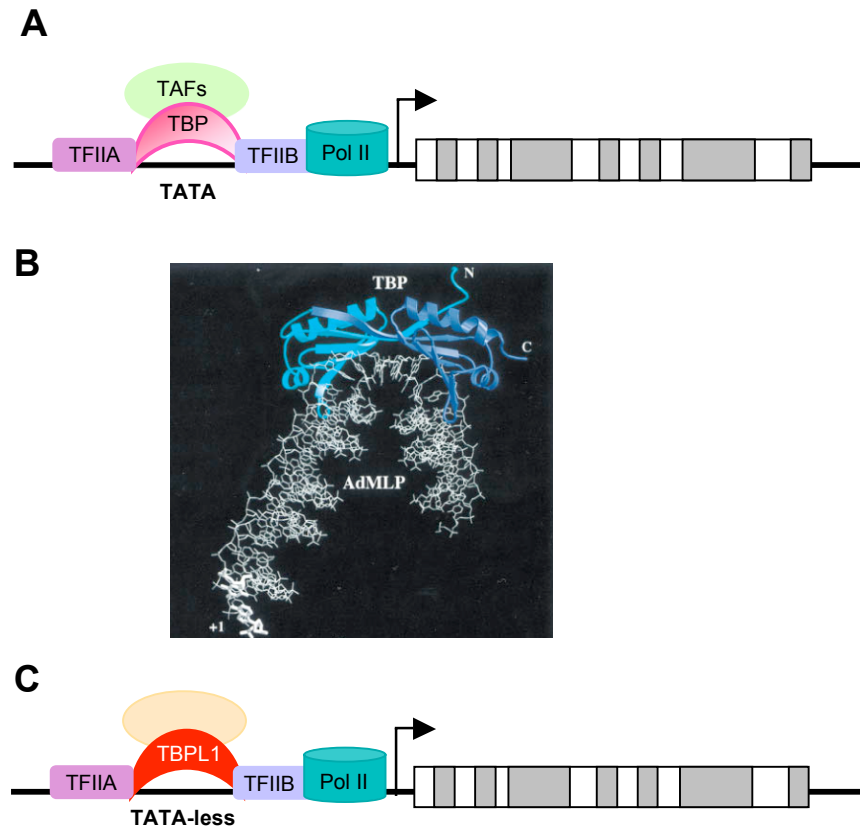


Figure 1. Schematic view of Pol II-dependent transcription initiation and crystal structure of TBP-DNA complex. (A) Simplified view of the preinitiation complex on the TATA-containing promoter. TFIID, containing TBP protein that recognizes the TATA box and TAFs, nucleates the formation of the preinitiation complex. TFIIA and TFIIB stabilize the binding of TFIID complex on DNA, and allow the recruitment of the other transcription factors together with RNA Pol II, which initiates transcription. (B) Crystal structure of TBP complexed with the TATA element of the adenovirus major late promoter (AdMLP). TBP is depicted as ribbon drawing and colored in light blue for TBP N-terminus and first repeat, and dark blue color for TBP second repeat. DNA is shown as a stick figure with hypothetical, linear, B-form extensions at both ends. The transcription start site of the AdMLP is labeled with +1 (adapted from Nikolov and Burley, 1997). (C) Simplified view of transcription initiation from a TATA-less promoter which uses TBPL1 as nucleating factor of the PIC. TBPL1, the TBP-like factor has a saddle-like shape similar to TPB. It binds a TATA-less promoter and contacts TFIIA and TFIIB probably in a similar way as TBP does.

3.3. The TATA Binding Protein

TFIID is a multiprotein complex composed of TBP and 13 or 14 TAFs [22, 23]. TFIID assembly on the TATA-containing promoters starts with the binding of TBP to the TATA element [24, 25]. In addition to its central role in Pol II transcription, TBP was found in multiprotein complexes of Pol I and Pol III, also functioning in promoter recognition.

All organisms except eubacteria possess TBP. In the last fifteen years many structural studies of different TBP species were performed by crystallizing TBP alone or DNA/co-factors associated. TBP has a bipartite structure with a C-terminal core domain highly conserved and approximately 80% identical in yeast and mammals. The N-terminal TBP region is variable between all the eukaryotes, but is well conserved amongst vertebrates [26, 27]. The three-dimensional structure of the C-terminal portion of TBP composed of 180 amino acids has a saddle shape [28-30]. TBP consists of two almost-identical domains due to the presence of two direct imperfect repeats found in the core domain (called N- and C-terminal repeats) (Figure 1B). Therefore, it was suggested that TBP evolved from a true dimer of two identical chains of approximately 90 amino acid residues [31]. The core domain is responsible for the DNA-binding through the concave underside of the saddle, and for the transcription machinery components and other regulatory proteins interaction through the convex upper surface of the saddle. In order to prevent unwanted transcription, TBP forms a homodimer that is inactive for the DNA binding [28, 30, 32].

Several cocrystal structural analyzes of DNA-TBP from different species suggest an induced-fit mechanism of protein-DNA recognition [33]. TBP modifies the TATA box DNA by binding to the minor groove which relies on hydrophobic interactions, unwinding partially the DNA duplex due to the insertion of phenylalanine residues, and bending the B-DNA at both 5' and 3' ends of the TATA box (Figure 1B, [34]). The N-terminal domain of the conserved portion of TBP contacts the 3' half of a consensus TATA box, and the C-terminal domain contacts the 5' half. However, the orientation of the transcription machinery is given by the TATA box in combination with other promoter elements such as BRE, the TFIIB recognition element [35-37]. The crystal structure of TBP-cTFIIB-TATA ternary complex revealed that TFIIB binds the major groove upstream of the TATA box and the minor groove downstream of the TATA box in the AdML promoter [36]. TFIIB upstream binding site was called BRE^u and the sequence G/C-G/C-G/A-C-G-C-C is preferred for the interaction with TFIIB [38]. This TFIIB-BRE^u interaction can occur independent of TBP and helps orienting the

preinitiation complex [38, 39]. The consensus for downstream BRE (BRE^d) was found to be G/A-T-T/G/A-T/G-G/T-T/G-T/G, and the TFIIB binding seems to require prior TBP binding [40]. These BRE elements were found in the TATA-containing promoters, as well as in the TATA-less promoters. It was suggested that TFIIB probably enhances TFIID binding to the core promoter region by stabilizing this interaction through additional DNA contacts [40]. Except for TFIIB, TFIIA is necessary to stabilize the TBP binding to the TATA box [16].

In *Xenopus* and zebrafish TBP is expressed already at the onset of zygotic transcription and during all the stages of embryonic development [41, 42]. Moreover, the *TBP*^{-/-} murine embryos arrest in development at embryonic blastocyst stage [43]. However, TBP depletion produced a loss of Pol I and Pol III transcription, but not Pol II, suggesting that Pol II transcription can run through different mechanisms independent of TBP.

3.4. The TATA Binding Protein-Like Factor

Since TBP was found assembled in different complexes required for the transcriptional activation, it was considered the “universal transcription factor”. Recent studies, however, led to the discovery and analysis of TBP-related factors (TRF1, TRF2 and TRF3), showing that TBP is indeed not the universal transcription factor, and that Pol II transcription still present in TBP null embryos might be due to one of these factors.

TRF1 found only in *Drosophila*, and TRF3 found in most vertebrates except *Drosophila* and *C.elegans*, resemble TBP in the facts that bind the TATA box, TFIIA and TFIIB, but seem to activate only a specific set of genes transcription [44-49].

3.4.1. The Role of TBPL1 in Transcription

TRF2/TRP/TLP/TLF is a TBP-related factor and will be further called in this work as TBPL1, based on the Mouse Genome Database nomenclature committee annotation. TBPL1 has been described in many metazoans and in the unicellular dinoflagellate *Cryptothecodinium cohnii*, but not in plants, yeast or archaea [42, 50-60]. Like TBP, TBPL1 factor has a bipartite structure with a variable N-terminal domain and a highly conserved C-terminal core domain containing two direct repeats [50]. The murine TBPL1 core-domain presents 76% similarity and 39% identity with the corresponding domain of mouse TBP, and the binding sites for TFIIA and TFIIB are conserved. Indeed, studies showed that TBPL1 binds TFIIA and TFIIB transcription factors, but not the TATA box (Figure 1C, [54-57]). *Drosophila* TBPL1 co-

purified in a large multisubunit complex unlike TBPL1 overexpressed in human cells, which was found in a small complex with nearly stoichiometric amounts of TFIIA and without TAFs [55, 56, 59, 61].

TBPL1 activates transcription from different TATA-less promoters, and repress transcription from the TATA box-containing promoters, probably because it has a higher affinity for TFIIA than TBP has (Figure 1C, [55-57, 62-64]).

TBPL1 subcellular localization is unexpected for a basic transcription factor. TBPL1 is nucleolar in HeLa and Cos7 cells, cytoplasmic in DT40 chick cells, and either nuclear or cytoplasmic in mouse male germ cells [43, 60, 65, 66].

3.4.2. The Role of TBPL1 in Animal Development

Sequence comparison of the core domains in the TBPL1 family reveals that they are less conserved in evolution (40 to 45% identity among the metazoan species) than the TBP core domains (about 80% identity between yeast and humans) [50]. Thus, while the role of TBP is similar in different species, the function of TBPL1 may have evolved into different regulatory pathways in evolutionarily distant species.

The difference in the biological functions of TBPL1 in various species is evident. The depletion studies in *C.elegans*, *Xenopus*, zebrafish and *Drosophila* using RNA interference, antisense oligonucleotides, homozygous gene inactivation or dominant negative approaches resulted in early embryonic arrests and a loss of expression of some genes required for differentiation [42, 51, 52, 59, 61]. Therefore, it was suggested that TBPL1 is directly required for the expression of a specific set of genes necessary for early development, or indirectly required for the expression of other necessary genes, such as transcription factors [52]. The loss of TBPL1 caused the expression of several genes normally not expressed at early stages of *C. elegans* embryogenesis, suggesting that TBPL1 may be a repressor of transcription in early embryo [51]. The depletion of TBP or TBPL1 in *Xenopus* and zebrafish revealed that there is an independent as well a complementary requirement for TBP and TBPL1 for some genes, strengthening the idea that TBPL1 is necessary for transcription of a certain set of genes [41, 42].

Analysis of *TBPL1* expression revealed that *TBPL1* was expressed in most human and mouse tissues, with the highest level in testis [53, 55]. The total inactivation of *TBPL1* mouse gene by homologous recombination revealed that the mice were viable, which came unexpected

considering the lethal phenotype obtained by the inactivation of *TBPL1* in *C. elegans*, *Drosophila*, zebrafish, *Xenopus* and *Drosophila* [67, 68]. Male mice were sterile because of a late arrest in spermiogenesis, but females were fertile indicating that maternal and zygotic TBPL1 expression is not essential for embryogenesis. The *TBPL1*^{-/-} mice have an arrest at the transition of round spermatids to elongating spermatids at a stage when not much transcription is still going on. In addition, most of the round spermatids underwent apoptosis. Several testis-specific genes such as *MTEST640*, *641*, and *643*, *protamine 1* and *transition protein (Tp1)* genes were affected, suggesting a role of TBPL1 in the transcriptional regulation of a testis specific set of genes. In addition, the null mice have spermatids with defects in assembly of centromeric heterochromatin in chromocenter, suggesting a TBPL1 role in the organization of spermatid heterochromatin. This phenotype correlates very well with the recent results obtained using the *Drosophila* TBPL1 viable mutant [61]. Thus, the decreased TBPL1 transcription in the mutant flies lead to abnormalities in chromatin condensation preceding the first meiotic division in both oocytes and mature primary spermatocytes and to other aberrations in germ cell development.

4. Chromatin Remodeling Activities

4.1. Spermatogenesis

Gene regulatory mechanisms in germ cells differ from those in somatic cells. Male primordial germ cells (PGCs) differentiate into pluripotent spermatogonia cells, which divide mitotically and enter spermatogenesis in mice at 5 days post-partum (pp) (Figure 2, [69, 70]). These progenitor cells undergo a serie of mitoses and around day 10 pp the first wave of spermatogenic differentiation takes place, giving rise to the primary spermatocytes [70]. Meiosis starts, and after the first division the secondary spermatocytes are produced, which divide again around day 21 pp resulting in the formation of the first haploid round spermatids. Then spermiogenesis starts, and the round spermatids undergoing the elongation phase take the shape of the mature spermatozoa and are released into the lumen of the seminiferous tubules by day 35 pp. In the spermatids an intense chromatin remodeling process occurs. Histones are first replaced by the transition proteins (Tpn) in the round spermatids, and subsequently by protamines (Prm) in the elongating spermatids, a time that coincides with a stop of transcription and a start of translation (Figure 2, [71]).

After meiosis, spermiogenesis starts with a massive wave of transcriptional activity, when

many essential postmeiotic genes are activated [72]. Transcription is temporally restricted in germ cells, but the high levels of basic transcription factors (TBP, TFIIB, Pol II) and the presence of testis-specific transcription factors (TFIIA τ , TAF_{II}55) compensate this fact. Moreover, many testis-specific genes lack a TATA box, and TBP-related proteins are likely to be utilized in transcription initiation from the TATA-less promoters during spermatogenesis [72]. Thus, germ cells present cell-specific transcription initiation complexes to accurately activate many different gene networks required for proper embryonic development.

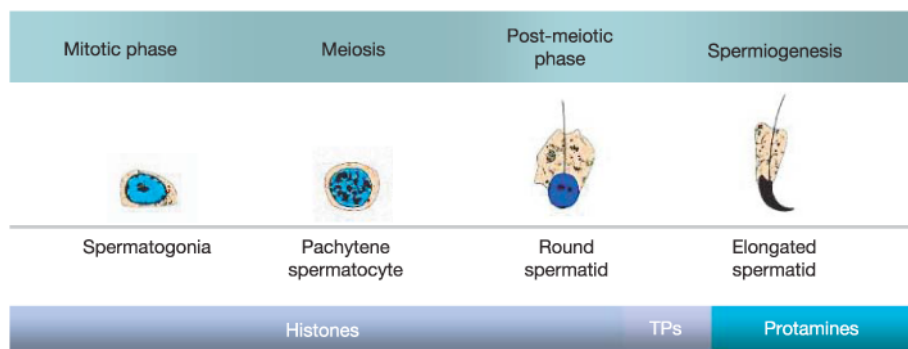


Figure 2. Chromatin remodeling in male germ cells development. The spermatogonia divide mitotically and generate the primary spermatocytes which enter meiosis. Next, the round spermatids enter the spermiogenic phase. During the last phase of spermiogenesis, the chromatin is highly compacted. The sperm head is totally reshaped, a process which includes a replacement of most histones with transition proteins, subsequently replaced by protamines (Adapted from Kimmins and Sassone-Corsi, 2005).

4.2. Polycomb Group Proteins

One mechanism to maintain the repression of genes functions through the products of the Polycomb group (PcG) of genes which modify the histone proteins around which the DNA is wrapped, blocking the access of the transcription factors.

Polycomb group proteins are known for their role in maintenance of the *homeotic* gene repression [73, 74]. *In vitro*, purified polycomb complexes inhibit the action of the SWI/SNF complex on a nucleosome array, suggesting that polycombs silencing might block the access of transcription factors by preventing the nucleosome remodeling [74, 75]. Biochemical and genetic characterization of Polycomb group proteins revealed 15 proteins that exist in distinct complexes. The Polycomb Repressive Complex 1 (PRC1) contains four core proteins in *Drosophila*, namely polycomb (PC), polyhomeotic (PH), posterior sex combs (PSC), and dRING1 [74, 75]. The PRC2 complex is a histone methyltransferase complex, which adds a

methyl histone H3 mark necessary for the subsequent recruitment of the PRC1 complex [76-78]. The human PRC1-like complex (PRC1L) establishes a new covalent modification, mono-ubiquitination of histone H2A necessary for the gene silencing [79].

Recent studies show that not only *Hox* genes expression is regulated by PcG, but many other mammalian genes are repressed to maintain pluripotency in the embryonic stem cells by PcG [80, 81]. Another study shows that genes repressed during cell differentiation are already bound by the PcG proteins in non-differentiated cells, despite being actively transcribed [82]. The mechanisms for gene silencing promoted by PcG proteins are complex, and may interfere with specific functions of the transcriptional machinery other than generally preventing the access of transcription factors by covalently modifying the histone chromatin. Thus, PcG complexes interact with the promoter factors such as TBP and TAFs on repressed gene promoters [83, 84]. Along the same line of evidence, polycombs does not prevent the binding of TBP, RNA polymerase, or HSF to the *hsp26* promoter, but interfere in some early steps of transcriptional initiation, affecting directly and specifically the ability of RNA polymerase to form the initiation complex [85].

4.3. Geminin

Luo et al. identified geminin protein as a new member of the PRC1 complex, its transient association with PcG complex being dependent on the cell cycle phases (Figure 3A, [86, 87]). Thus, geminin was found to repress *Hox* proteins function during embryogenesis by direct association with Polycomb members on *Hox* regulatory chromatin elements and by impairing *Hox* gene action on their target genes through a direct binding to the homeodomain of *Hox* proteins [87]. In a similar way, geminin directly interacts and antagonizes the role of another homeobox protein, *Six3* [88].

Geminin plays an important role in the cell cycle preventing DNA re-replication after the DNA replication was initiated by sequestering Cdt1, one of the key licensing factors [89, 90]. The interaction of geminin with *Hox* and *Six* proteins directly competes with geminin-Cdt1 interaction (Figure 3B, [86]). This finding presents geminin as a protein with dual functions, which connects embryonic development and cell division.

Except for its role on preventing DNA replication during the same cell cycle, geminin was found to prevent centrosome duplication, regulating multiple steps of the chromosome inheritance cycle [91].

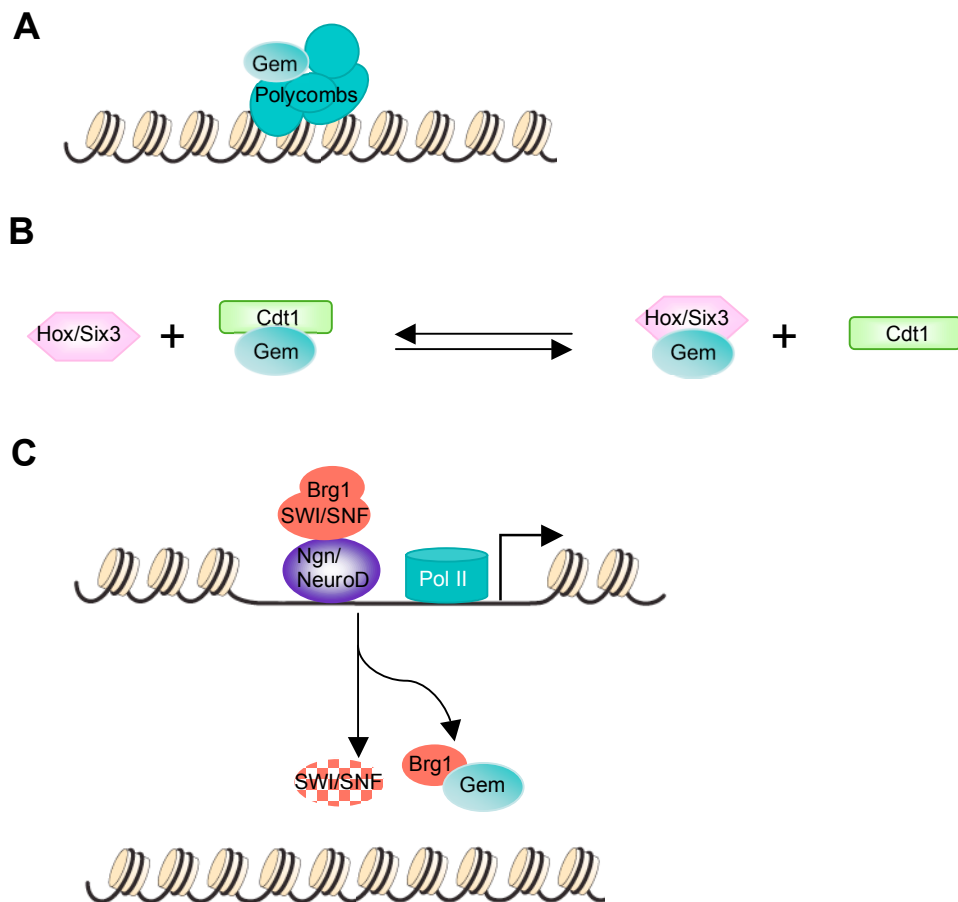


Figure 3. Geminin functions. (A) Geminin associates transiently with Polycomb proteins and functions as polycomb-like factor [87]. (B) Schematic representation of the equilibrium between geminin in proliferation and in differentiation. The Cdt1-geminin complex can be converted into a Hox/Six3–geminin complex depending on the availability of free ligands (adapted from Pitulescu et al, 2005, [87, 88]). (C) SWI/SNF mediates the transactivation of proneural target genes Ngn and NeuroD. Geminin recruits Brg1 catalytic unit of SWI/SNF complex and suppresses neuronal differentiation by preventing proneural gene transcription [92].

Geminin is multifunctional, being a protein initially isolated in *Xenopus* in an expression-cloning screen where was proposed to play a role in neural domain specification during early embryogenesis [93]. Recently, the same group showed that unlike the neural inducing function in early development, geminin prevents neuronal differentiation later in development. This occurs by sequestering Brg1, the catalytic subunit of SWI/SNF complex, and thus prohibiting a transcriptional activator effect of pro-neural basic helix-loop-helix (bHLH) transcription factors neurogenin 2 (Ngn2) and NeuroD on their neuron-specific target genes (Figure 3C, [92]). Geminin has an additional role in neurogenesis, through its association with AP4 repressing the expression of neuron-specific genes in non-neuronal cells, thus preventing precocious expression of target gene in fetal brain [94]. Thus, geminin

functions on multiple levels, connecting cell proliferation with embryonic development.

Geminin is a multifunctional protein with different biochemical roles in transcription gene regulation, DNA replication, centrosome duplication and chromosome segregation. Therefore, is possible to understand the dual life of geminin as regulator of cell proliferation and differentiation. However, it was already found that its activities are strongly related to the cell type, cell cycle phases, its cellular dosage and binding proteins. Therefore, as many details we know concerning its interaction with other players, the complexes to which it takes part, and the processes in which it is involved, the more we can understand how it can connect and balance different pathways.

5. Aim of the Thesis

A previously unidentified mouse protein, TIPT, was defined as geminin interacting partner in a yeast two-hybrid screen. Therefore, the aim of this work was the biochemical characterization of this completely novel protein. This implies the study of cellular and subcellular localization of the protein, the identification of interacting partners, and the investigation of TIPT functional role in relation to multifaceted regulator geminin and to the binding partners newly identified.

Results

1. TIPT DNA, RNA and Protein

1.1. TIPT Identification in a Yeast Two-Hybrid Screen

The full-length TIPT cDNA was isolated by Lingfei Luo in a yeast two-hybrid screen of a day 8.5 mouse embryo cDNA library for identifying geminin interacting partners (Figure 4, [87]). Eight yeast clones were positives and encoded parts of the homeodomain proteins Hoxd10 and Hoxa11, the polycomb factor Scmh1 protein (homologous to the “Sex comb on midleg” *Drosophila* protein), and a completely uncharacterized protein, designated TIPT (see below) (Figure 4).

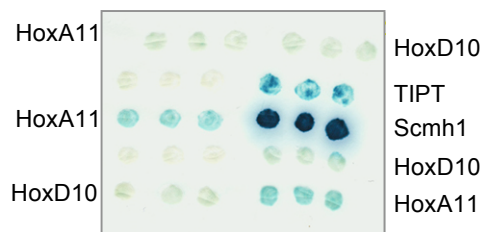


Figure 4. TIPT identification in a yeast two-hybrid screen. β -galactosidase activity was assayed for the all eight cDNA clones found as positives for geminin binding in the first round of screen [87].

1.2. TIPT is Conserved in Mammalian Vertebrates

The novel clone identified in the two-hybrid screen was sequenced, and a poly(A)⁺ tailed cDNA of 715 base pairs (bp) length was obtained. The cDNA clone was analyzed using the NCBI Blast platform for sequence homology. The clone contained a full-length Riken cDNA identified in the NCBI database under NM_029485 accession number. Initially the cDNA encoded an unknown product, and only recently, a data base entry identified it as coding for TIPT isoform 2 protein (TATA binding protein-like factor-interacting protein) (GI:56553512, submitted by Brancorsini, S., and Sassone-Corsi, P.) (Figure 5A). The murine gene found under the 5133400G04Rik name with additional aliases AU016220, 2700012K08Rik, and 4930583E11Rik is localized on mouse chromosome 18, cytogenetic band B3.

The full open reading frame (ORF) of mouse TIPT isoform 2 contains 618 bp and spans 5497 bp in the genome (Figure 5A). By comparison of its cDNA and mouse genomic sequences

available in the electronic databases (NCBI, Celera, ENSEMBL) the exon-intron structure of the gene was determined (Figure 5B).

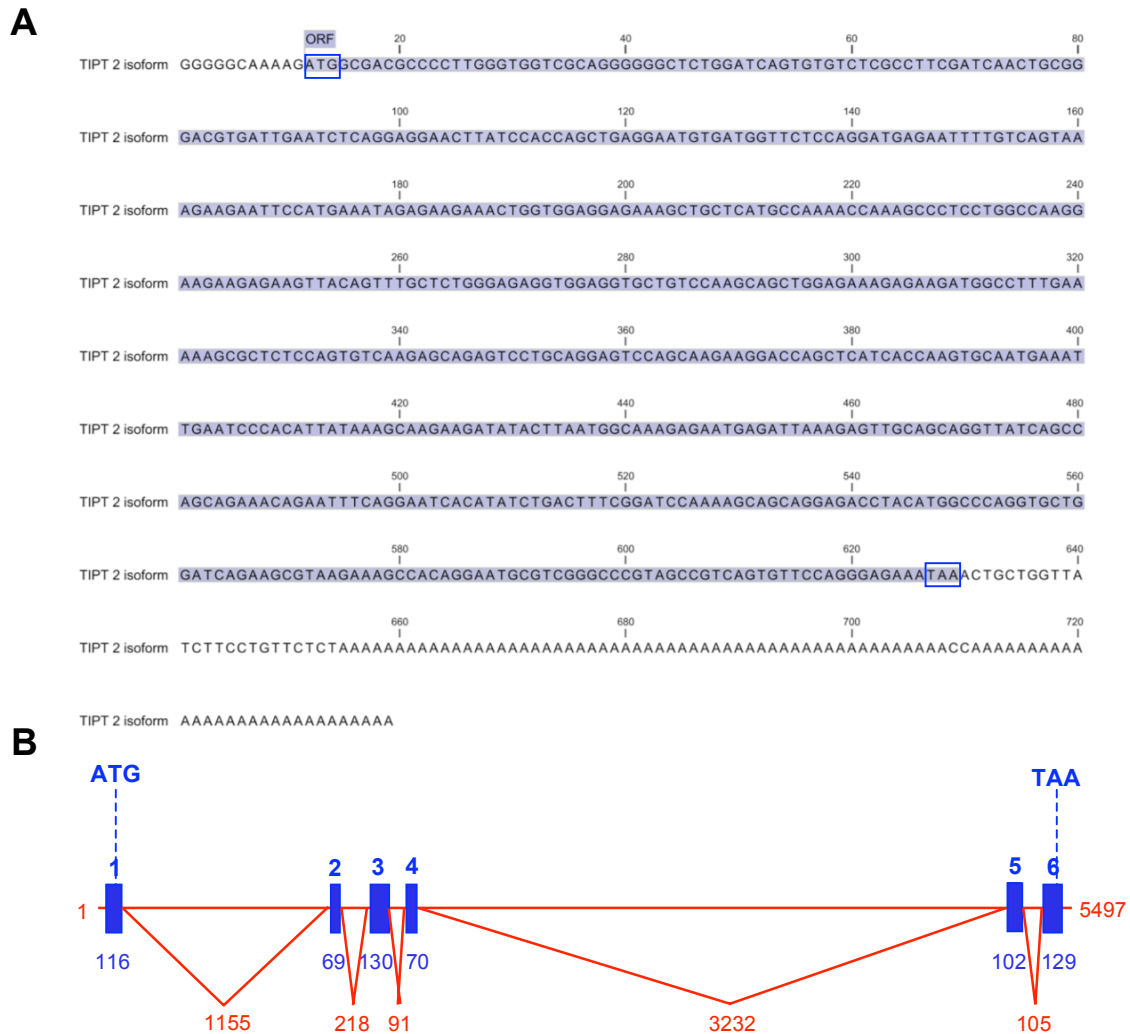


Figure 5. TIPT cDNA and genomic sequences. **(A)** Nucleotide sequence of mouse TIPT isoform 2 full-length cDNA (Accession number NM_029485, NCBI database). The ORF, between the start and stop codon, is highlighted in blue. **(B)** Schematic representation of the exon-intron structure of mouse *TIPT* gene. Boxes indicate the positions of the exons in the gene. Blue numbers above the boxes indicate the exon number, and the ones below represent the size of the exons in bp. The red line represents the intronic sequence and the red numbers indicate the size of the introns. The start codon (ATG) is positioned in the first exon, and the stop codon (TAA) in the last exon.

To find all the TIPT orthologs BLASTP function from the NCBI database was used. The alignment of mouse and human TIPT isoform sequences is presented in figure 6 and was realized using the CLC protein Workbench software. The amino acid sequence comparison of mouse TIPT and its orthologs revealed a high degree of conservation across mammalian species. No orthologs were found in other eukaryotes, with one exception for *Strongylocentrous purpuratus* where the percent identity was fairly low (Table 1).

TIPT protein does not have high similarities with any other known protein, and no conserved domain was found. Using different prediction softwares from ExPASy database (<http://www.expasy.ch>) three coiled-coil domains (amino acids 19-39; 74-112; 134-161) known to be protein-protein interaction domains were detected for the murine TIPT isoform 2 protein.

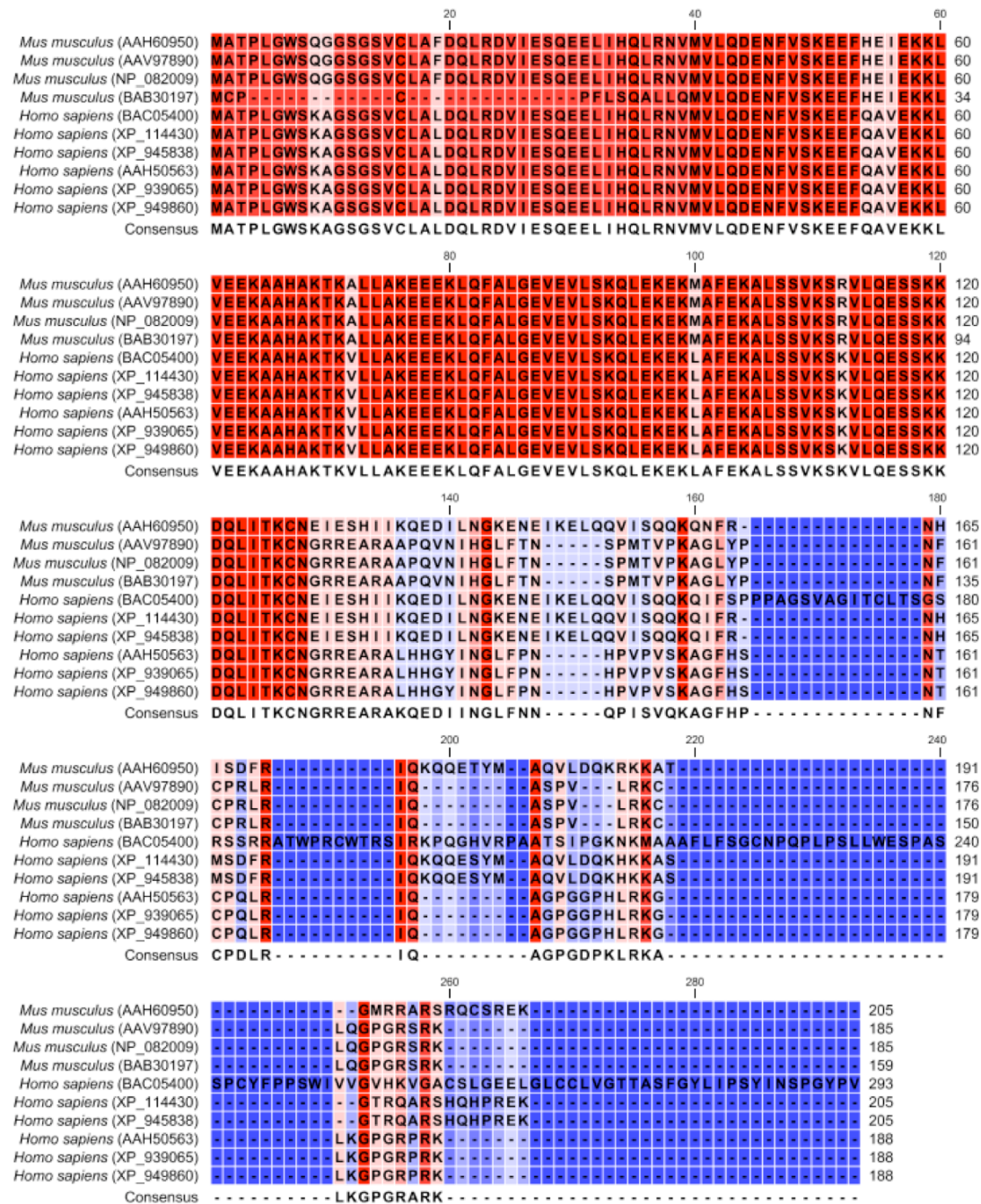


Figure 6. Sequence comparison of mouse and human TIPT isoforms. The amino acids are presented on a background colour, which varies in a gradient from red (the most conserved residues) to light blue (less conserved residues) and dark blue (unconserved residues). In the left side are indicated the species and the accession numbers and on the right side, the amino acids number. The consensus sequence is depicted below the alignment.

<i>Specie</i>	<i>NCBI protein name</i>	<i>NCBI accession number</i>	<i>No. of AA residue</i>
<i>Mus musculus</i>	TIPT isoform 2	AAH60950	205
	TIPT isoform 1	AAV97890	185
	unnamed protein	BAB30197	159
<i>Homo sapiens</i>	TIPT isoform 2 isoform 1	XP_114430	205
	hypothetical protein LOC202051	AAH50563	188
	TIPT isoform 1 isoform 2	XP_939065	188
	unnamed protein	BAC05400	293
<i>Rattus norvegicus</i>	similar to TIPT	XP_214584	362
<i>Macaca fascicularis</i>	unnamed protein	BAE00938	205
<i>Macaca mulatta</i>	TIPT isoform 2 isoform 1	XP_001083280	205
	TIPT isoform 1 isoform 2	XP_001083410	188
<i>Canis familiaris</i>	TIPT isoform 2 isoform 2	XP_848310	205
	TIPT isoform 1 isoform 3	XP_855732	188
<i>Bos taurus</i>	TIPT isoform 2 isoform 1	XP_582494	205
	TIPT isoform 2 isoform 2	XP_874082	261
	TIPT isoform 1 isoform 5	XP_887261	218
	TIPT isoform 1 isoform 4	XP_887249	188
	TIPT isoform 1 isoform 3	XP_887237	154
<i>Strongylocentrotus purpuratus</i>	similar to TIPT	XP_782021	159

Table 1. TIPT orthologs. The BLASTP search for homologs in other species was done using TIPT mouse protein as query. In the first column are indicated the species in which TIPT proteins were identified. All the NCBI accession numbers for different protein isoform identified are shown in the second column, as well as their names found in the database in the third column. In bold is indicated the accession number of TIPT isoform 2. The last column presents the length in amino acids of each protein identified.

1.3. TIPT RNA and Protein Expression

1.3.1. TIPT RNA Expression

In order to characterize TIPT expression, several methods were used: RT-PCR, Northern blot, whole-mount in situ analysis, immunoanalysis on cells and tissue sections.

The temporal expression pattern of TIPT was analyzed by a two-step RT-PCR technique in comparison with the expression of GAPDH housekeeping gene (Figure 7A). Embryonic RNA was extracted from day 7.5 to 11.5 mouse embryos, dissecting the embryos in three parts, anterior (above first the branchial arch), medial (between the first branchial arch and the hindlimbs), and posterior (the rest). TIPT was found in all the embryonic stages analyzed and it showed anterior, medial and posterior distribution.

To assess TIPT gene expression across tissues, an adult mouse Northern blot was hybridized with a TIPT probe. The result confirmed the expected size of TIPT isoform 2 transcript and the unrestricted expression pattern (Figure 7B). TIPT expression was present in adult all tissues, less abundant in liver and highly expressed in testis.

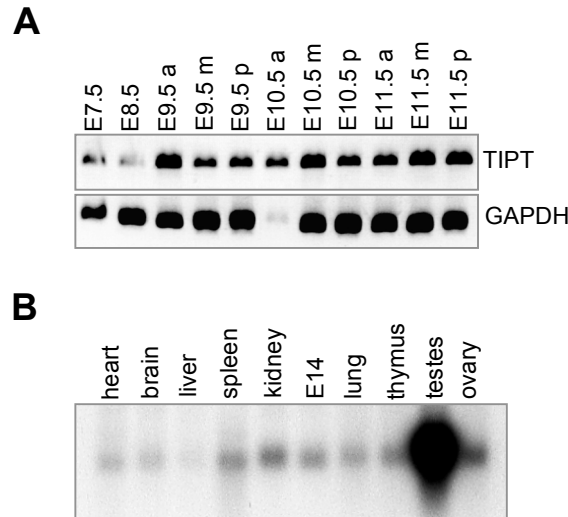
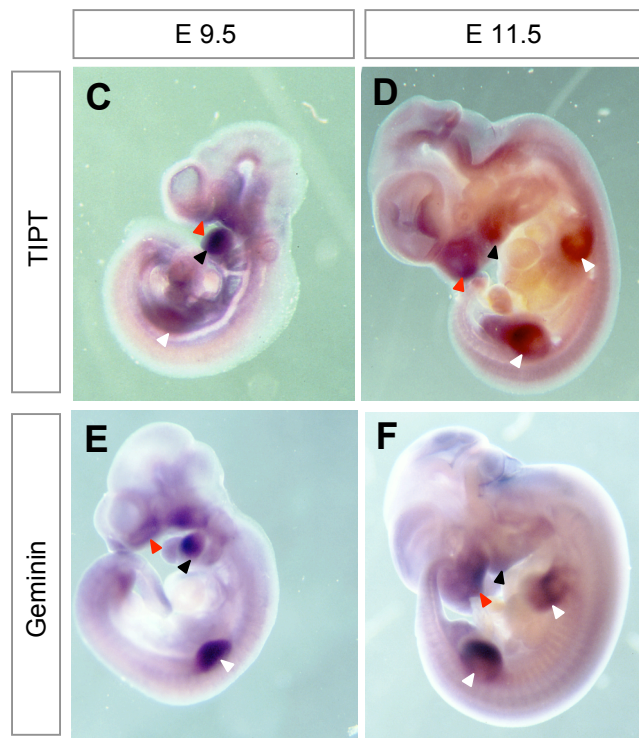


Figure 7. TIPT expression in mouse. **(A)** Temporal curve of TIPT expression. a-anterior region, m-middle region, p-posterior region. **(B)** TIPT adult tissues and E14-embryo expression. **(C-D)** TIPT expression in mouse embryos on day 9.5 and 11.5. **(E-F)** Geminin expression in mouse embryos on day 9.5 and 11.5. Red arrowheads-frontonasal prominence; black arrowhead-branchial arch; white arrowheads-fore- and hindlimbs;



Whole-mount in situ analysis was performed on different embryonic mouse stages. In day 8.5 mouse embryos TIPT expression is low and ubiquitous (data not shown). It increases and becomes more restricted in day 9.5 with a stronger detection of the transcript in the first branchial arch, frontonasal prominence, forelimb buds and extraembryonic tissues (Figure

7C). In day 11.5 mouse embryos TIPT expression is restricted to the nasal process, branchial arches, in the fore- and hindlimbs (Figure 7D). TIPT expression resembles to a degree the geminin expression pattern in day 9.5 and 11.5 mouse embryos (Figure 7E, F).

Taken together, the embryonal and adult TIPT analyses at the RNA level indicate a widespread expression.

1.3.2. Anti-TIPT Antibodies

For further descriptive and functional analysis of TIPT at cellular and subcellular level a polyclonal antibody was created. Full-length TIPT was cloned into pGEX-KT vector which contains a GST tag downstream of the Thrombin cleavage site, and into pET-15b vector provided with a His tag. Four *E. coli* cell strains were used as hosts for the expression of tagged TIPT mouse proteins: BL21(DE3), BL21(DE3)C41, BL21(DE3)CodonPlus-RIL and XLBlue-1. An expression screening aiming to characterize the best cell strain for TIPT protein production was performed. Optimal conditions for GST-tagged protein production expression and solubility were achieved using BL21(DE3)CodonPlus-RIL bacterial strain, inducing protein expression at 17°C with 0.2mM IPTG, and growing the cells overnight. The His-tagged protein could not be overexpressed under conditions tested. GST-TIPT protein was purified using affinity tag column chromatography (Figure 8A). The tag was removed by cleavage with Thrombin, and the untagged protein was subjected to purification by electroelution from SDS-PAGE gel and sent for rabbit immunization to a commercial producer.

The serum was affinity purified and tested by Western blot against the pure TIPT proteins tagged and untagged (Figure 8B). The antibodies recognized the recombinant GST-TIPT protein as well as the protein used for rabbit immunization. This protein was the untagged version, which was purified and controlled for the right amino acid sequence by mass spectrometry analysis. Still, the antibodies recognized an additional upper band, which suggested that the protein formed dimer during storage. The antibodies were tested also against cell extracts (Figure 8C). The predicted TIPT molecular weight is 23,6700 Da however, TIPT migrates slightly slower than expected, around 28,500 Da. In addition, a second band was frequently detected at the double size, corresponding to a dimer size, identical to the band observed on untagged TIPT protein. Dimer formation could not be avoided using freshly added DTT, cooking the samples at 70°C for 20 minutes, or boiling them for 10 minutes. However, if the extract was freshly prepared and immediately subjected to analysis, dimerization could be prevented. The specificity of the antibodies was tested in a

competition assay, incubating the blot membrane with ten fold excess of pure recombinant protein and antibodies. The outcome was a completely blank blot, demonstrating the high specificity of TIPT antibodies (data not shown).

The antigen was detected in both cytoplasmic and nuclear HeLa cell extract (Figure 8C). In order to find out in which cellular compartment antibodies identify TIPT, a protease protection assay using HeLa cell extracts was performed (Figure 8D). TIPT was detected in the 3,000 g pellet representing the nuclear fraction and the non-disrupted cells. The supernatant was divided in two and treated in parallel with trypsin or trypsin inhibitor. Both samples were spun down at 100,000 g, and the supernatants and pellets were analyzed by Western blotting. TIPT was found only in the protease inhibitor (PI) treated sample, both in the supernatant and pellet, which demonstrates its cytoplasmic localization as soluble form and attached to the membrane, but not integrated into the membrane.

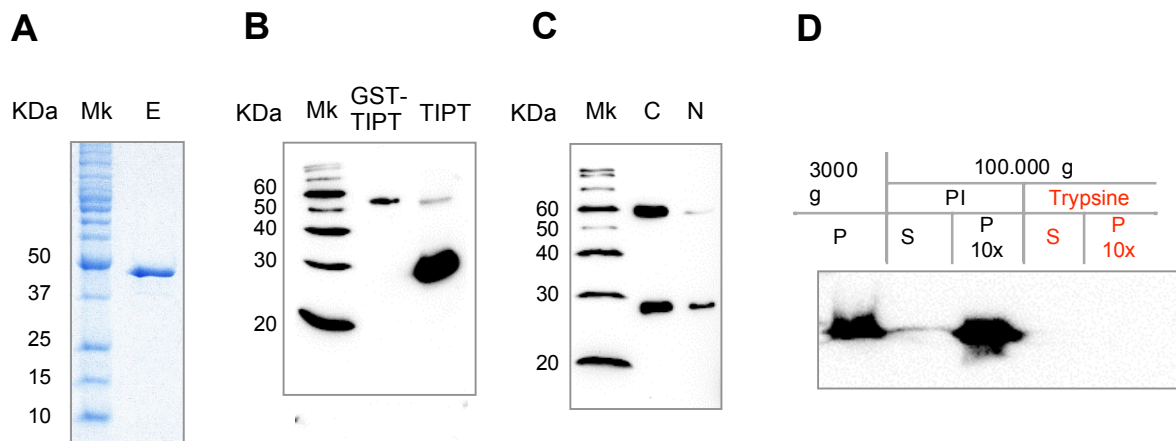


Figure 8. TIPT antibodies characterization. (A). Purification of GST recombinant full length mouse TIPT by glutathione sepharose affinity purification. Recombinant GST-TIPT protein has 48 kDa and more than 90% purity according to the Coomassie blue staining. Lane Mk contained molecular size markers (Bio-Rad; indicated in kilodaltons on the left). (B) Purified antibodies recognize GST-TIPT *E.coli* purified protein and the protein subjected for immunization. Lane Mk contained chemiluminescent molecular size markers (Invitrogen; indicated in kilodaltons on the left). (C) Antibodies detect two bands in cytoplasmic and nuclear HeLa extracts frozen and thawed (monomer and dimer TIPT). (D) Protease protection assay. TIPT is present in nuclear fraction (3,000 g pellet). Cytoplasmic TIPT was found in soluble and membrane attached forms. Pellet fraction was loaded 10 fold more in comparison to the supernatant fraction. Abbreviations: E, elution; C, cytoplasmic; Mk, marker; N, nuclear; P, pellet; PI, proteinase inhibitor; S, supernatant.

1.3.3. TIPT Phosphorylation

In order to find whether TIPT can be posttranslational modified by phosphorylation, NetPhos2.0 (<http://www.cbs.dtu.dk/services/NetPhos/>), the software for phosphorylation prediction sites was used. Nine serine phosphorylation sites were found, with a prediction

score higher than 0.9 for eight of them (Ser 28, 49, 106, 107, 116, 117, 197, 201), and one with a score above 0.5 (Ser 110) (Figure 9A). Using another Phospho.ELM database (<http://phospho.elm.eu.org>), the kinase phosphorylation recognition sites were predicted: casein kinase II (CKII) phosphorylation sites- amino acids 28-31; casein kinase I (CKI) phosphorylation sites- residues 107-110; glycogen synthase kinase 3 (GSK3) phosphorylation sites- amino acids 6-12 and 195-201; protein kinase B (PKB) phosphorylation sites- residues 196-202.

In order to identify if TIPT is phosphorylated *in vivo*, an immunoprecipitation assay was performed, aiming for the MALDI peptide mass fingerprint analysis of precipitated TIPT. The anti-TIPT rabbit polyclonal antibodies could not immunoprecipitate TIPT from HeLa, U2OS and 3T3 total cell extracts or fractionated nuclear and cytoplasmic extracts. Therefore, the immunoprecipitation was performed from total cell extract overexpressing HA tagged TIPT using tag antibodies. In parallel with a Western blot analysis realized in order to check whether the immunoprecipitation was successful, a gel was silver stained and analyzed by mass spectrometry. The analysis re-confirmed that TIPT was successfully precipitated by HA antibodies, and led to the identification of a peptide phosphorylated at Ser 28: DVIESQEELIHQLR (data not shown). This site is predicted to be a casein-kinase II target. To confirm that CKII phosphorylates TIPT an *in vitro* CKII phosphorylation assay was performed. The gel stained with Coomassie blue to confirm the equal loading of product reactions was further exposed to a film. CKII transfers γ -ATP-[32 P] in a dose dependent manner to GST-TIPT, but not to GST alone (Figure 9B).

In order to find in which cellular compartment the phosphorylated form of TIPT predominates a more *in vivo* assay was performed, treating the cells with phosphatase or phospho-kinase inhibitors. Okadaic acid, a Ser/Thr phosphatase inhibitor, was used to inhibit de-phosphorylation. After a short treatment (6 hours) U2OS cells were almost normal (Figure 9C), but upon a longer treatment (24 hours) the TIPT subcellular localization was changed: the protein disappeared almost completely from nucleoli and was redistributed in cytoplasm, and accumulated in dot-like structures (Figure 9D).

DRB, 5,6-dichloro-1-beta-D-ribofuranosylbenzimidazole, is an adenosine analogue that inhibits casein kinase II [95]. Human U2OS and HeLa cells were treated with 50 μ g/ml DRB during a period of 15 min or 1h, but almost no change was observed in comparison with the control (data not shown, Figure 9E). Increasing the level by a factor of 100 for 15 min changed drastically TIPT localization, increasing the amount of nucleolar fraction with a

decrease in the cytoplasmic localization (Figure 9F). Altogether, these data prove that TIPT protein is phosphorylated by CKII at least on one serine site. The inhibition of dephosphorylation directs more TIPT into the cytoplasm, and on the contrary, the inhibition of phosphorylation localizes more TIPT into the nucleolus. Thus, TIPT localization is dependent on posttranslational phosphorylation.

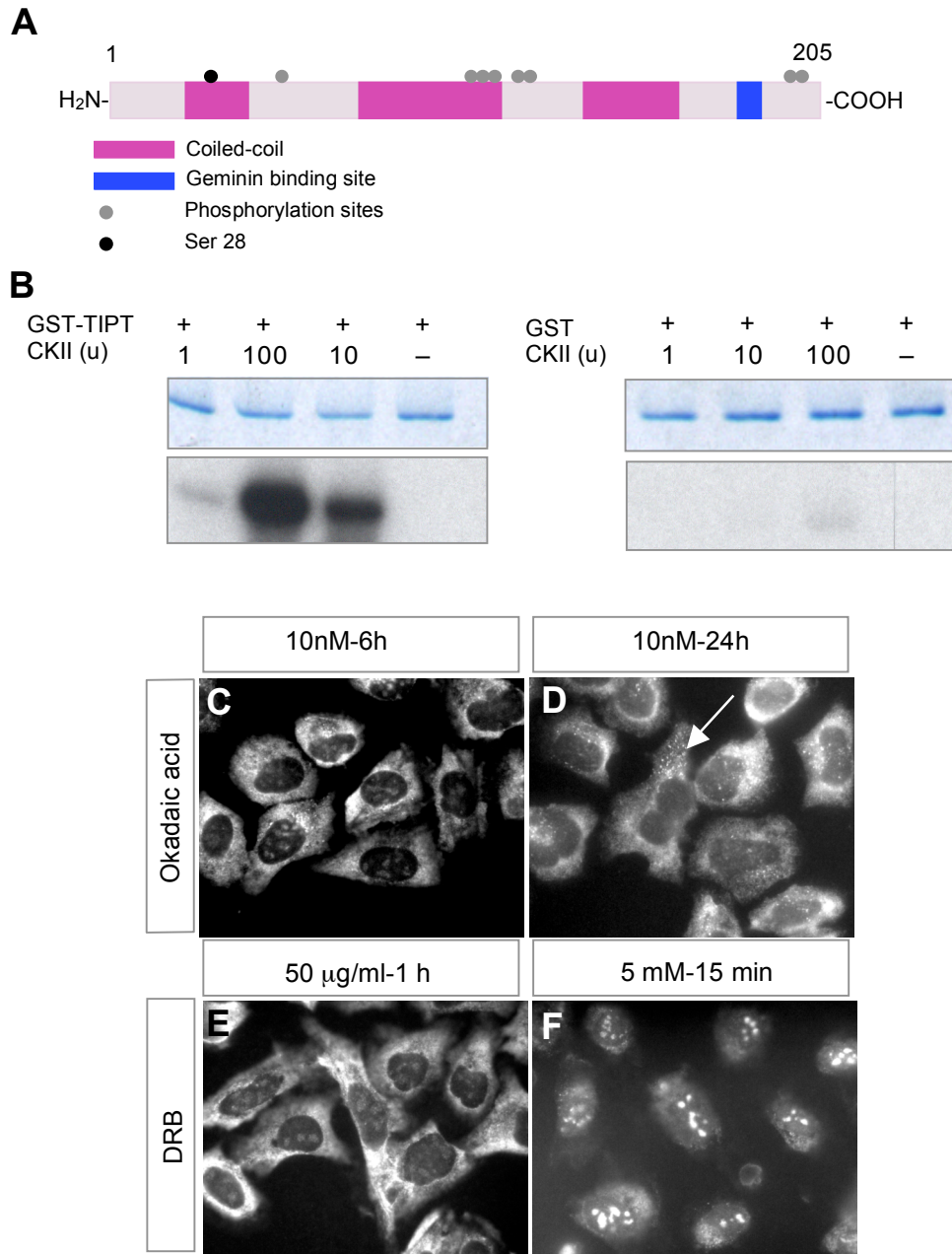


Figure 9. TIPT is phosphorylated. (A) Phosphorylation predicted sites using NetPhos2.0 software. Mouse TIPT 2 isoform (205 amino acids) is depicted with coiled-coil domains and binding site for geminin (see section 2.1). (B) Casein kinase II phosphorylates TIPT in an *in vitro* binding assay. 1-100 unit CKII transfers 20 mCi [³²P]-γ-ATP on 2 µg GST-TIPT recombinant protein, but not on 2 µg of GST. Elutions were separated on SDS-PAGE gel stained with Coomassie blue and exposed to an X-ray film. (C-D) Okadaic acid inhibits de-phosphorylation. 10 nM Okadaic acid applied for 24 h changes TIPT localization in U2OS cells. (E-F) DRB inhibits CKII. 5 nM DRB applied for 15 min determines nucleolar recruitment of TIPT in U2OS cells.

1.3.4. TIPT Expression in Embryonic Brain and Neurons

In order to analyze whether TIPT has a restricted expression pattern in brain, day 16.5 mouse embryo were subjected to immunohistochemistry. TIPT protein was found in the proliferative neuroepithelium, the mitral cell layer, and external plexiform layer of the olfactory bulb, as well as in the frontal orbital cortex (Figure 10A, B). In cortex, TIPT is abundant in the entire cortical plate, in the subplate, in the ventricular (VZ) and in subventricular zone, but not in the intermediate zone (Figure 10C, D). In the VZ, TIPT was detected in the basal (abventricular) progenitors, which divide symmetrically and give rise to neuronal lineage (Figure 10D). By contrary, TIPT was not found in the asymmetrically dividing multipotent radial glial cells located at the ventricular surface. Hippocampal TIPT expression is restricted to the dentate gyrus (Figure 10E, F). In the diencephalon, TIPT localizes to the dorsal thalamus, in lateral habenula, as well as in a very defined population of cells, reticular thalamic nucleus (Figure 10G, H). In telencephalon TIPT is very strongly expressed in basal ganglia, confined to globus pallidus, caudate putamen and amygdala (Figure 10I-L). Moreover, TIPT is localized in pontine nuclei of pons, and in the external germinative layer of cerebellum (data not shown).

To study the expression of TIPT at cellular level neurons were differentiated from mouse embryonic stem cells (ES) and a double labeling with neuronal tubulin marker (Tuj1) was performed. TIPT was detected in the nucleoli, not only in differentiated neurons but also in the supporting fibroblasts used as feeder layer (Figure 11A-C). In order to further analyze TIPT expression in neurons, a hippocampal neuronal culture was prepared from newborn rats, followed by double co-immunostaining with a synaptic vesicle protein marker (synaptotagmin I) (Figure 11D-F). TIPT is present only in neurons while it does not appear to be expressed in supporting astrocytes. As indicated from analysis of mouse brains and ES cell derived neurons, also in hippocampal rat neurons TIPT was found in the neuronal cell body. However, TIPT is not enriched in nucleoli, is rather found diffuse in the nucleoplasm and at the nucleolar periphery (Figure 11G). TIPT antibodies also stain very strongly the neuronal processes (Figure 11G-I). When compared to the synaptic vesicle pattern, TIPT appears to follow the axons in a filamentous pattern, and does not enrich substantially in synaptic buttons.

These data indicate that TIPT expression is confined to proliferating precursor cell populations and in regions where neurons are maturing. At the cellular level, analysis of

mouse brains, ES cell derived mouse neurons and hippocampal rat neurons indicate TIPT expression not only in neuronal cell body but also in neuronal processes.

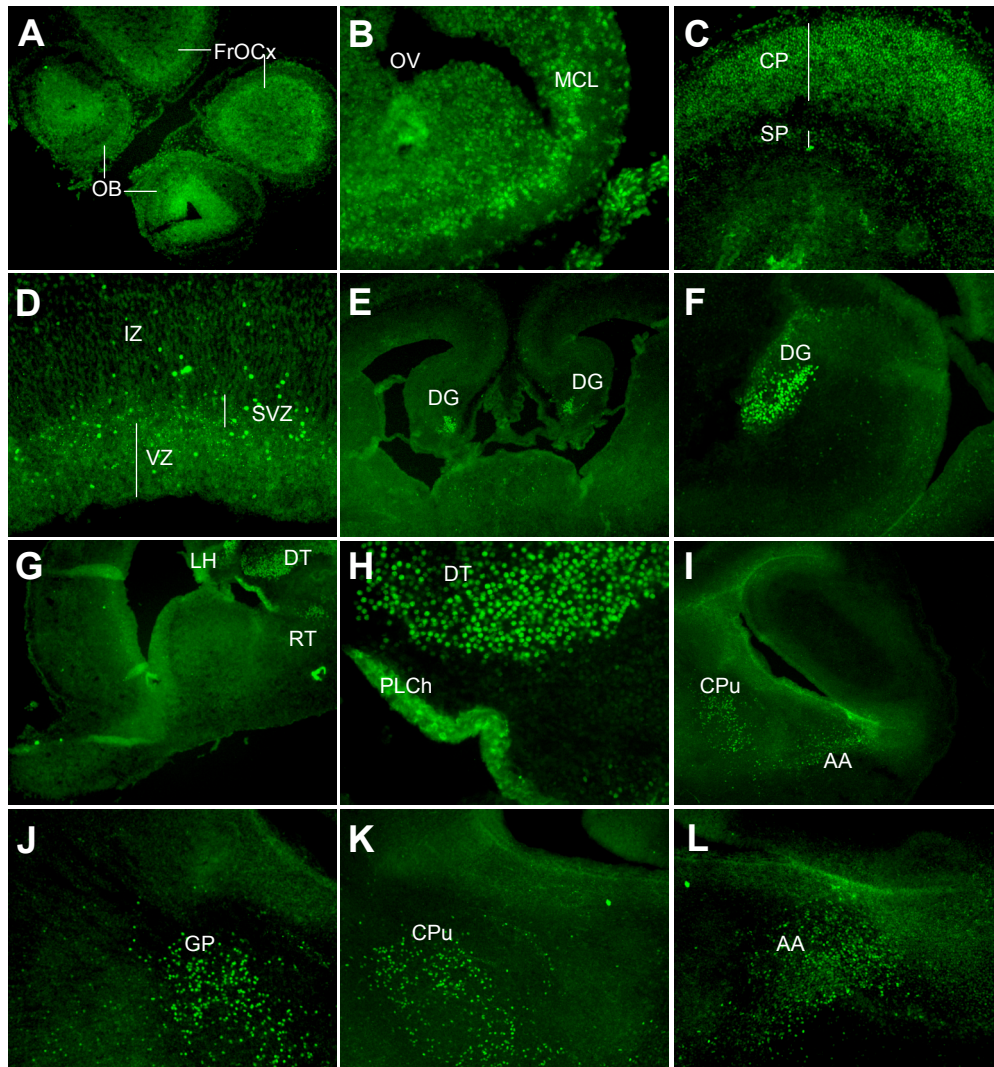


Figure 10. TIPT expression in brain day 16.5 mouse embryo. (A-C) TIPT expression in rostral cortex (crosssections). (D) TIPT expression in basal layer of VZ and SVZ (sagittal section). (E-F) TIPT expression in dentate gyrus (cross and sagittal section). (G-H) TIPT expression in thalamus (sagittal section). (I-L) TIPT expression in basal ganglia on sagittal sections. Abbreviations: AA, amygdala; CP, cortical plate; CPu, caudate putamen; DG, dentate gyrus; DT, dorsal thalamus; FrOCx, frontal orbital cortex; GP, globus pallidum; IZ, intermediate zone; LH, lateral habenula; MCL, mitral cell layer; OV, olfactory ventricle; PLCh, plexus choroids; RT, reticular nucleus; SVZ, subventricular zone; VZ, ventricular zone.

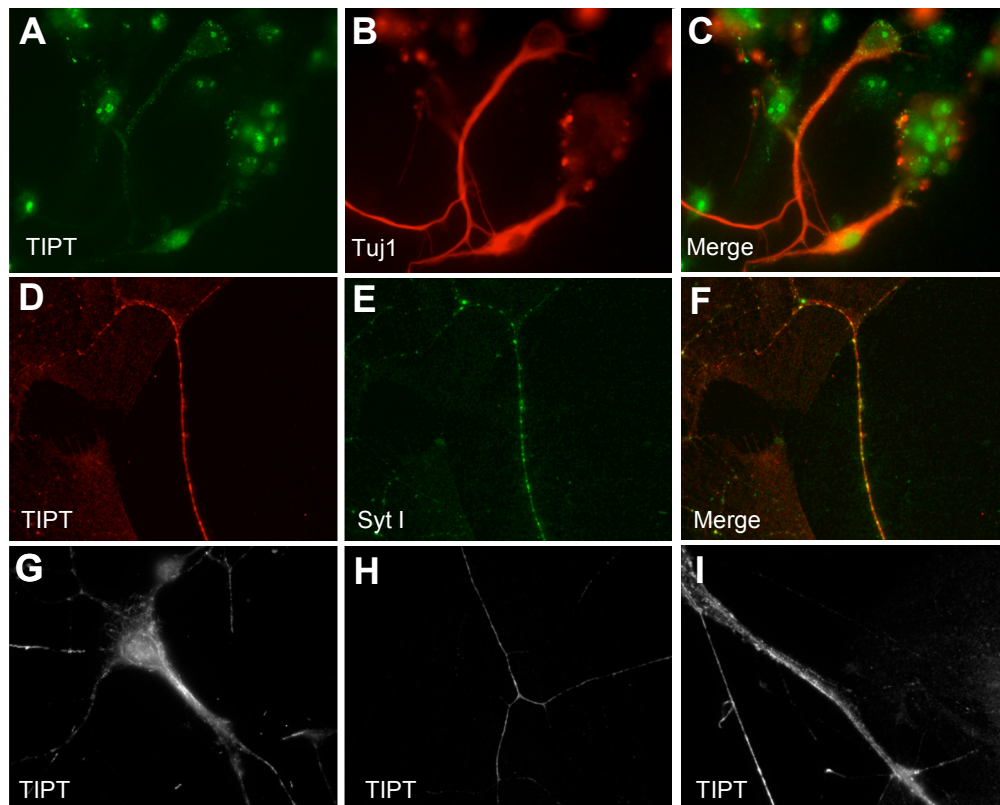


Figure 11. TIPT expression in mouse differentiated neurons and rat hippocampal neuronal culture. **(A-C)** Immunohistochemistry of ES cell derived neurons. TIPT and Tuj1 expression. **(D-I)** Immunohistochemistry of rat hippocampal neuronal culture. **(D-F)** TIPT co-localization with Synaptotagmin I. **(G)** TIPT expression in neuronal cell body. **(H-I)** TIPT expression in neuronal processes. Enlarged view presented in I. Abbreviations: Tuj1, tubulin; Syt I, synaptotagmin I; merge, co-localization.

1.3.5. TIPT Expression in Testis

TIPT expression in adult testis relative to other tissues is explicitly high, therefore a detailed analysis of TIPT during male germ cell development was performed.

For this study testes derived from wild-type mice in different developmental stages, and from mutant mice with well-defined arrest in germ cell differentiation were used. Total testicular RNAs from mice of different postnatal developmental stages, namely 7, 11, 15, 19, 21, 23, 25, 30 days old and adult were prepared. Except for TIPT isoform 1 and 2, also geminin, AF10 and TBPL1 were included in analysis. The latter are expressed in high levels during testes development, and were further included in the biochemical characterization of TIPT function (see below).

TIPT-1 isoform follows an expression dynamics with a start at day 21 pp, increases at day 23 pp and then decreases, but does not disappear completely in day 25 and 30 pp, to be also highly expressed in adult (Figure 12A). This correlates with the appearance of the first

spermatids and indicates the presence of TIPT-1 isoform in all haploid spermatids. TIPT-2 RNA is almost undetectable at day 21 pp, becomes higher at day 23 pp, and disappears at day 25 pp to be present again in adult testis. This pattern suggests that TIPT-2 transcript is expressed in early haploid spermatids, but not in late spermatids (Figure 12A). A similar RNA expression pattern was obtained for geminin, AF10 and TBPL1 (Figure 12A).

For an analysis of TIPT protein expression during development, total testicular protein extracts from different postnatal mouse stages, namely 15, 19, 21, 23, 25 days old and adult were prepared. The Western blot was performed using TIPT and Vimentin antibodies as loading control (Figure 12B). A protein band, which runs at 25 kDa, corresponding probably to TIPT-1 (predicted size 20.8 kDa), was detected in mouse testis 23, 25 days pp and adult (Figure 12B). The protein band corresponding to TIPT-2 was detectable only after a much longer exposure, and followed the TIPT-1 profile. These data suggest that TIPT-1 is the predominating isoform in testis, and the translation starts 2 days later than its transcription.

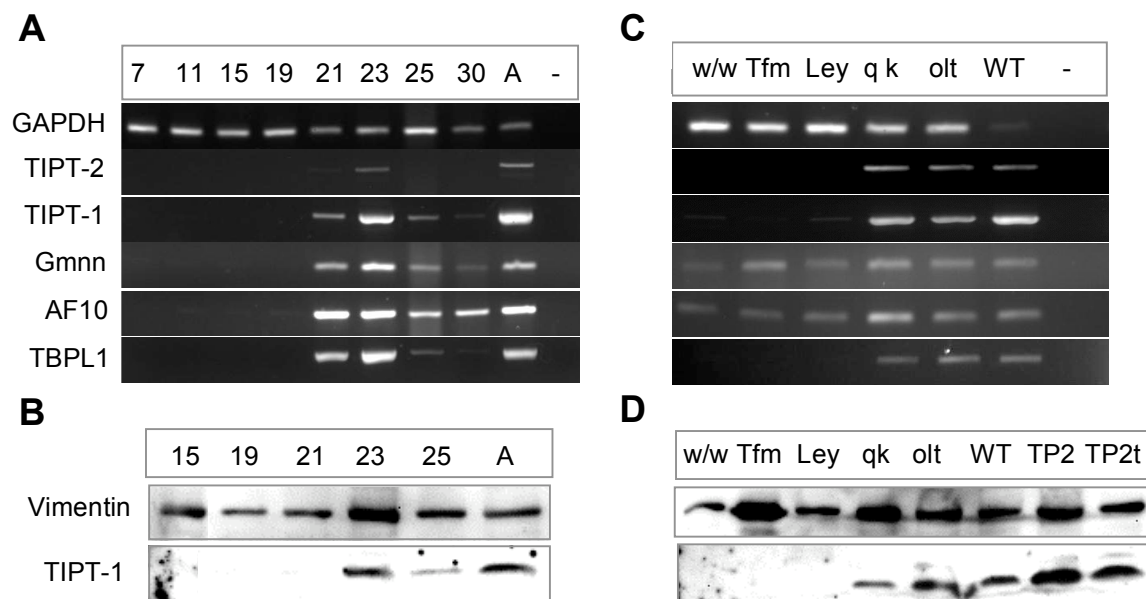


Figure 12. Expression of TIPT 1 and 2 isoforms, geminin, AF10 and TBPL1 in male germ cells. (A) RNA from different mouse testis developmental stages was reverse-transcribed and TIPT-1, TIPT-2, geminin, AF10 and TBPL1 expression was determined. (B) TIPT protein expression during development. (C) RNA from mouse mutants arrested at different developmental stages was reverse-transcribed to amplify TIPT isoforms, geminin, AF10 and TBPL1. (D) TIPT protein expression in testis extracts from mouse mutants. Abbreviations: A, adult; Ley, *Leyl*^{-/-} mutants; olt, *olt/olt* mice mutants; qk, *qk/qk* mice; Tfm, *Tfm/y* mice mutants; TP2, *Tpn2*^{-/-} null mice; TP2t, *Tpn2* CAT transgenic mice; w/w, *W/W^v* mutants; -, negative control, ddH₂O.

RT-PCRs were performed using testis from different mouse mutants with well-known arrest of germ cell differentiation [96]. The mutant mice used were: *W/W^v*, *Tfm/y*, *Leyl*^{-/-}, *olt/olt*,

qk/qk, *TPn2*^{-/-} and *Tpn2* transgene. *W/W*^V mice are characterized by only a few primary spermatogonia [97]. In *Tfm/y* (testicular feminization) mutants germ cells arrest as primary spermatocytes [98, 99]. *Leyl*^{-/-}(*insl3*) deficient mice have arrest at secondary spermatocytes stage [100]. *olt/olt* (oligotriche) mutants arrest in spermatogenesis at round spermatids. *qk/qk* (quaking) mutants arrest at elongating spermatids [98, 99]. Both TIPT isoform transcripts are present in mutants with germ cells arrest at spermatids level, which correlates with the developmental expression data (Figure 12C). These results suggest that TIPT-1 and 2 are expressed in secondary spermatocytes and haploid spermatids.

RT-PCR analysis for TBPL1 transcript follows TIPT expression profile (Figure 12C). This finding more or less goes along with a very detailed report on TBPL1 stage-specific expression during spermatogenesis where high levels of TBPL1 transcript were found in pachytene spermatocytes and lower levels in spermatids [43]. Geminin transcript was detected in every mutant, with a lower expression in *W/W*^V mutants (Figure 12C). This observation is partially consistent with a previous work where geminin was found expressed in primary spermatocytes and some spermatogonia cells [101]. AF10 transcript, like geminin, was present in all the mutants, with higher expression in *qk/qk* and *olt/olt* (Figure 12C). In a previous study AF10 was found expressed in postmeiotic germ cells, especially in spermatids from around stage VI to VIII [102].

To compare TIPT developmental pattern with information obtained from mutants analysis, it was necessary to check also TIPT protein levels in mutants. Except for the mutants characterized above, two other mice mutants for transition protein 2 gene (*Tnp2*) were examined: *Tnp2*^{-/-} and *Tnp2*-CAT transgenic. *Tnp2*-null mice present abnormal focal condensations in step 11 spermatids, while in *Tnp2* transgenic mice a CAT reporter gene is driven by *Tnp2* rat promoter in postmeiotic male germ cells [103]. As in the developmental blot, a protein band with 25 kDa mobility in *qk/qk* and *olt/olt* mutants was observed, doubled by TIPT-2 protein band after a long exposure, confirming transcriptional profile obtained from mutants RNA (Figure 12D). In addition, TIPT is increased if TP2 is absent or overproduced in haploid spermatids.

Taken together, these data indicate that TIPT-1 and 2 constitute a coexpression group together with TBPL1, AF10 and geminin. In testis, transcriptional start happens 2 days before TIPT proteins are produced, which is characterized by late spermatocytes and postmeiotic germcells expression.

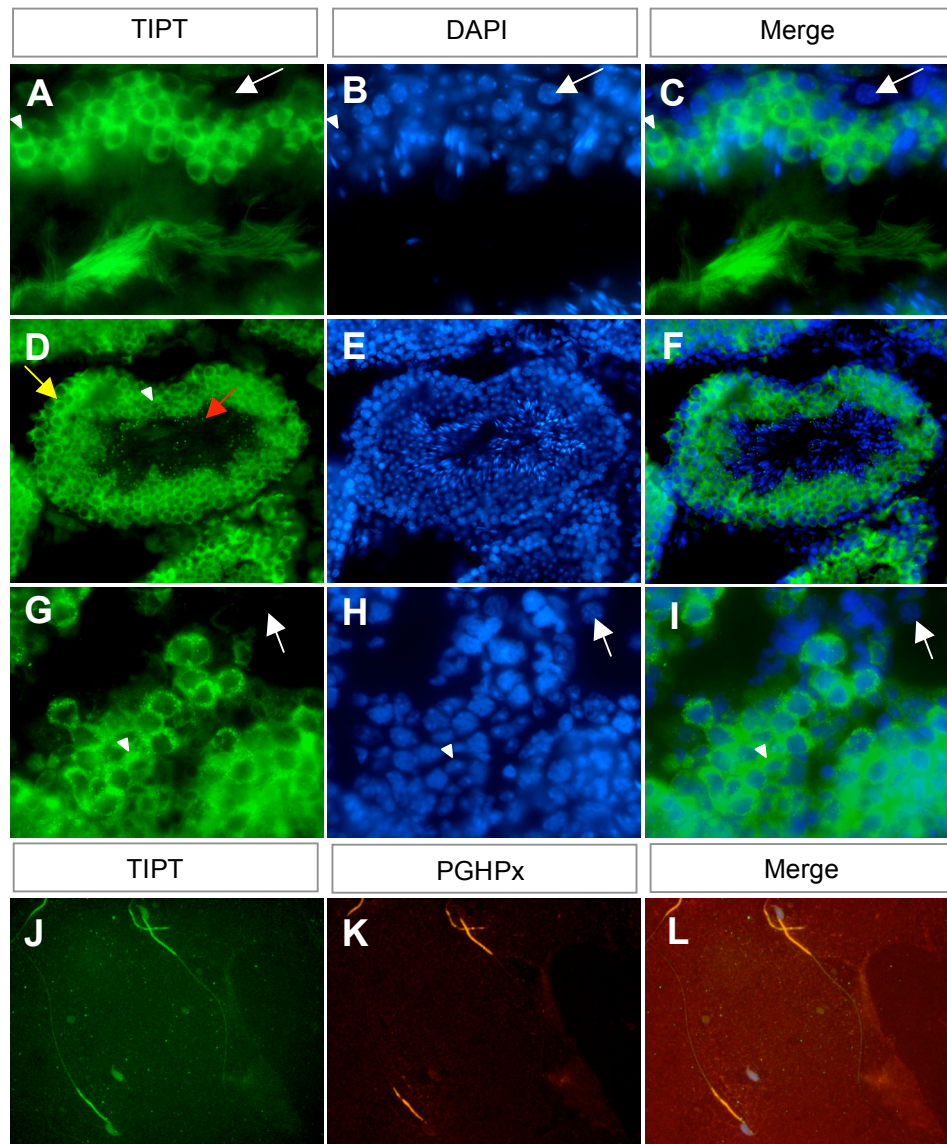


Figure 13. Immunostaining of TIPT on mouse testis cryosections, cell suspension and spermatozoa smear. (A-F) TIPT immunostaining on adult mouse testis cryosections. (A, D) TIPT expression in spermatocytes, round spermatids and elongating spermatids, but not in spermatogonia. (B, E) DNA staining of seminiferous tubules with DAPI. (C, F) TIPT co-localization with DAPI staining. (G-I) TIPT immunostaining on adult testis cell suspension. (G) TIPT expression in spermatids and some spermatocytes. (H) DNA staining with DAPI. (I) TIPT immunostaining and DAPI overlay. (J-L) Co-localization of PHGPx and TIPT in the midpiece of mouse spermatozoa. (J) TIPT staining of midpiece tail and head sperm. (K) PGHPx stains midpiece tail sperm. (L) TIPT and PGHPx immunostainings overlay. Symbols: white arrow, no TIPT staining; white arrowhead, round spermatids staining; yellow arrow, TIPT spermatocytes staining; red arrow, TIPT tail's midpiece staining of elongating spermatids.

Immunostaining on cryosections or cellular suspensions from adult testis detected TIPT not in all cell types. No TIPT expression occurred in spermatogonia (Figure 13A-C). Different stages of seminiferous tubules were stained, and TIPT was detected in cytoplasm of round spermatids and in some spermatocytes (Figure 13A-I). In addition TIPT was found in the

midpiece of elongated spermatids (Figure 13D). To confirm this finding, a spermatozoa smear was prepared from epididymal mouse sperm, followed by co-staining with phospholipid hydroperoxide glutathione peroxidase (PHGPx), a spermatozoa midpiece marker (Figure 13J-L). While the co-localization with this marker reports TIPT presence in midpiece, a week staining was also observed in spermatozoa head.

These findings reveal TIPT localization in late meiotic and postmeiotic germ cells, as well in the midpiece of elongating spermatids and spermatozoa.

1.3.6. TIPT Subcellular Expression

To analyze systematically the subcellular localization of TIPT different cell lines were used: mouse embryonic stem cells, SNL and NIH 3T3 mouse fibroblasts cells, Cos-7 monkey cells, RD rhabdomyosarcoma rat cells, HeLa cervical cancer human cells and U2OS human osteosarcoma cells. In all of these TIPT was localized in cytoplasm, and additionally in some nuclear structures suggesting nucleolar localization (Figure 14A, D, G, J and data not shown). To confirm the nucleolar staining, co-localization with TBPL1 was investigated, a protein previously identified in the nucleolus [65]. Both of TIPT and TBPL1 antibodies clearly label the same subcellular structures, demonstrating that they correspond to nucleoli (Figure 14B, E, H).

TIPT expression does not change during the cell cycle, being detected in all the cells of an asynchronous population. A more careful look on the cellular distribution, revealed a dot-like structure localized in the cytoplasm, in human and mouse cell lines. The number of these structures varied from 1-2 in the majority of mouse and human cells analyzed, to a higher number of structures in a small percent of human malignant cells. Such structures may correspond to centrosomes, cytoplasmic structures whose distribution and number is related to the cell cycle phases: a single centrosome in G1 phase, a doublet during S and G2 phase, and as well doublet, but separated to the spindle poles during subsequent mitotic stages, prometaphase, metaphase, and anaphase. To test this, the cells were double-labeled with anti-TIPT and anti- γ -tubulin antibodies (Figure 14J-O). γ -tubulin binds microtubule minus ends and is responsible for mediating the link between microtubules and the centrosome, functioning as the microtubule organizing centre [104, 105]. The cells in the cell cycle phases were examined, and TIPT was found present in centrosomes not only in interphase cells, but also in all the mitotic cellular phases. As an example, in figure 14M-O TIPT is presented the

prometaphase centrosomal localization. Moreover, TIPT is not only localized to the spindle poles, but also on the mitotic spindles (Figure 14M).

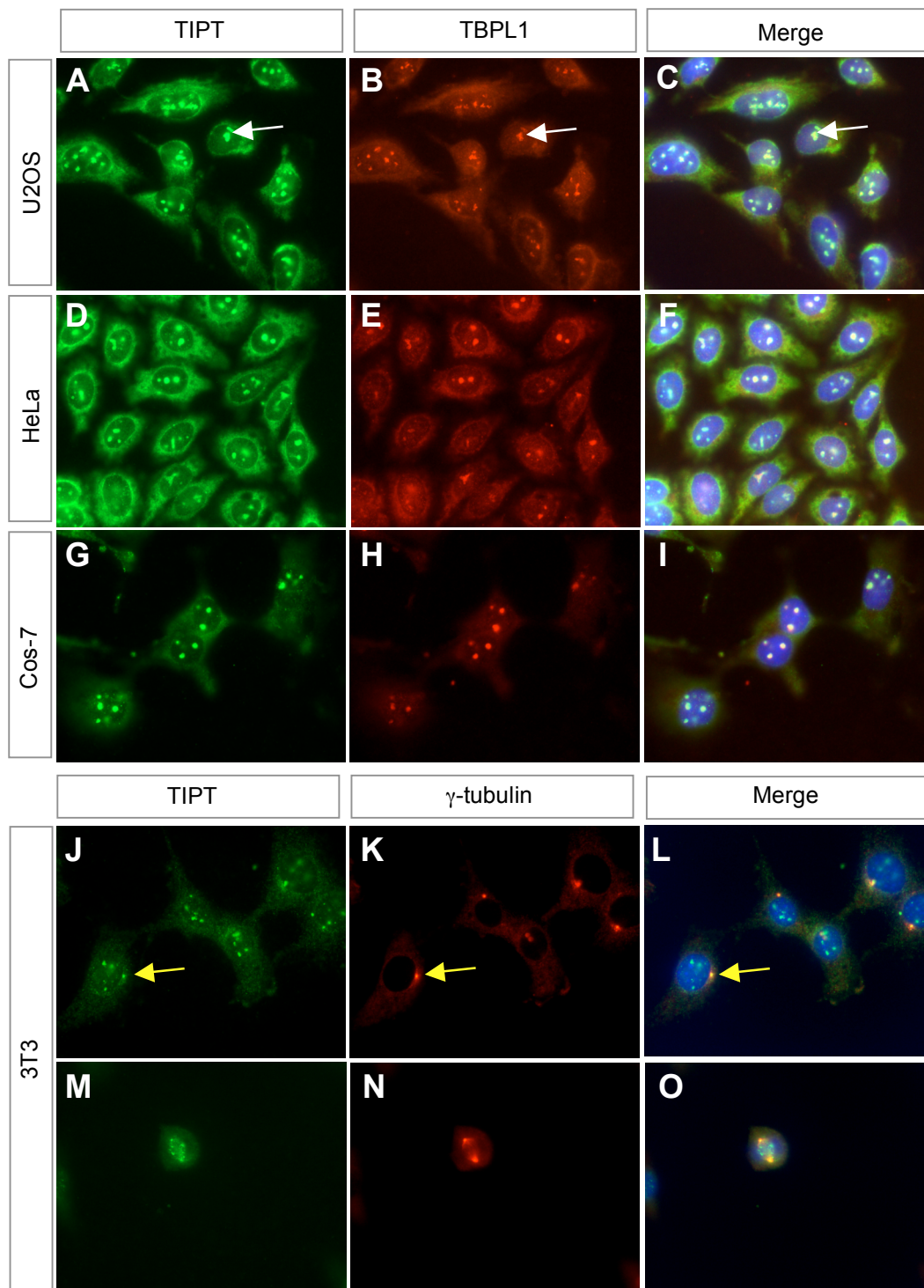


Figure 14. Cytoplasmic, nucleolar and centrosomal localization of TIPT in different cell lines. (A-G) TIPT nucleolar co-localization with TBPL1 in human osteosarcoma cells (A-C), human HeLa cells (D-F), and monkey Cos-7 cells (G-I). (J-O) TIPT co-staining with γ -tubulin in centrosomes of 3T3 mouse fibroblast cells. (J-L) TIPT co-localizes with γ -tubulin in centrosomes of interphase cells. (M-O) TIPT and γ -tubulin co-localization on centrosomes of pro-metaphase cells. In addition, TIPT localizes on mitotic spindle in pro-metaphase cells in M. Symbols: white arrow, nucleoli; yellow arrow, centrosome.

2. The TIPT Interactome

In order to find interacting partners for TIPT, several methods and strategies were used including pull-down assay, yeast two-hybrid screen and co-immunoprecipitation.

2.1. Candidates Testing Approach

2.1.1. Geminin

To ensure that TIPT really interacts directly with geminin, an *in vitro* binding assay was employed. The full length geminin sequence was inserted into pSP64 vector which contains an SP6 promoter and a poly(A)⁺tail. Geminin protein was synthesized by *in vitro* transcription-translation and tested for binding to the pure recombinant GST-TIPT protein, and pure GST as control. The interaction of geminin with TIPT was confirmed in this assay (Figure 15A).

To better characterize this interaction, the binding site of geminin on TIPT protein was delineated. The full-length amino acid sequence of TIPT was subdivided into sixty-three peptides twenty amino acid-length each, starting with the N-terminus, with 17 amino acids overlapping between adjacent peptides. The peptides were synthesized and spotted onto a cellulose membrane by Jerini company. Binding of His-geminin to TIPT revealed a basic amino acid rich domain, close to the C-terminus of protein (KRKK, amino acids 185-189) (Figure 9A, 15 B). In order to check that this is the real binding site for geminin, two lysines were substituted with aspartates (KRKK was mutated to DRDK). The GST-TIPT mutated protein was overexpressed in *E.coli* BL21DE3RIL bacterial strain, purified, and the interaction with *in vitro* translated geminin was controlled (Figure 15A). Indeed, no interaction was detected upon mutation of geminin binding site.

In vivo geminin-TIPT direct interaction was checked by immunoprecipitation. The experiment was performed using geminin polyclonal antibodies and total cell extract from day 8.5 mouse embryos or human HeLa and U2OS cells. However, TIPT protein could not be detected in the immunoprecipitated sample (data not shown). The next question asked was whether geminin can be precipitated together with HA-TIPT from HA tagged TIPT transfected cells. Once more, the result was negative (data not shown). These results suggest that under these experimental conditions tested geminin and TIPT do not interact *in vivo*.

2.1.2. Polycomb Group Proteins

The original two-hybrid screening for identification of geminin binding partners raised the idea that TIPT might be a component of the Polycomb group complex, like geminin is. Thus, some members of this complex were tested for TIPT binding, using *in vitro* pull down binding assay (Figure 15C). The SAM/SPM domain of Scmh1, the full-length Mph2, Ring1B and Mel18 were cloned into pSP64 vector. In these *in vitro* binding assays, Scmh1, Ring1B and Mph2 bound significantly to GST-TIPT in comparison to GST alone. In contrary, Mel18 cannot be recorded as TIPT partner because the level of interaction was almost the same as for GST alone. The finding that TIPT interacts directly with geminin, Scmh1, Ring1B and Mph2 raise the possibility that TIPT belongs to the Polycomb group complex, at least transiently. Further investigations will be necessary in order to elucidate the significance of this finding.

2.1.3. TATA Binding Protein and TATA Binding Protein-Like Factor

The strikingly similar subcellular localization of TIPT and TBPL1, and the interaction of TIPT with proteins involved in co-transcriptional regulation, geminin and AF10 (see section 2.2) prompted the investigation of a direct interaction. In addition, a data base entry recently appeared indicated that 5133400g04 Riken clone corresponds to TIPT isoform 2 (TATA binding protein-like factor-interacting protein) (see section 1.2). Full-length TBPL1 *in vitro* transcribed and translated from pSP64-TBPL1 plasmid interacted strongly with recombinant GST-TIPT, but not with pure GST (Figure 15C). TBPL1 belongs to the TBP family, therefore the TIPT interaction with TBP was also investigated. The same result was obtained, indicating that TIPT interacts *in vitro* with both TBPL1 and TBP proteins, most probably on a similar domain (Figure 15C).

In addition, the interaction between TIPT and basic transcription factors was tested *in vivo*. Immunoprecipitation was performed using HA antibodies and a total cell extract prepared from HA-TIPT stable cell line (see section 3.2). An *in vivo* interaction was impossible to detect, either checking endogenous TBPL1 or overexpressed GFP-TBPL1 in these cells. This failure might be explained by the fact that TBPL1 antibodies used could not detect the protein in the extract by Western blot. In contrary, TBP was found as TIPT interactor *in vivo* (data not shown). TFIIA was also tested, but could not be proved any interaction with TIPT (data not shown).

Moreover, because geminin is a binding partner of TIPT, its relation with TBP and TBPL1 was explored. Surprisingly, GST-geminin appeared to interact *in vitro* with both TBP family members (Figure 15D).

In conclusion, TIPT and geminin interact directly with each other and with basic transcription factors.

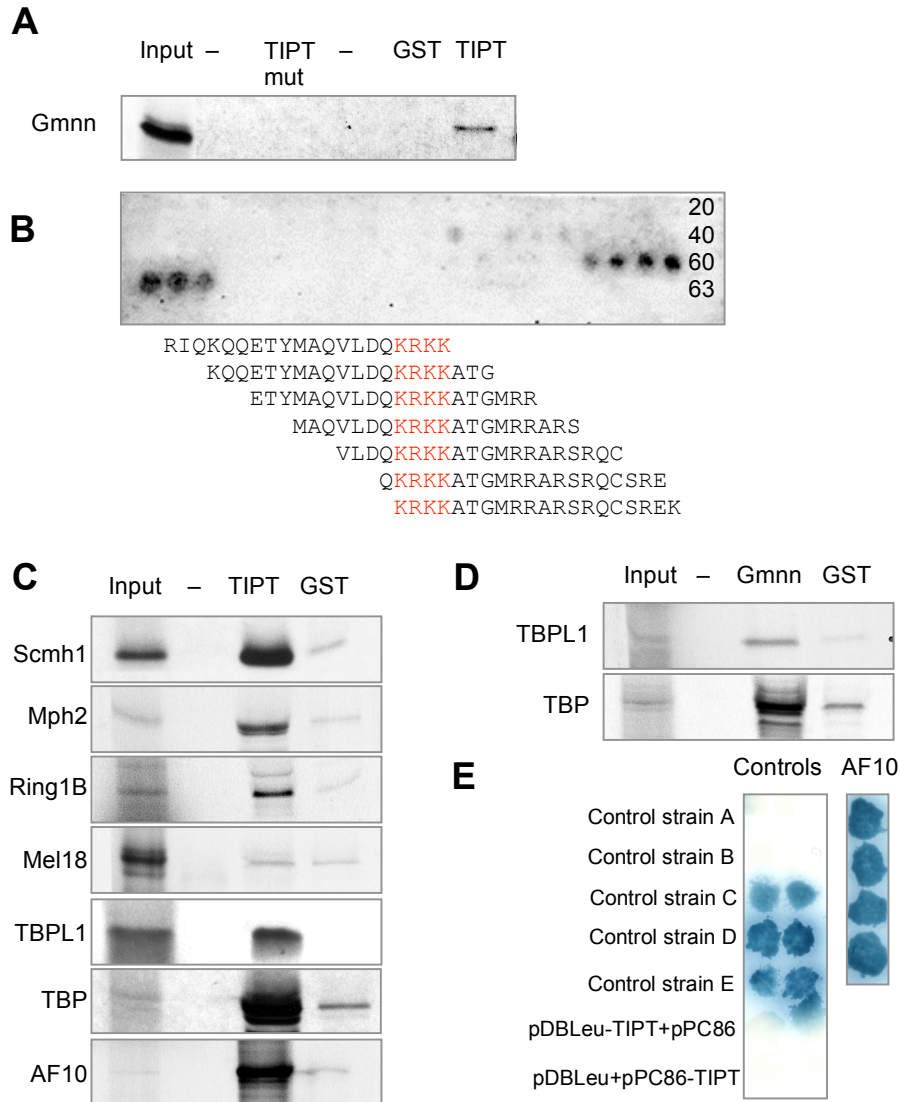


Figure 15. The interaction partners of TIPT and geminin (Gmn). **(A)** *In vitro* translated geminin interacts with GST-TIPT, but not with TIPT mutated for geminin binding site or GST. **(B)** Binding of His-geminin to a TIPT peptide array. Below, His-geminin bound peptides are listed (number 57-63). Amino acids 185-189 of TIPT comprise the geminin-binding site (KRKK). **(C)** Pull-down assays. The interactions of *in vitro* transcribed and translated Scmh1, Mph2, Ring1B, Mel18, TBPL1, TBP, and AF10 with GST-TIPT and GST were tested **(D)** The interactions of *in vitro* transcribed and translated TBPL1 and TBP with GST-geminin and GST were tested. **(E)** Yeast two-hybrid screen. The induction of the *lacZ* (blue in X-Gal assay) reporter gene was analyzed for the control strains A-E, in the self-activation test and for the AF10 clone. The AF10 clone is indicated by 4 different colonies and each control clone - by 2 different colonies. Control strains C, D, E are moderate, strong and very strong interactors as revealed by LacZ activity. AF10 clone was found positive, as visualized by X-gal staining in the second round of screen.

2.2. Yeast Two-Hybrid Screen

A yeast two-hybrid screening approach was taken to search for the putative TIPT's interaction partners during embryogenesis. The full-length TIPT cloned in frame with the Gal4 DNA binding domain in the pDBLeu vector, was used as bait and transformed into yeast strain MaV203 containing *HIS3* and *lacZ* reporter genes. 50 mM 3AT was established as concentration sufficient to determine *HIS3* gene expression by even weak interacting proteins and was enough to inhibit also bait self-activation. The day 8.5 mouse embryo cDNA library containing the preys, cloned in frame with Gal4 DNA activation domain in pPC86 vector was used for screening. This cDNA library was heat shocked in the pre-transformed pDBLeu-TIPT MaV203 yeast strain and 428 independent colonies were selected out from the first round of screen on plates lacking leucine, tryptophan and histidine, and supplemented with 50 mM 3AT. Next, all these clones were applied to the second round of screen in which β -galactosidase activity was assayed for every clone. From this step, 88 candidate clones were identified and sorted according to the X-Gal staining: 51 strong interactors, 27 moderate, and 10 weak interactors.

<i>Number of clones</i>	<i>TIPT interactors</i>
1	mAF10 (Mlt10)
2	D/tpvp (decidual/ trophoblast prolactin related protein)
1	1600014E20Rik (adult female placenta)
1	Brp44l (brain protein 44-like)
1	Ctla-2a (cytotoxic T lymphocyte-associated protein 2 alpha precursor)
1	Dap-1 (death-associated protein)
1	Bok/Mtd (Bcl-2-related ovarian killer protein/apoptosis activator matador)

Table 2. Outcome of the two-hybrid screening using the full length TIPT fused to the Gal4 DNA binding domain. The first column indicates the number of identified clones for each gene. The second column indicates the interesting clones resulted from the second screen.

To analyze all the sequence data the NCBI Blast platform for sequence homology was used. 48 clones coding for desmin were identified and many others encoding proteins related to cytoskeleton, proteins involved in transport function, mitochondrial, ribosomal and proteasomal proteins. These clones are probably false positive readouts as suggested by previous studies (<http://fccc.edu/research/labs/golemis/Table1.html>, [106]). The

retransformation step necessary to confirm the interactions was skipped because only one interesting candidate from the eight positive clones was further investigated.

The clone that was taken into consideration encodes mouse AF10 (mllt10) protein (Figure 15D). AF10 was previously identified as a frequent fusion partner of MLL and CALM in human acute leukemias [107, 108]. From the screen a partial cDNA was obtained which starts at nucleotide 1677 and codes for the last two thirds of the protein, from amino acid 559 to 1068. This C terminal part is the 3' end of cDNA and carry a poly(A)⁺ tail. The C-terminal part of AF10 was detected in two other two hybrid-screens performed in order to identify functional partners for hDOT1L and SYT [109, 110].

In order to confirm the protein-protein interaction, the full length AF10 clone purchased from Open-bioscience was cloned into pSP64 vector. Radioactively marked *in vitro* translated AF10 protein was tested for binding to the pure recombinant GST-TIPT protein, and pure GST as control (Figure 15C). The result confirmed the interaction indicated by the yeast two-hybrid screen system.

2.3. Co-Immunoprecipitation Assay

To find more binding partners for TIPT that could serve as indications for its function, *in vivo* pull-down assay was performed. Immunoprecipitation was done using HA antibodies from cells either transiently or stable transfected with HA tagged-TIPT plasmid. In Table 3 several candidates which were obtained from mass spectrometry analysis are listed. The output is constituted mainly from nucleolar and centrosomal proteins, which is in agreement with the subcellular localization of TIPT. Nucleolin and nucleophosmin are multifunctional proteins, very abundant in nucleoli, with major role in rRNA processing [111]. Nuclear DNA helicase II is a protein localized in nucleolus, with multiple functions in transcription and RNA transport [112, 113]. Nucleophosmin and Eg5 are proteins with role in centrosomal duplication [114]. All these findings may constitute starting points for TIPT functional analysis.

In conclusion, using several approaches many TIPT interactors were obtained. They can be classified into different categories: transcriptional regulators, chromatin remodellers, nucleolar and centrosomal proteins. Therefore, several experiments were suggested and assays for the identification of TIPT function in cell cycle regulation, transcription and rRNA processing were performed.

<i>Protein name</i>	<i>Number of peptides</i>	<i>Localization</i>
Kinesin-related protein (Eg5/ Kif11)	5	Centrosome
RNA helicase A (Nuclear DNA helicase II)	2	Nucleolus, nucleoplasm
Nucleolin (C23)	3	Nucleolus, cytosol
NPM1 (nucleophosmin 1/ B23)	1	Nucleolus, centrosome
GNB2L1 (G protein beta polypeptide 2 like 1/ RACK1/ receptor of activated kinase 1)	4	Nucleus, nuclear envelope, associated with polysomes, cytoplasm
Similar to heterogenous nuclear ribonucleoprotein U isoform b isoform 5	3	In polysomes

Table 3. Mass-spectrometry results of HA-TIPT co-immunoprecipitations. The first column presents the protein corresponding to peptides found in the immunoprecipitated samples. The second column indicates the number of identified peptides for each protein. The last column refers to the reported cellular localization of these proteins.

3. TIPT and Cell Cycle

The modulation of geminin, TBP and TBPL1 protein levels in cells changed the length of cell cycle phases and affected cell proliferation [60, 115, 116]. From previous approaches TIPT was identified as binding partner of geminin, TBP and TBPL1, therefore its role on the cell cycle regulation was investigated. In order to test this, the protein level was modified, either transiently or stably overexpressing HA-TIPT construct in human osteosarcoma cells.

3.1. Transient Overexpression of HA-TIPT Affects Cell Cycle Phases

The cells were transiently transfected with HA-TIPT overexpression plasmid, or with empty HA vector, as control. Afterwards, the cells were synchronized with aphidicolin (an inhibitor of DNA polymerase alpha which blocks replication arresting the cells at G1/S border) for a period of 18 hours, then released from the block and collected every 2 hours for a period of 12 hours (Figure 16A). The cells were subjected to fluorescent activated cell sorting (FACS) analysis and the results are shown in Table 4. The normal distribution of human osteosarcoma cells was: 36% cells in G1, 46% cells in S phase, and 18% in G2 and M phases. Fugene6 did not affect cell distribution over the cell cycle, but asynchronous cells overexpressing TIPT had a minor increase in S phase cell population (Table 4). All the DNA histograms collected were cumulated and three different graphs for cell distribution in different cell cycle phases were constructed. Control and overexpressing TIPT cells when released from aphidicolin block had a similar content in G1 population during all 12 hours recorded (Figure 16B, left).

However, there were significant differences in S and G2/M population (Figure 16B, middle, respectively right). There are much more cells containing increased amount of TIPT in S phase at 4 and 6 hours of releasing from the block (Table 4). In addition, there are more control cells in G2/M phase at 6 hours from block releasing. The differences are considered significant because the modifications are more than 5% and the results were reproducible. These findings indicate that TIPT overexpressing cells remain longer in S phase in comparison to the control cells.

<i>Method</i>	<i>Overexpression</i>	<i>G1 %</i>	<i>S%</i>	<i>G2/M%</i>
Asynchron	Nontransfected	36.00	46.13	17.87
	Fugene	35.44	47.51	17.05
	HA-CMV	39.16	42.18	18.66
	HA-TIPT	31.41	48.84	19.74
Aphidicolin 0h	HA-CMV	55.30	40.38	4.32
	HA-TIPT	62.75	34.3	2.95
Aphidicolin 2h	HA-CMV	58.40	41.96	0.00
	HA-TIPT	52.98	47.02	0.00
Aphidicolin 4h	HA-CMV	20.41	79.2	0.40
	HA-TIPT	11.56	88.44	0.00
Aphidicolin 6h	HA-CMV	1.96	63.47	34.57
	HA-TIPT	0	98.27	1.73
Aphidicolin 8h	HA-CMV	10.41	37.74	51.85
	HA-TIPT	7.02	35.54	57.04
Aphidicolin 10h	HA-CMV	16.28	29.74	53.98
	HA-TIPT	10.46	27.16	62.38
Aphidicolin 12h	HA-CMV	19.64	24.66	55.70
	HA-TIPT	17.07	24.73	58.19

Table 4. FACS analysis of U2OS transfected cells asynchronized or synchronized with aphidicolin. First column indicates which sort of cells were analyzed: asynchronous cells, or cells synchronized with aphidicolin and released from the G1/S block. The second column indicates what is the reagent/plasmid received by the cells. The following columns indicate what is the cell distribution according to DNA staining.

3.2. Stable Overexpression of HA-TIPT Does not Affect Cell Proliferation

To find out if the cell cycle length was changed, stable cell lines overexpressing HA-TIPT were constructed. Human U2OS cells were transfected with a HA-TIPT plasmid containing a neomycin gene, which conferred resistance in eukaryotic cells. The minimum concentration of Neomycin (G418) to which only the transfected cells are alive, but control cells are dead, was determined experimentally at 500 µg/ml. 17 clones were selected and some of them were analyzed by Western blotting (Figure 16C). Clone 4 was selected because was resistant to

neomycin drug, but does not overexpress HA-TIPT, suggesting that genomic integration was in a silenced locus. Other clones like 1, 2, 7, 8 and 9 presented an additional HA-TIPT protein level which varied in relation to the endogenous TIPT level.

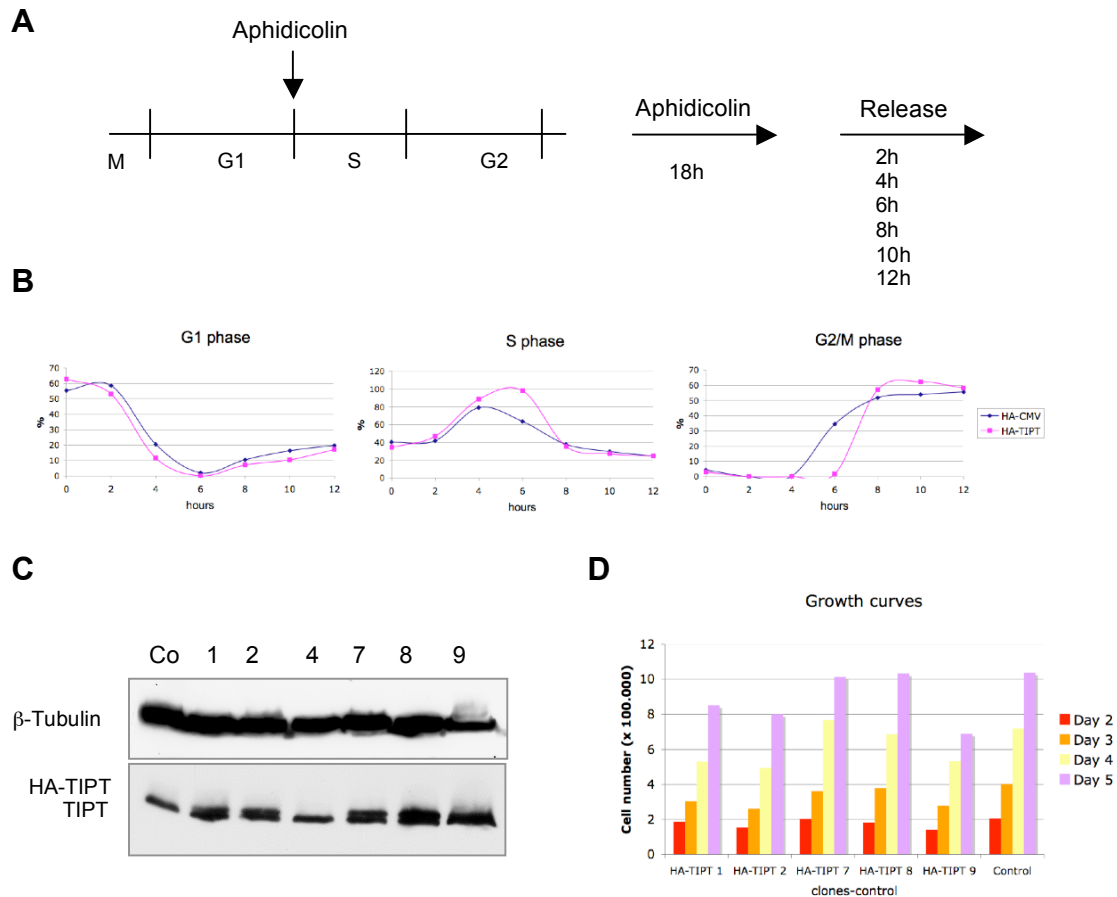


Figure 16. HA-TIPT transient and stable transfection of human U2OS cells. **(A)** Aphidicolin synchronization scheme of transient transfected cells. **(B)** HA-TIPT-expressing cells released from Aphidicolin block for up to 12 hours and FACS analyzed in cell cycle phases distribution every 2 hours in comparison to empty vector transfected cells: G1 phase (left), S phase (middle), G2/M phase (right). **(C)** Different clones of HA-TIPT stable expressing U2OS cells analyzed at protein level by Western blotting. **(D)** Growth curves of different stable clones in comparison to the wild-type cells. 6×10^4 cells were plated at day 0. Viable cells were counted 2, 3, 4, 5 day after seeding. The results indicate one of the three experiments performed. Abbreviations: cell cycle phases: G1, S, G2, M; Co, control wild type cells.

To test if the cell cycle length was affected by a TIPT increased level, different clones were cultured starting from the same number of cells, and grown in identical conditions. The growth curves were performed for a period of five days. The experiment was repeated three times and one is represented in the figure 16D. No significant differences can be observed between the wild-type U2OS cells and the overexpressing TIPT clones.

Together, these data show that overexpressing TIPT cell proliferation is not affected, but the length of the cell cycle phases changes, with longer S phase and shorter G2/M phase.

3.3. TIPT Cannot be Down-Regulated

To explore the real effect of TIPT on cell cycle a knock-down approach was used. Several siRNAs, or short hairpin vectors to silence TIPT mouse or human expression were used. All siRNAs used to down-regulate TIPT produced a silencing effect on mRNA level, with the highest knock-down effect (more than 90%) obtained by the combination of four siRNAs from Dharmacon *SMART*pool (Figure 17A). However, none of them produced a decrease in the TIPT protein level even if the cells were cultured for 5 days or were re-transfected 2-3 times (data not shown). This effect can be explained if TIPT protein has a long protein turnover. In order to find this, U2OS cells were cultured in a medium containing 10 μ g/ml cycloheximide, a reversible inhibitor of protein synthesis. The cells were collected for the indicated time points. TIPT expression was detected after 1 day of protein synthesis block, but disappeared after 2 days. A long exposure time showed that some TIPT protein was left. Tubulin α used as a control was detected even at 48 hours (Figure 17B).

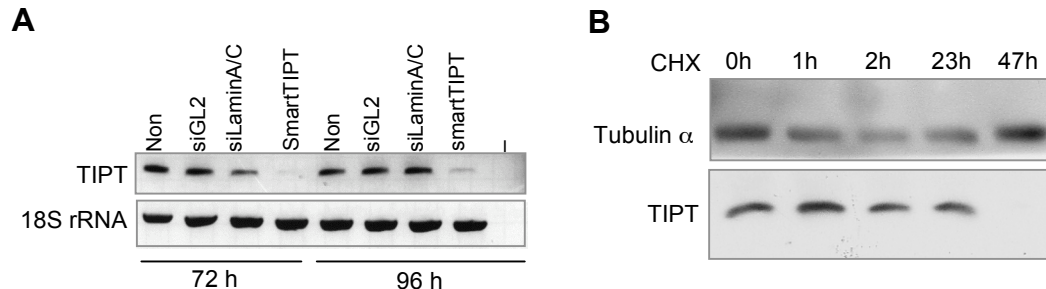


Figure 17. TIPT down-regulation. (A) TIPT silencing with siRNA SMART pool from Dharmacon in U2OS cells. The effect was tested at 72, respectively 96 hours from transfection. As controls were used siGL2 and siLaminA/C, and 18S rRNA was amplified from the same amount of RNA as for TIPT. (B) TIPT protein half-life determination by inhibiting protein synthesis in U2OS cells with 10 μ g/ml cycloheximide. Abbreviations: CHX, cycloheximide; -, negative control, ddH₂O.

These experiments indicate that TIPT protein level cannot be decreased using these methods even if it was found that TIPT has not a long turnover, rather a moderate one. This suggests that TIPT might be an important protein very necessary for the life of the cell, so it can be protected by different posttranslational modifications.

4. TIPT and Pol I

4.1. Evidence for a Role of TIPT in rRNA Synthesis

The nucleolar localization of TIPT and the interactions observed with several nucleolar proteins (nucleolin, nucleophosmin and RNA helicase I) suggested that TIPT might play a role in Pol I dependent transcription or in rRNA processing. First, to reveal the functional significance of TIPT nucleolar localization, the effect of actinomycin D (ActD) on TIPT localization was tested. Actinomycin D is an adenosine analogue that intercalates between G-C base pairs and blocks the progression of RNA polymerase. When used at low concentrations, 0.04 µg/ml, and for a short period of time it blocks specifically the synthesis of rRNA [117]. When used for longer time or at higher concentration, 1 µg/ml, ActD blocks total RNA synthesis. In human osteosarcoma and mouse 3T3 cells treated to inhibit rRNA synthesis, TIPT lost its nucleolar localization almost completely (Figure 18B, E) in comparison to the control cells grew in a medium with DMSO (Figure 18A, D). If in human cells TIPT relocated to cytoplasm, in mouse fibroblasts TIPT was redistributed to the nucleoplasm almost completely and a small amount could still be detected at the nucleolar periphery. A more drastic effect was obtained when total RNA synthesis was impaired (Figure 18C, F). However, in mouse treated cells TIPT was found in nucleoplasm, in dot-like structures. Altogether, these findings indicate a possible role of TIPT in Pol I-dependent transcription.

4.2. TIPT Activates Pol I Transcription

In order to investigate whether TIPT has a role in Pol I-dependent transcription, a collaboration with Dr. Christine Mayer and Prof. Ingrid Grummt from Division of Molecular Biology of the Cell II, German Cancer Research Center from Heidelberg, was started (experiments from section 4.2 and 4.3 were performed by Dr. Christine Mayer). To check if TIPT activates RNA polymerase I transcription, Northern blots for endogenous and reporter transcription were performed. To analyze the effect of TIPT on endogenous transcription, human 293T embryonic kidney cells were transfected with increasing amounts of HA-TIPT plasmid. For Northern blot analysis of human pre-rRNA, pGem3-Hr was used as a template for riboprobe synthesis (Figure 18G). The TIPT overexpression was controlled at the protein

level. The stimulation of pre-rRNA precursor synthesis suggested the possibility that TIPT activates endogenous RNA polymerase I transcription.

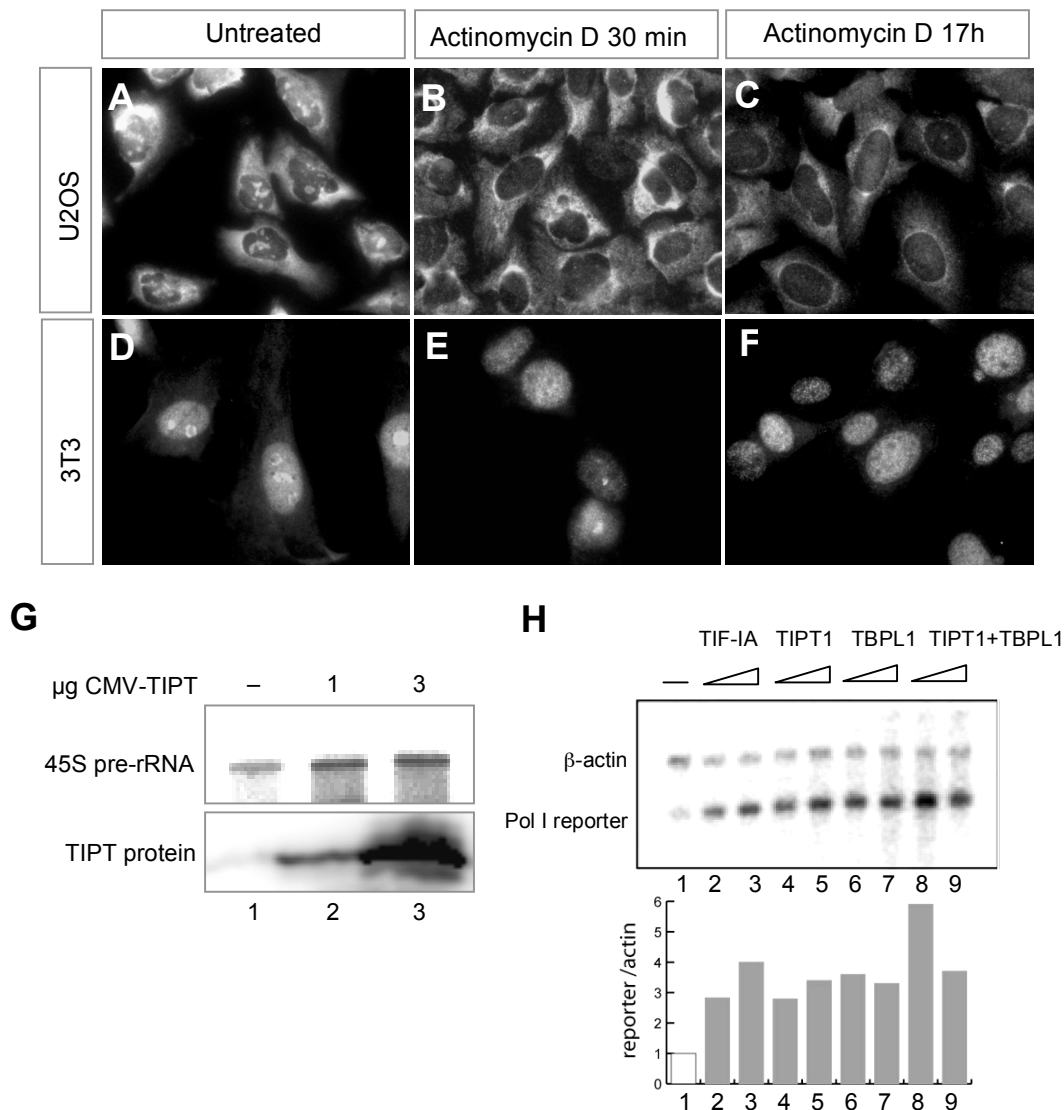


Figure 18. TIPT role in Pol I transcription. (A-F) Actinomycin D effect on TIPT nucleolar localization. (A, D) DMSO does not change the nucleolar localization of TIPT in U2OS, respectively 3T3 cells. (B, E) 0.04 µg/ml ActD for 30 min depletes TIPT from nucleous in U2OS, respectively 3T3 cells. (C, F) Total RNA synthesis inhibition by 0.04 µg/ml ActD for 17 hour prevents nucleolar localization of TIPT. (G) Activation of endogenous RNA polymerase I transcription. Northern blot (2 µg of RNA was loaded on the gel), control Western blot (25 µl of cell lysates were loaded on the 12% gel. Lane1- 293T mock, lane2- 293T cells transfected with 1µg of HA-tagged TIPT, lane3- 293T transfected with 3 µg of HA-tagged TIPT). (H) TIPT influences reporter transcription. 2 µg of RNA was loaded on the 1% gel (reporter transcription, 293T cells transfected with: lane 1– mock transfected, 2- 0,25 µg of TIF-IA, 3- 0,5 µg of TIF-IA, 4- 0,25 µg of HA-tagged TIPT, 5- 0,5 µg of HA-tagged TIPT, 6- 0,25 µg of Flag-tagged TBPL1, 7- 0,5 µg of Flag-tagged TBPL1, 8- 0,25 µg from HA-tagged TIPT and Flag-tagged TBPL1, 9- 0,5 µg from HA-tagged TIPT and Flag-tagged TBPL1). The membrane was blotted with Pol I reporter probe and for the internal control with β-actin probe. Effect of TIF-IA, TIPT and TBPL1 on Pol I transcription was calculated using Aida software in comparison to internal control.

Next, the cells were transfected with reporter for Pol I transcription and gradually increasing amounts of HA-TIPT. For Northern blot analysis detection of reporter transcripts pTβUC

probe was used, and for internal loading control a riboprobe against β -actin. The effect of TIPT on transcription was calculated using Aida software in comparison to internal control. Lower amounts of TIPT produced activation, whereas higher amounts led to a decrease of reporter activity (data not shown). This finding suggested a common phenomenon found in transcription, squelching [118].

In order to interpret the significance of the effect produced by TIPT overexpression on Pol I a comparison with TIF-IA was made. TIF-IA is a component of the Pol I preinitiation complex which phosphorylates Pol I and activates transcription initiation [8]. A similar experiment as the one described above was performed, transfecting the cells with Pol I reporter and expression plasmids for TIF-IA, HA-TIPT, Flag-TBPL1, Flag-TBPL1 plus HA-TIPT (Figure 18H). The reason to introduce TBPL1 as a new player in this experiment is that it is a basic transcription factor interacting with TIPT, localized to the nucleoli, and possibly having a function in Pol I transcription [65]. TIPT and TBPL1 have a similar effect to TIF-IA on Pol I reporter transcription, and the effect is slightly synergic when are co-expressed (Figure 18H).

4.3. TIPT Interacts neither with Pol I and TIF-IA Proteins, nor with rDNA

Promoter and Coding Regions

Since these experiments suggested an activatory role of TIPT on Pol I transcription, to gain more insights, protein-protein and protein-DNA interactions were verified. Because proteins interacting with RNA polymerase I complex very often may be detected with TIF-IA, for co-immunoprecipitation experiments antibodies against Pol I and TIF-IA were used. Nuclear extracts from 293T cells transfected with HA-tagged TIPT and non-transfected cells were used. However, no interaction between TIPT and RNA Polymerase I or with TIF-IA was detected (data not shown). The interaction with SLI complex containing TBP basic transcription factor needs to be further investigated. Chromatin immunoprecipitation (ChIP) experiments were used to check if TIPT interacts directly with rDNA human promoter and human coding region. ChIP analysis was done using 293T cells transfected with HA-TIPT or HA-CSB plasmid as control. TIPT could not be detected on these DNA regions, suggesting that it may be indirectly involved in Pol I transcription. Taken together, these data indicate that the nucleolar TIPT is involved in Pol I-dependent transcriptional activation, but they don't suggest a direct effect.

4.4. TIPT Has no Role in Ribosomal RNA Processing

In several studies it was reported that nucleophosmin and nucleolin have a role in rRNA processing. Since these proteins were found as TIPT binding partners during an immunoprecipitation experiment (see section 2.3), it was interesting to investigate if TIPT has a role in rRNA processing. The interaction of NPM with HA-TIPT was confirmed by co-immunoprecipitation from a stably HA-TIPT expressing U2OS cells (clone 8) (Figure 19A).

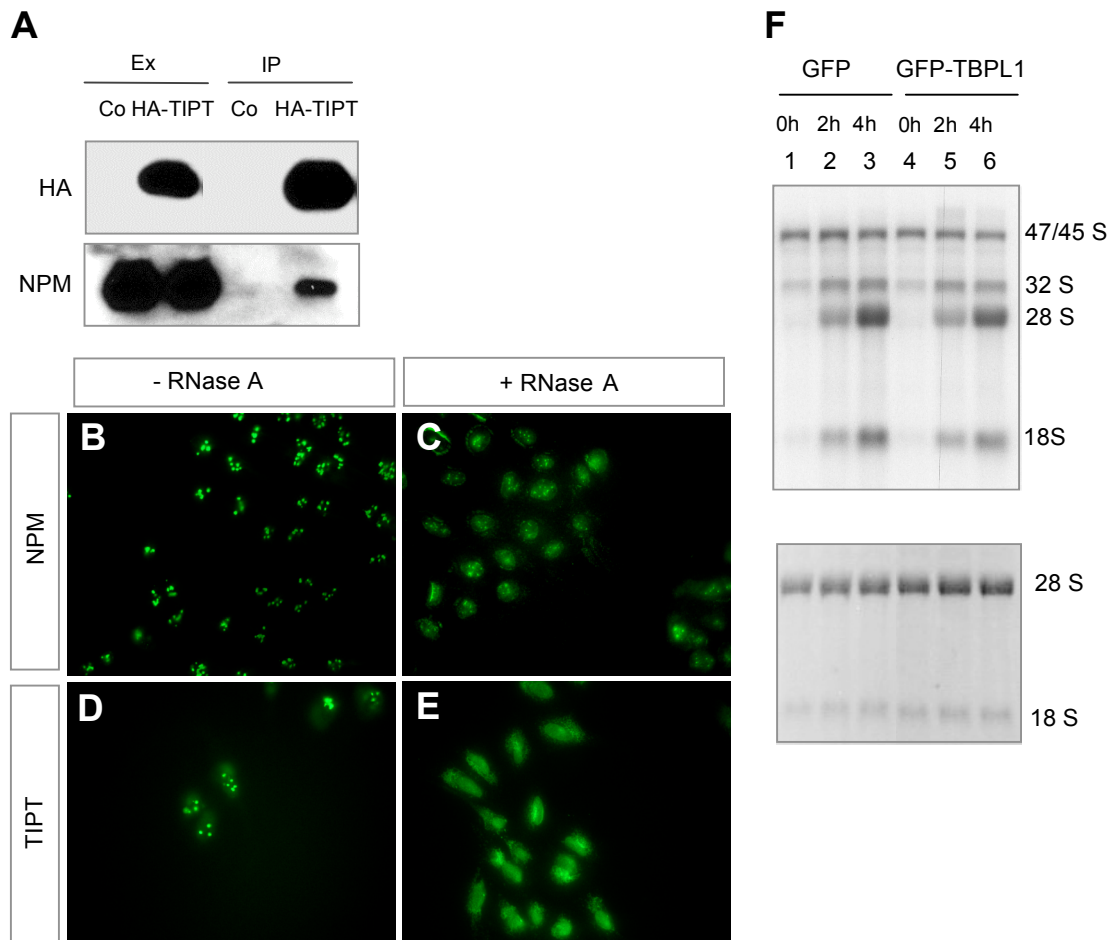


Figure 19. TIPT has no role in rRNA processing. **(A)** HA-TIPT interacts *in vivo* with nucleophosmin in HA-TIPT stable cell line. Immunoprecipitation using HA antibodies was performed from HA-TIPT stable transfected and wild-type U2OS cell extracts. The eluates were transferred by Western blotting and membranes were probed with anti-NPM antibody, and anti-HA antibody. **(B-E)** Both TIPT and NPM require RNA for their nucleolar localization in U2OS cells. **(B, D)** NPM and TIPT localize in nucleoli of U2OS cells permeabilized with saponin. **(C, E)** NPM and TIPT redistribute into the whole nucleoplasm after 1mg/ml RNase A treatment. **(F)** *In vivo* metabolic labeling of cells. U2OS cells were transfected with GFP-TBPL1 or GFP, metabolically labeled for 1.5 hours with [32 P]-orthophosphate, and chased for indicated times. RNA was isolated and loaded on a formaldehyde/agarose gel. The equal loading was verified by staining the gel with ethidium bromide (lower panel). The transfer was performed on a Hybond N+ membrane, and the radioactivity was determined with a Phosphorimager (upper panel). Abbreviations: Co, control wild type cells; Ex, input extracts; IP, co-immunoprecipitation eluates.

Next, it was checked if TIPT nucleolar localization requires RNA. Immunostaining on human U2OS cells treated with 1 mg/ml RNase A revealed that TIPT redistributes in the entire cell (Figure 19E). In addition, TBPL1 followed exactly the same distribution pattern like TIPT (data not shown), and NPM was confined to the entire nucleoplasm (Figure 19C). These results suggest that all three proteins require the presence of certain RNA species for their nucleolar localization.

TIPT is localized to the nucleolus, requires RNA for its nucleolar localization, and interacts with proteins involved in rRNA processing. Therefore, was checked if indeed it has a role on rRNA processing. Because the knocking-down of TIPT protein proved impossible, a dominant-negative like experiment was designed to investigate its role in processing. TBPL1 interacts with TIPT and theoretically, more TIPT would be bound by overexpressed TBPL1 and less TIPT would be available to perform its functions. For this purpose, GFP-TBPL1 and GFP transfected human U2OS cells, were labeled for 1.5 hours with [32 P]-orthophosphate containing medium and were chased for 2 and 4 hours with growth medium. An equal amount of RNA was loaded on formaldehyde/ agarose gel and stained with ethidium bromide to check the loading (Figure 19F lower panel). The gel was blotted and radioactive membrane was exposed to Phosphoimager, followed by interpretation of rRNA band densities obtained after background subtraction in comparison to the control, using the software Quantity One (Table 5). The results indicate that TBPL1 overexpression has no effect on rRNA processing, it rather produced a global decrease of processed rRNAs (~ 30% in comparison to the control) from 45/47S precursor to 18 S and 5 S rRNA (Figure 19F upper panel). This result suggests that TIPT affects rRNA transcription on another level, other than the processing.

<i>rRNA</i>	<i>Chase time</i>	<i>% Decrease</i>
47S	2h	37
	4h	25
32S	2h	11
	4h	38
28S	2h	15
	4h	31
18S	2h	13
	4h	35

Table 5. *In vivo* metabolic labeling of rRNA. The densities of radioactive 47S, 32S, 28S and 18S rRNA bands were calculated after background subtraction, and the decrease in comparison to the control is shown in the last column.

5. TIPT and Pol II

5.1. TBPL1 Protein Model is Similar to TBP's.

TBP and TBPL1 are basic transcription factors, which nucleate the formation of transcription preinitiation complex on different promoters, TATA box-containing, respectively on some of the TATA-less promoters. They belong to the same protein family, but the identity between the C-terminal core domain of murine TBP and TBPL1 protein is only 39%. Because of this, was highly interesting to see if TBPL1 resembles TBP structure. TBPL1 protein structure was modeled by Dr. Reinhard Klement (Max Planck Institute for biophysical chemistry, Göttingen).

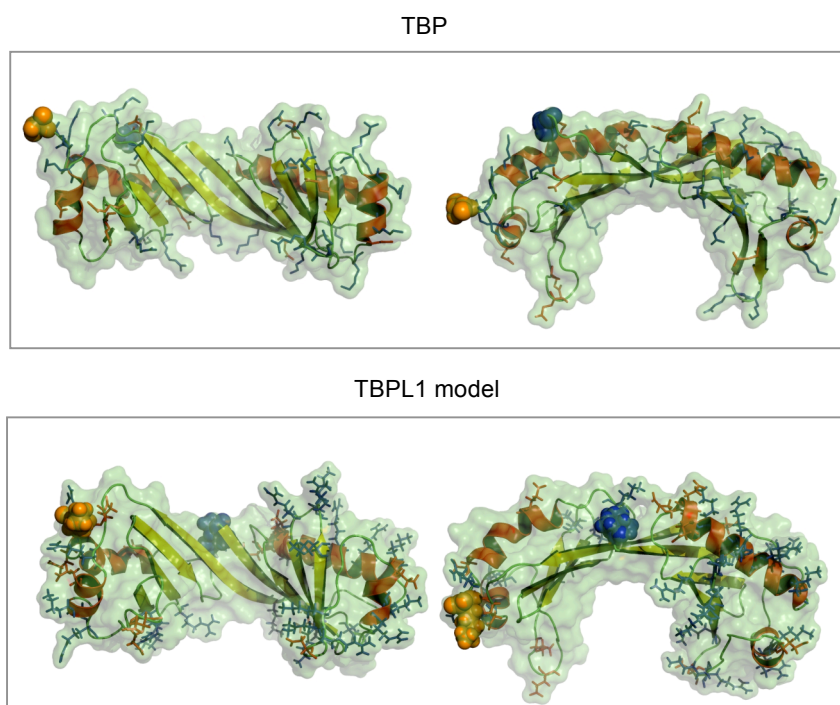


Figure 20. The model of human TBPL1 protein compared to TBP crystal structure. TBP and TBPL1 have a similar saddle-like structure. TBPL1 model was obtained using TBP/TFIIA/DNA crystal structure from PDB database [119]. TBP and TBPL1 are depicted as ribbon drawing and colored in yellow for the β -strands, red for the α -helices, blue for the N-terminus, orange for the C-terminus, and in green the solvent accessible surface.

The TBPL1 primary sequence (amino acids 13-183) was compared to TBP crystal structures from PDB databank using SWISS-Model software (<http://swissmodel.expasy.org>), automated and manually. The best model was obtained using a TBP-TFIIA-DNA crystal structure (1nvp) [119]. The read-out came up surprisingly because of the low similarities between these two proteins. TBPL1 structure preserved the saddle-like shape, which is very similar to TBP's

(Figure 20). The internal pseudo-symmetry specific for TBP was maintained due to the similar disposition of the structural elements (β -sheets strands and α -helices). The DNA-binding C-terminal region of TBP has two identically folded domains, each with five-strand β -sheets, a long and short α -helix [31]. The twisted β -sheet of TBP forms the saddle surface that is the key to DNA binding. For TBPL1 each folded domain contained five β -sheets (from which one was very reduced in size) and shorter α -helices (Figure 20). Moreover, the N- and C-terminus were not close together located like in the case of TBP, the N-terminus being placed in the middle of the TBPL1 structure. Altogether, these findings suggest that TBPL1 may have a similar function to TBP, and indicate that the apparent structural differences may be the reason for a differential affinity to the TATA box DNA sequence.

5.2. TIPT Activates Pol II Transcription from TATA box Promoters

5.2.1. TIPT Binds the Adenovirus Major Late Promoter

TIPT interacts with TBP and TBPL1 basic transcription factors. Therefore, to characterize a possible role of TIPT in Pol II transcription first, it was necessary to investigate if TIPT forms a complex with TBP and DNA. For that purpose, a very well investigated piece of promoter that belongs to the adenovirus major late promoter (-40 to -15) was used as DNA oligonucleotide containing a TATA box. It turned out that TIPT bound strongly to the labeled oligonucleotide (Figure 21A). To check if the binding was specific, this interaction was competed with increasing amounts of competitors like poly(dG-dC) (Figure 21A lanes 2, 3), poly(dI-dC) (lanes 4, 5), Pax6 binding oligonucleotides (lanes 6, 7) and cold adMLP oligonucleotides (lanes 8, 9). The result showed that the TIPT-DNA interaction could be competed only by cold AdMLP oligo, which proves that the binding is specific. It is worth noting that multiple bands were detected in the gel shift assay suggesting that a TIPT multimer interacts with DNA (Figure 21A). In a pull down assay using *in vitro* translated radioactively labeled TIPT and recombinant GST-TIPT was found that TIPT interacts strongly with itself, but not with GST alone used as control (data not shown). Altogether, these data promote the idea that TIPT binds DNA both as monomer and multimer.

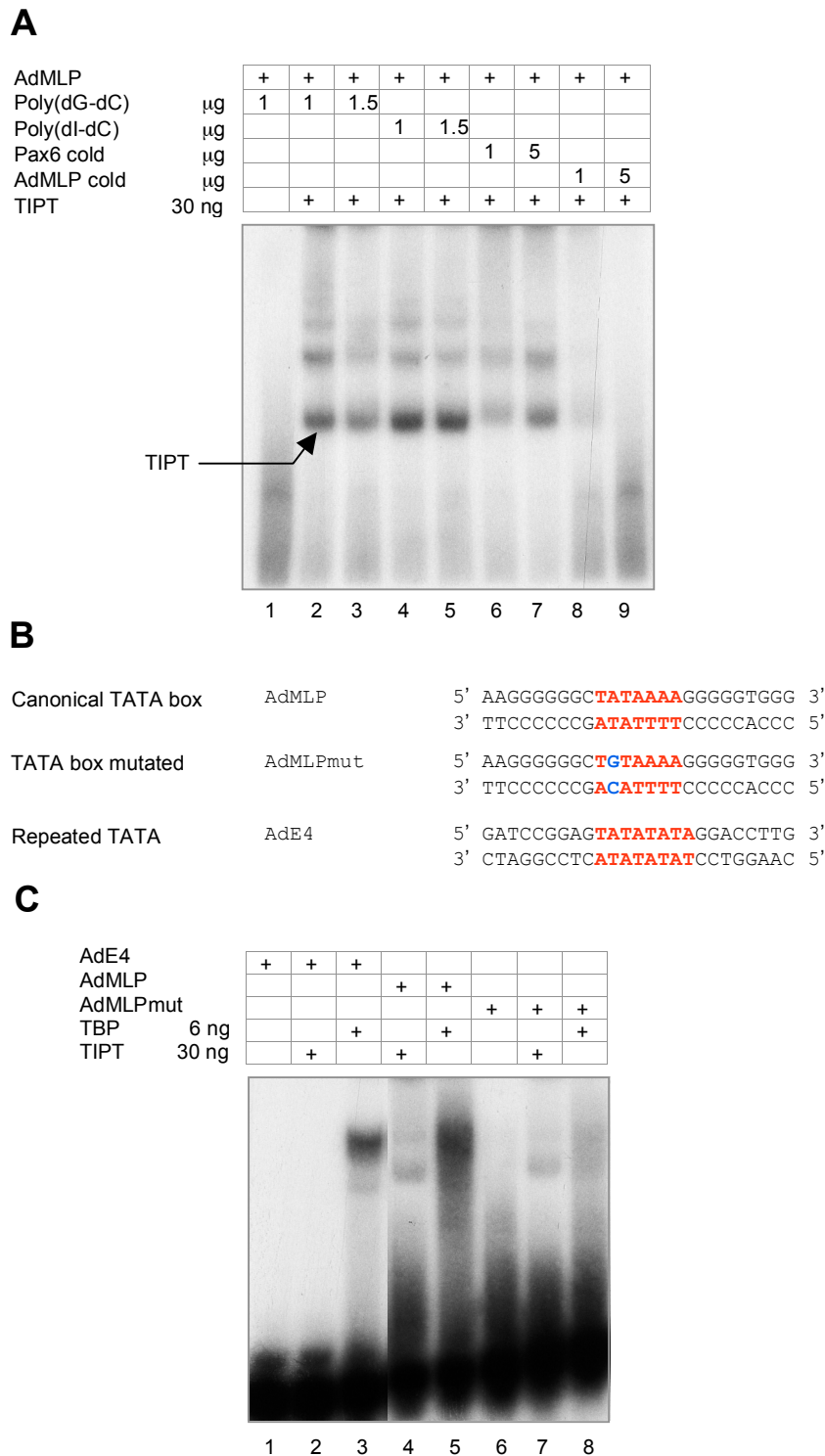


Figure 21. TIPT binds to the adenovirus major late promoter, but not to the adenovirus E4 (AdE4). **(A)** Analysis of TIPT binding to AdMLP. GST-TIPT was assayed for DNA-binding activity using labeled AdMLP oligonucleotide. The specificity of the DNA-binding activity was analyzed by competition with increasing amounts of competitors as indicated. The arrow indicates retarded TIPT-AdMLP DNA complex. **(B)** Alignment of three different double stranded oligonucleotides: AdMLP, AdMLPmut containing mutated TATA box, and DNA oligonucleotide containing the repeated TATA motif from AdE4 promoter. In bold red is depicted the TATA motif, and with bold blue is indicated the mutation performed. **(C)** DNA-binding assay using TBP and TIPT as described for panel A. Human TBP, or GST-TIPT were incubated with radioactively labeled AdMLP, AdMLPmut, and AdE4 oligonucleotides.

5.2.1.1. TIPT Binds the BRE^u Element of the Adenovirus Major Late Promoter

To define the TIPT binding sequence for the AdMLP, the interaction to the TATA element was first investigated. A gel shift assay was performed using either a mutated TATA element (AdMLPmut), or a piece of DNA containing a repeated TATA box from the adenovirus E4 promoter (AdE4) (Figure 21B, [57]). Mutated form of TATA was found in a complex with TIPT (Figure 21C lane 7), but not with human TBP (lane 8). In addition, TIPT does not bind to the AdE4 oligonucleotide (lane 2) to which TBP binds strongly (lane 3), suggesting that TATA box is not the important sequence for TIPT binding, rather the flanking sequences from the AdML promoter outside of TATA.

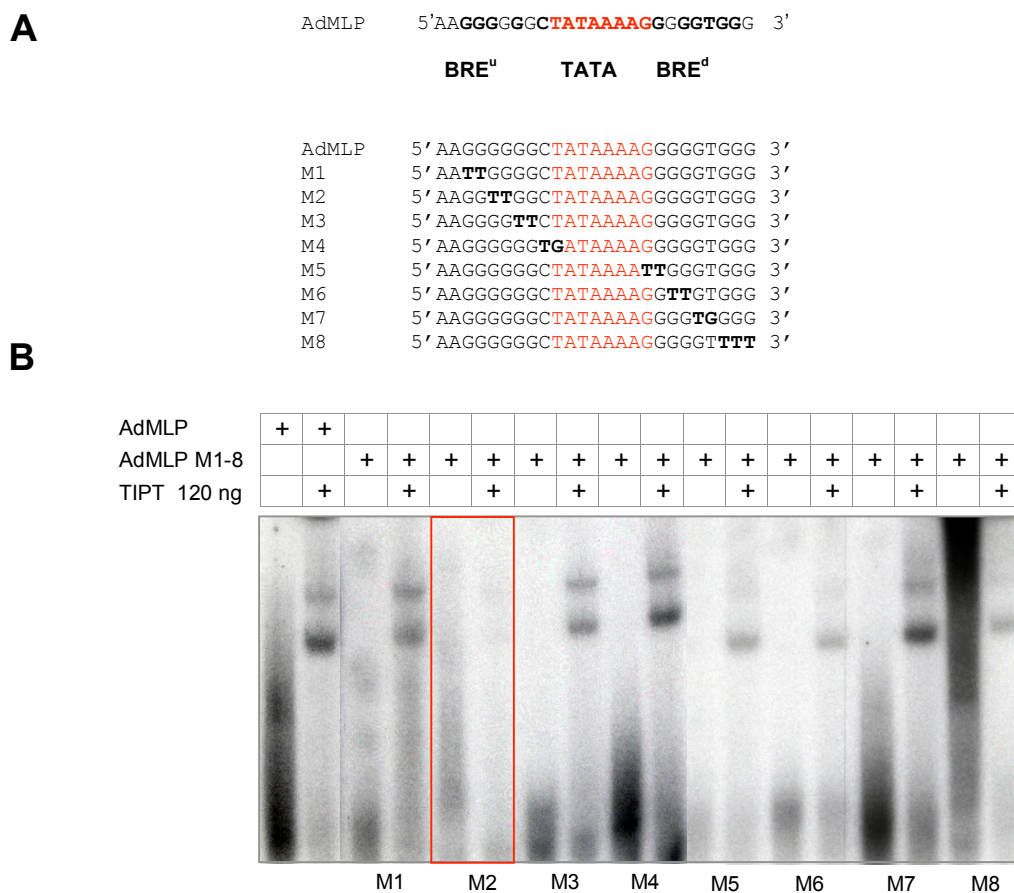


Figure 22. TIPT binds the BRE^u element, but not the TATA motif of AdMLP. (A) BRE^u (nucleotides are in bold black), TATA box (in bold red), and BRE^d elements (6/7 bold nucleotides match) are depicted on AdMLP oligonucleotide. Below, the sequential mutations performed in AdMLP oligonucleotide to find TIPT binding site, as indicated in the figure (in bold black). The mutated oligonucleotides are numbered M1-M8. (B) TIPT binding motif identification to the AdMLP oligonucleotide. GST-TIPT protein was assayed for DNA-binding activity by using labeled DNA fragments representing the wild-type AdMLP and mutated forms as indicated in panel A. In red rectangle is highlighted the impaired binding reaction.

The AdMLP contains an additional DNA binding sequence, the BRE^u element, located immediately upstream of TATA box motif where TFIIB was reported to bind (Figure 22A).

Downstream of the TATA sequence is a region also highly rich in Gs, a “downstream G track”, which contains six/seven match to the consensus BRE^d sequence (5'-G/A-T-T/G/A-T/G-G/T-T/G-T/G-3'), considered to be a secondary binding site for TFIIB, only after TBP binds [38, 40]. To reveal the location of TIPT binding site, sequential mutations in TATA flanking sequences were done (Figure 22A). A gel shift retardation assay was performed using the same amount of DNA and TIPT protein in each binding reaction. The binding was obviously impaired only when substitutions were performed in the middle of the Gs from the BRE^u element (AdMLP M2) (Figure 22B). This indicates that TIPT binds the BRE^u sequence. It cannot be excluded that a shift decrease is also observed for M6, an oligonucleotide with a mutation in BRE^d.

This experiment proves that TIPT is a DNA binding protein, which interacts with the BRE^u element of the adenovirus major late promoter.

5.2.1.2. TIPT, TBP and AdMLP Form a Ternary Complex

The formation of a ternary complex between TIPT, TBP and the AdMLP oligonucleotides was studied by gel shift assay. Indeed, the presence of both proteins revealed a new DNA binding pattern. The shift produced by TBP-DNA (Figure 23A band 1) was missing in TBP-TIPT-DNA reaction. In addition, was observed that the more retarded band of TBP-TIPT-DNA reaction (band 3) was more intense and migrated differently than the one from the TIPT-DNA complex. This observation suggests that the two interacting proteins TIPT and TBP may bind adjacently on the AdMLP, contacting the BRE^u and the TATA box, respectively.

5.2.1.3. TIPT, TBP and Geminin Activate Synergistically the AdML promoter

To follow the significance of the protein-DNA interaction *in vivo* reporter assays were performed using the AdML promoter (-58 to +11) cloned into pGL3 firefly luciferase reporter vector. Human U2OS cells were transfected, and the total amount of DNA was equalized using a CMV-GFP plasmid. All the transfections were performed on the basis of significant endogenous levels of TIPT, TBP and geminin, which cannot be depleted for technical and/or biological reasons. Therefore, a careful transfection titration was performed in order to optimize conditions for a good ratio reporter: expression plasmid. A squelching effect was avoided by using 1: 10 ratio of TBP expression plasmid: reporter construct.

GFP-TBP produced only a small activation of the reporter (Figure 23B). Transfection of HA-tagged TIPT produced a much stronger, dose-dependent activation. Co-expression of GFP-TBP increased this activation (about three fold) suggesting that TIPT and TBP act synergistically to activate TATA-containing AdML promoter.

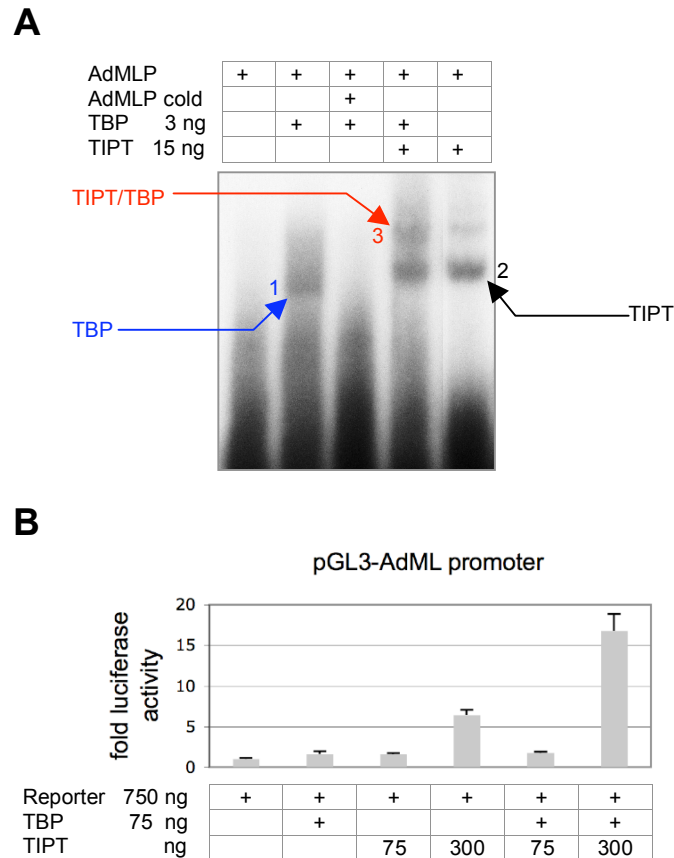


Figure 23. TBP and TIPT bind simultaneously to the AdMLP and activate synergistically the AdML promoter in reporter assay. **(A)** Binding of TIPT to TBP-DNA complex. Human TBP or GST-TIPT was assayed for DNA binding activity by using labeled AdMLP oligonucleotide. The specificity of TBP-DNA complex was analyzed by competition, using double-strand cold oligonucleotides. **(B)** TIPT activates dose dependent alone or synergistic with TBP the AdMLP reporter. A reporter luciferase assay was performed in U2OS cells in 24 well format, using AdML promoter (-58 to +11) fused to firefly luciferase gene. Total DNA transfected in each condition was equalized to 1125 ng by the addition of pEGFP-C3.

Since geminin was found to interact with both TIPT and TBP, it was included into reporter assays. Due to the fact that this time the cells received a higher amount of DNA, and more plasmids were co-transfected, the activation produced by TBP and TIPT was much more reduced (Figure 24A). Co-transfection of TBP and geminin produced almost the same activation of the reporter like TBP and TIPT did. Surprisingly, TIPT and geminin produced a very strong increase in AdMLP luciferase activity. To test if this activation was dependent on the direct interaction between geminin and TIPT, geminin was co-expressed with a GFP

construct of TIPT mutated for geminin binding site (TIPTmut). As expected, the activation was reduced about a half, which demonstrates that the effect produced depends on the direct TIPT-geminin protein interaction *in vivo*.

Next, to find whether geminin has an activator or repressive role on the effect produced by TBP and TIPT on AdMLP, all three expression constructs were co-transfected. The result was an even stronger activation than produced by geminin and TIPT. Also, the co-expression of TIPTmut with geminin and TBP decreased the activation level about one third. In contrast to TBP, TBPL1 does not activate AdMLP. A co-transfection performed replacing GFP-TBP plasmid by GFP-TBPL1 construct revealed that the effect produced by TBP, TIPT and geminin was TBP-specific (Figure 24A).

These results suggest that TIPT synergize with geminin and TBP in order to activate a TATA-containing promoter.

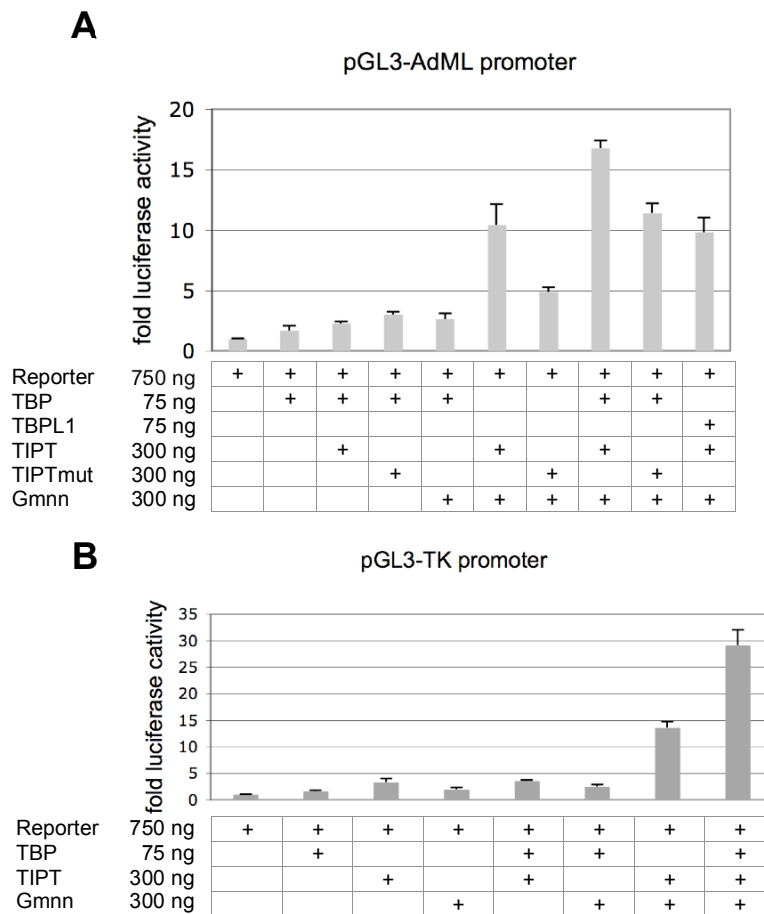


Figure 24. TBP, TIPT and geminin activate synergistically AdML and HSV TK promoter in reporter luciferase assay. **(A)** TIPT, TBP and geminin activate synergistically the AdML promoter. Total DNA transfected /24 well was equalized to 1425 ng by the addition of pEGFP-C3. The fold luciferase activities were calculated as before. **(B)** TIPT, TBP and geminin activate synergistically the TK promoter. TK promoter was fused to firefly luciferase gene.

5.2.2. TIPT, TBP and Geminin Activate Synergistically the Herpes Virus Thymidine Kinase Promoter

To find whether TIPT, TBP and geminin activate another TATA-containing promoter, the herpes virus thymidine kinase luciferase reporter was assayed. The promoter used is a large piece of about 750 nucleotides and contains besides a TATA box-like element, several other DNA binding elements like CCAAT box and CpGs elements. The BRE element cannot be found upstream of the TATA box. Using the same experimental conditions as before, it was found that TIPT together with geminin and TBP activate very strongly and synergistically the TK promoter (Figure 24B). This effect was proven to be TBP-specific, because replacement of TBP by TBPL1 manifested a decrease in the level of activation (data not shown).

5.2.3. Geminin Decreases the Binding of TBP to the Adenovirus E4 Promoter

In order to better define on which type of TATA-containing promoters TIPT acts together with TBP and geminin to produce activation, adenoviral E4 promoter was used as model. TIPT does not form a complex with AdE4 oligo proved in a gel shift assay (Figure 21B, 25 lane 3). To determine whether it forms a complex with TBP and DNA, increasing amounts of TIPT were added on TBP-DNA complex (lanes 5, 6). No ternary complex was observed suggesting that the TATA box is not sufficient to nucleate the formation of a TBP-TIPT-DNA complex. However, geminin decreased significantly the formation of TBP-DNA complex (lane 7). TIPT or anti-geminin antibodies could rescue partially this decrease because geminin was titrated out from the system in a certain proportion (lanes 8, 9, 10).

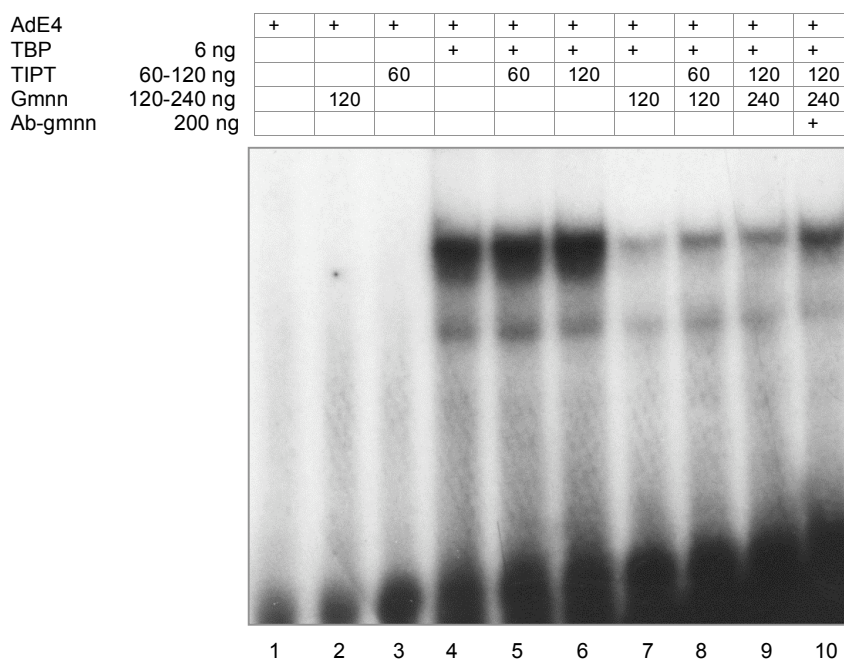


Figure 25. Geminin inhibits TBP-AdE4 promoter complex formation. Human TBP, GST-TIPT, or His-geminin was assayed for DNA-binding activity using labeled DNA fragments containing the AdE4 TATA repeated motif. Increasing amounts of GST-TIPT were incubated with TBP-DNA complex to assess whether a ternary complex was formed. His-geminin was added to TBP-DNA complex. Increasing amounts of GST-TIPT, or anti-geminin antibody were added to the previous reaction as indicated in the figure.

Taken together, these results suggest that geminin represses TBP binding to AdE4 promoter through a direct interaction with TBP, and TIPT can overcome this negative effect.

5.3. TIPT Activates Pol II Transcription from TATA-less Promoter

TBPL1 activates some of the TATA-less promoters and represses transcription from TATA box-containing promoters. TIPT interaction with TBPL1 transcription factor was demonstrated *in vitro* (see section 2.1.3.) and since such an important effect of TIPT on TATA box-containing promoter activation was observed (see section 5.2), prompted the investigation of TIPT effect on the TATA-less promoter activity.

5.3.1. TIPT, TBPL1 and Neurofibromin Promoter DNA Form a Ternary Complex

One of the TATA-less promoters on which TBPL1 was shown to have an activatory effect is the neurofibromin promoter [63]. Recently it was demonstrated *in vitro* and *in vivo* binding of TBPL1 to a piece of 103 bp from NF1 promoter. To delineate more precisely the binding site, it was proven that the interaction between TBPL1 and DNA could be competed by two smaller pieces from this promoter region.

In order to demonstrate that TIPT has a role on TBPL1-dependent transcription, several assays were performed. To find out if TIPT forms a ternary complex together with TBPL1 and DNA, the influence of TIPT on TBPL1-DNA complex mobility was analyzed on a gel shift assay. Because TBPL1 shifts the DNA only in complex with TFIIA, this complex was purified from both cytoplasmic and nuclear extracts of HeLa cell line stable overexpressing Flag-TBPL1 [56]. The sequence to which TBPL1 was shown to bind was further used in the gel shift assays with the remark that was extended 6 bp upstream and downstream (-286 to -250). TBPL1 was complexed significantly with DNA (Figure 26A lane 3). From the analysis of shifted band mobility can be observed that was not too retarded from the free oligo, suggesting that TBPL1 alone (20 kDa size) formed a complex with the NF1 oligo without the involvement of TFIIA complex, which probably helped only for the stabilization of the complex. Unexpectedly, TIPT bound this DNA oligonucleotide producing a double shift (lane

4) like the one obtained with AdMLP oligonucleotide. Increasing amounts of TIPT resulted in a quantitative chase of the TBPL1-DNA complex to one that migrated more slowly, suggesting that TIPT and TBPL1 form a ternary complex with the NF1 promoter (lanes 5, 6). In addition, can be observed that TBPL1 binding mostly abolished TIPT binding to DNA. Geminin does not form a complex together with TBPL1 and DNA, on the contrary it decreases the complex formation (lane 8). This effect is similar to what was observed for TBP-AdE4 complex formation, suggesting that geminin competes with DNA for binding to TBPL1. Next, it was analyzed whether geminin affects TIPT-TBPL1-DNA ternary complex formation. Increasing amounts of geminin produced a decrease of TBPL1-DNA band, on the extent of more NF1 oligonucleotides shifted in complex with TBPL1 and TIPT (lanes 9, 10). Geminin does not supershift TIPT-TBPL1-DNA ternary complex, but increases it probably by stabilizing it, suggesting a possible “hit and run” mechanism for geminin.

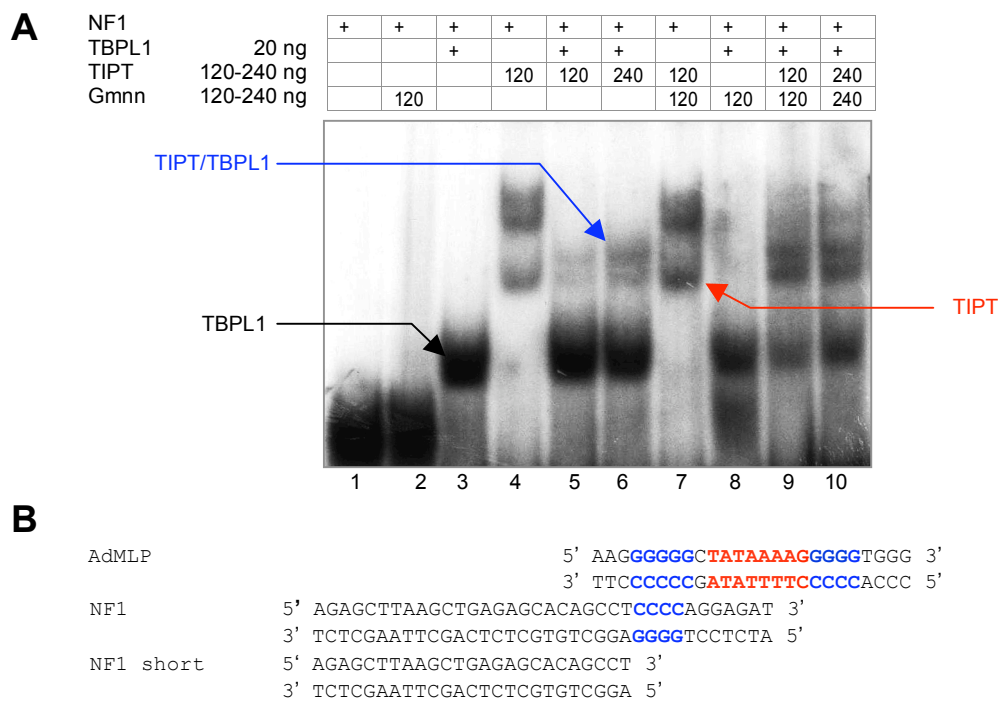


Figure 26. TBPL1 and TIPT form a ternary complex with neurofibromin (NF1) oligonucleotides *in vitro*. **(A)** Binding of TIPT and geminin to TBPL1-DNA complex. Human TBPL1-TFIIA complex or GST-TIPT were assayed for DNA-binding activity using labeled DNA fragments containing the NF1 promoter extending from -286 to -250. Increasing amounts of TIPT were incubated with TBPL1-TFIIA-DNA complex. His-geminin was incubated with TIPT or TBPL1-DNA complexes to check the effect. Increasing amounts of geminin were added to TIPT-TBPL1-DNA complex. **(B)** Alignment of the AdMLP and NF1 oligonucleotides. In red bold is depicted the TATA motif and in blue bold the G/C rich regions. NF1 short oligonucleotide has a deletion of the C-terminal region.

In order to find the reason why TIPT binds to both NF1 and AdMLP oligonucleotides, their sequences were aligned (Figure 26B). The only common similarity was a C/G rich region, which for NF1 represents a stretch of six C/Gs located at its C-terminal part, interrupted by one T/A nucleotide. In order to test if this finding has significance a new NF1 shorter oligonucleotide, containing a deletion of the last C-terminal 11 nucleotides (including the stretch of 4 C/Gs), was labeled and used in a gel shift assay (Figure 26B). Neither TBPL1 nor TIPT was found in a complex with NF1 short oligonucleotide, suggesting that this G/C stretch is important for their binding (data not shown).

In conclusion, these experiments suggest that TIPT DNA binding site may represent a G/C nucleotide stretch.

5.3.2. TIPT, Geminin and TBPL1 Activate Synergistically the NF1 Promoter

To find if TIPT has *in vivo* role on human NF1 promoter, a luciferase reporter assay was done. For this purpose, 350 bp from the NF1 promoter (-334 to +16) was cloned into pGL3 luciferase reporter vector [63, 120]. In order to improve the effect of TBPL1 on NF1, upstream of this piece of promoter were cloned fourfold-reiterated TBPL1 binding site (-280 to -256) (Figure 27A [63]). U2OS cells were transfected, and the total amount of DNA was equalized using a CMV-GFP plasmid.

First, were performed transfections with increasing amounts of TIPT, varying TBPL1:TIPT ratio. This experiment revealed that TBPL1 and TIPT activate synergistically NF1 promoter in a dose-dependent manner, and 1:4 ratio produced the best NF1 activation (37 fold activation) (Figure 27A). Further experiments were performed using TBPL1: TIPT ratio that produced the highest NF1 reporter activation.

Geminin was introduced in this assay in order to prove that has *in vivo* the same role as was observed *in vitro*. The activation produced by TBPL1 and TIPT was much more reduced (to 5 fold), probably due to the fact that cells received a higher amount of DNA than before, and more plasmids were co-transfected (Figure 27B). Very similar to AdMLP reporter assay (Figure 24A) TIPT and geminin produced a very strong increase of NF1 luciferase activity (16 fold) (Figure 27B). Also, it was determined that geminin, TIPT and TBPL1 activate synergistically NF1 promoter, producing 67 fold increase in the luciferase activity. A co-transfection performed replacing GFP-TBPL1 plasmid by GFP-TBP, revealed that NF1 activation was TBPL1-specific (data not shown).

These results suggest that TIPT activates TATA-less NF1 promoter transcription synergizing with TBPL1, and geminin boost this activation due most probably to protein-protein interactions with both TIPT and TBPL1.

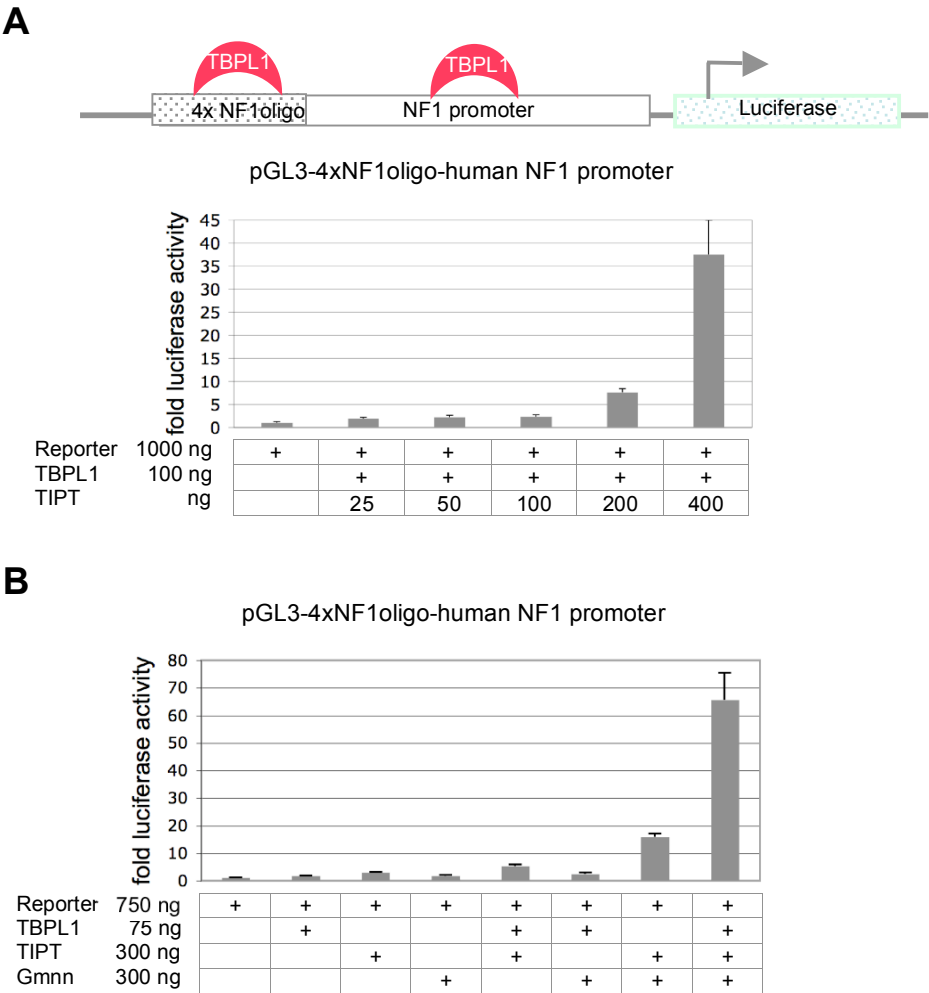


Figure 27. TBPL1, TIPT and geminin activate synergistically human NF1 promoter in reporter luciferase assay. **(A)** TIPT activates synergistically in dose-dependent manner together with TBPL1 the NF1promoter. pGL3-NF1 reporter construct was designed by cloning 4x oligo3 binding site (-280 to -256) upstream of 350 bp human NF1 promoter (-334 to +16) fused to firefly luciferase gene. The reporter luciferase assay was performed in U2OS cells in 24 well plates. Total DNA transfected in each condition was equalized to 1500 ng by the addition of pEGFP-C3. **(B)** TIPT, TBPL1 and geminin activate synergistically the human NF1 promoter. A reporter luciferase assay was performed as indicated in panel A. Total DNA transfected in each condition was equalized to 1425 ng by the addition of pEGFP-C3.

Discussion

1. TIPT Expression

Murine TIPT was identified as geminin binding partner in a yeast two-hybrid screen. Several TIPT homologs were identified in all mammalian genomes sequenced till present, which show a high identity between species, indicating that there are no important evolutionary differences, and the same TIPT isoform may have similar function in different organisms. However, among the same specie even if TIPT isoforms have a high degree of identity, there are significant differences which indicating different functions.

1.1. The Embryonic and Postnatal TIPT Expression

TIPT is widely expressed in embryos and different animal tissues analyzed, which suggests that it may have a general role. In brain day 16.5 mouse embryo TIPT is expressed restrictedly in some proliferative and differentiated areas. The expression of TIPT in proliferative areas of mouse embryonic brain suggests that it may be linked to neurogenesis as known to be the case for other genes also expressed in the cortical VZ and SVZ, such as Pax6 and nestin [121-124]. The fact that TIPT expression is also evident in zones of neuronal maturation indicates possible function for this gene in the neuronal differentiation.

TIPT interacts with TBP, TBPL1 and geminin, all proteins abundant in male germ cells. Many genes are expressed in male germ cells, which encode factors required for DNA replication and transcription initiation of testis specific genes [43, 61, 101, 125-131]. The facts that TIPT is expressed in late spermatocytes and haploid spermatids in a similar temporal window with TBPL1, and activates transcription synergistically with TBPL1 and TBP suggest that TIPT may play a similar role in regulating the differentiation program for spermiogenesis, by activating transcription of round-spermatids downstream targets.

Thus, TIPT is mainly localized in differentiated cells, suggesting that may have a role in activation of genes specifics for differentiated brain and testis cells.

1.2. The Subcellular Expression Domains of TIPT

TIPT interacts with TBPL1 and their expression was confined to nucleoli, a localization unexpected for transcription factors. Neither TIPT nor TBPL1 were detected in one of the

three proteomic screens of the human nucleolus [132-135]. The findings that TIPT interacts with nucleolin, nucleophosmin and RNA helicase A, and that may have a role on rDNA transcriptional activation suggest that TIPT is not only stored in nucleolus, but plays a specific role. However, the nucleolus was reported in several cases to act as a storage place for a number of factors that have no role in rRNA metabolism and exert regulatory functions, such as Hox and Polycomb group proteins and transcription factors like testis specific *Drosophila* TAFs [6, 127, 136].

The TIPT nucleolar and cytoplasmic distribution is regulated by phosphorylation, and CKII is shown to be at least one of the kinases that phosphorylate TIPT. In the nucleolus are found many phosphoproteins, however the unphosphorylated TIPT is confined to the nucleoli and the phosphorylated form to the cytoplasm.

TIPT is localized also in the centrosomes of human and mouse cells, not only in the nucleoli and the cytoplasm, despite the fact that TIPT was not identified in centrosomal proteomic approach [137]. TIPT interacts with nucleophosmin and geminin, both factors involved in centrosomal duplication. During a cell cycle, the centrosome can duplicate only once, and is prevented from re-duplication during late S and G2 phases by an intrinsic block [138]. Studies suggested that NPM may be a positive licensing factor which allows the centrosome duplication, and geminin may act as an anti-licensing factor prohibiting centrosome over-duplication in the same cell cycle [91, 114, 139]. Because geminin is not localized to the centrosomes, it cannot be considered as a centrosome-intrinsic inhibitor [139]. Thus, a geminin interacting protein present in G1 phase in centrosome could be potentially sequestered by geminin in S and G2 and thereby preventing centrosome over-duplication within one cell cycle. TIPT fulfills this criteria being present in G1 phase. However, its centrosome association is not cell cycle dependent, TIPT being present during the entire interphase and also in all the mitotic phases. TIPT could be considered as potential factor necessary for licensing only if one imagines that would be so tightly regulated and geminin would sequester a TIPT form different than TIPT remained in centrosome. TIPT interacts with Eg5, and its association with the mitotic spindle during the entire mitosis raises the possibility that it may have a similar function to Eg5 in spindle assembly and dynamics [140, 141].

2. The TIPT Interactome

In order to extend the characterization of TIPT from a descriptive to a more functional level, one of the goals of this work was to find TIPT interacting proteins. Using different approaches several interactors that fall into various functional classes were identified: chromatin remodeling proteins, transcription factors, nucleolar proteins and centrosomal proteins. These findings suggest that TIPT may be involved in several processes that take place in different subcellular compartments. At least few pertinent questions arise: How is TIPT regulated in order to act in different complexes? Is there a common feature of TIPT in all these processes? Can TIPT represent a link between chromatin remodeling and transcriptional regulation? How do these different functions integrate in the context of embryonic development?

2.1. TIPT Interaction with Geminin

The initial finding from the yeast two-hybrid screen that geminin interacts with TIPT was confirmed through *in vitro* assays. It was found that geminin binds TIPT on a basic region near the C-terminal end (KRKK). Mutations of the first and the second lysine from this region abolished the binding of TIPT to geminin, proving that this is the binding site. In mouse and human isoforms this site is not completely conserved except for the second lysine, suggesting that K/L-R/H-K-K/C/G is the signature of this site. *In vivo* association of geminin and TIPT could not be confirmed by immunoprecipitation from total cellular or embryonic extract, neither using geminin nor tag antibody. Several reasons could be found for this failure. The interaction might take place in relation to the cell-cycle phases. The complex might be formed on the chromatin and the total cell extract preparation excluded this phase. Also, the complex could be present only in centrosomes. Geminin and TIPT have multiple interaction partners suggesting that are engaged in many complexes, which lowers the chance to identify the interaction. Thus, this complex may exist *in vivo* in a small ratio in relation to the entire whole cell extract and the methods used have limited this finding.

2.2. TIPT Interaction with Polycomb Group Proteins

TIPT interacts with Scmh1, and in addition to Ring1B and Mph2. However, Mel18 does not bind to TIPT. Geminin associates transiently with the Polycomb complex, depending on the cell cycle phases [87]. There is no evidence for a cell cycle dependent expression of TIPT.

Geminin interacts directly with Scmh1 on a basic amino acid rich domain lying outside the SAM/SPM domain. TIPT interacts with SAM/SPM domain of Scmh1 indicating that it does not compete with geminin. TIPT does not colocalize with the Polycombs in the nucleus, suggesting that it is not a member of the PRC1 complex. However, in *Drosophila* and in a human nucleolar proteomic approach Polycomb members were identified in the nucleolus [127, 134]. In *Drosophila* differentiating primary spermatocytes two distinct populations of PcG proteins were found: one that stays on chromosomes and the other that goes to the nucleolus together with tTAFs. It was suggested that PcG may repress tTAFs targets, and at the moment when spermatocytes are differentiating these genes must be activated while tTAFs may chase the PcG proteins away to the nucleolus to store them and to prevent aberrant inactivation [127]. Therefore, it is possible that the interaction of TIPT with Polycomb group factors occurs outside the PRC1, maybe in the nucleolus, where could even inhibit the nuclear PRC1 formation.

2.3. TIPT Interaction with AF10

The transcription factor AF10 was detected as a strong TIPT interactor in a yeast two-hybrid screen. The cDNA clone obtained from the screen encodes the C-terminal region of the protein, which contains the leucine-zipper domain of the protein. Two other proteins, SYT and GAS41, bind the same leucine-zipper region of AF10 [110, 142]. Both proteins interact with members of the SWI/SNF complex, and AF10 itself was found to coimmunoprecipitate with Integrator Interactor 1 (INI1), the human homologue of the yeast SNF5 [142, 143]. Recently, it was shown that geminin inhibits SWI/SNF activatory function by removing Brg1, the ATPase of this complex [92]. TIPT interacts with geminin, which inhibits SWI/SNF function, and with AF10, which was suggested to activate transcription by recruiting SWI/SNF complex on the chromatin. Thus, would be interesting to find out whether TIPT has a more direct relation to the SWI/SNF complex.

2.4. TIPT Interaction with TBP and TBPL1

Polycomb group proteins were found on core promoter regions where they interact directly with components of the transcription machinery to repress their activity. PcG proteins interact with TAF proteins of the TFIID complex [83]. General transcription factors TFIIB, TFIIF, and TBP are present on PcG-repressed genes in cultured cells [84]. Thus, the simultaneous

presence and physical interaction of PcG and general transcription factors on the same promoters was unexpected and led to the hypothesis that PcG proteins maintain silencing by inhibiting GTF-mediated activation of transcription interfering with the formation of the preinitiation complex [84, 144]. Moreover, their co-existence seemed necessary in order to allow a relatively fast re-activation of PcG target genes.

TIPT interacts directly *in vitro* with the basic transcription factors TBP and TBPL1 and activates synergistically TATA-containing or TATA-less promoters. Thus, TIPT interacts with both Polycomb group complex and basic transcription factors, meaning with both repressing and activating factors.

Why TIPT contacts both TBP and TBPL1? Although the similarity between the primary structures is low and the secondary structures predict that the core domain is the conserved domain, with an intramolecular identity of the N-and C-terminal repeats lower for TBPL1 than for TBP, the tertiary structures are very similar, indicating a saddle-like structure. Therefore, maybe the binding site for TIPT is conserved between TBP and TBPL1. It is highly probable that TIPT interacts also with TRF3 because of its high identity with the core domain of TBP. Thus, TIPT may activate gene transcription from all three mammalian TBP family factors.

3. TIPT and Cell Cycle

Transient overexpression of TIPT in human U2OS cells elongates S phase and shortens G2/M phase during one cell cycle. However, proliferation in general is not affected by TIPT, as judged in stably overexpressing cells. The elongation of S phase suggests that an S phase checkpoint may become activated, blocking the entry into G2/M phase. It is known that a block of DNA synthesis, the re-replication, or the DNA damage can activate S phase checkpoints. Even if these mechanisms are separated, they act through a common pathway and activate ataxia telangectasia mutated (ATM) and ATM and Rad3 related (ATR) protein kinases. Chk1 and Chk2 protein kinases act downstream from and are substrates of the ATM/ATR kinases [145]. Therefore, the effect of TIPT on these pathways needs to be investigated in the future. Modulation of TBP, TBPL1, or geminin affects the length of cell cycle phases and cell proliferation [60, 65, 115, 116]. Therefore, lengthening of S phase by TIPT overexpression may have one of the following interpretations: TIPT interaction with

geminin may induce DNA re-replication and activation of intra-S phase checkpoint; TIPT activates TBP or TBPL1-dependent transcription of S phase checkpoint genes.

TIPT protein has not a long turnover, however TIPT protein level could not be reduced by RNA interference, despite the strong silencing effect produced at the RNA level. The real impact of TIPT on cell cycle, which could be informative from its down-regulation, is missing. Therefore, overexpression data are not sufficient to indicate a direct role of TIPT on cell cycle regulation.

4. TIPT and Pol I Transcription

Pol I-dependent transcription of *ribosomal DNA* genes results in the synthesis of rRNA, which takes place in nucleoli. TIPT co-localizes with TBPL1 in the nucleoli during the entire interphase. A role for TIPT in Pol I-dependent transcription was suggested by its release from the nucleoli when rRNA synthesis was inhibited with actinomycin D. A similar redistribution pattern was observed for TBPL1 [65]. However, some components of the rRNA transcription machinery are localized to the nucleolar periphery at the inactive rDNA sites when rRNA synthesis is inhibited [146-148]. The assembly of the preinitiation complex at the rDNA promoter does not represent a major mechanism for regulating rRNA synthesis [147]. Therefore, TIPT may play a role in regulating rRNA synthesis despite the fact that does not localize with the preinitiation complex when rRNA synthesis is blocked.

The need of rRNA synthesis and of RNA presence for TIPT nucleolar localization correlates well with the fact that TIPT activates significantly endogenous and reporter Pol I transcription at a similar level obtained with TIF-IA. However, the biochemical mechanism behind these effects could not be explained yet. TIPT does not associate *in vivo* neither with Pol I preinitiation complex, nor with ribosomal DNA promoter or coding region. Several reasons could be found for these failures. TIPT association with transcription machinery was investigated for Pol I and TIF-IA, but not for SLI/TIF-IB complex, to which is a high chance to interact because of TBP interaction with TIPT *in vitro* and *in vivo*. TIPT may be situated too far away from DNA and as a result it may be not cross-linked in a ChIP assay. Another explanation may be that the majority of TIPT amount involved in a complex with DNA is too low and cannot be detected during this assay. No role in rRNA processing was detected for TIPT, despite its interaction with nucleolin, nucleophosmin, and RNA helicase A, proteins with role in rRNA processing [149-151].

Further experiments will be necessary to clarify whether the TIPT effects on Pol I transcription are direct or secondary responses to the cell cycle alteration.

5. TIPT and Pol II Transcription

TBP and TBPL1 are basic transcription factors involved in Pol II transcriptional regulation from different core promoters. In this work it is shown that both TIPT and geminin interact directly with the above-mentioned basic transcription factors. Several experiments addressing the possible role of TIPT in Pol II transcription in relation with TBP and TBPL1 were carried out. Three major questions were asked. First, does TIPT form a complex with TBP or TBPL1 and DNA *in vitro*? Second, do they activate together TATA or TATA-less transient promoters? Third, does geminin have an effect on transcription, due to its interaction with TIPT, TBP and TBPL1?

5.1. TIPT and Geminin Effect on TATA-containing Promoters

The adenovirus major late promoter containing a TATA box is a widely applied model in the study of Pol II promoters [152]. TIPT binds specifically to this promoter *in vitro*. TIPT probably interacts not only as a monomer with DNA, but also as multimer, as judged from the bands with different mobilities shifted on a gel retardation assay. This makes sense after having observed that TIPT can interact *in vitro* with itself. Mutational analysis revealed that TIPT does not bind to TATA motif. The abundant GC base pairing which flank the TATA box of the adenovirus major late promoter was postulated to delimit the TATA element as a trap for transcription machinery assembly [153]. Actually, recently it was reported that this track of Gs located upstream is a BRE^u element, where TFIIB binds independent of TBP binding, and the G region downstream to TATA sequence resembles approximately to consensus BRE^d sequence considered a secondary TFIIB binding site, after TBP binds [38, 40]. The effects of nucleotides substitutions in the sequences of AdML promoter flanking the TATA box were investigated. In this study it was found that mutations of the upstream BRE element influence the dissociation of TIPT from the AdMLP. In addition, the BRE^d element appeared as a weak secondary binding site for TIPT. Therefore, the AdMLP sequence must be taken as an ensemble, in which the G/C rich flanking sequences of the AdMLP TATA box create a shape of double-stranded DNA recognized by TIPT.

The experiments performed revealed that TIPT, TBP, and DNA form a ternary complex *in vitro*. Probably, a heterodimer constituted between TIPT and TBP contacts the DNA. The following model arises: TIPT binds the TATA box adjacent sequences probably on both sides, bending the DNA in the same way as TFIIB does, and in addition contacts TBP which binds the TATA DNA sequence of the AdMLP. Wolner and Gralla showed that sequences flanking the core TATA box influence the basal level of transcription as well as the response to activators [15]. The synergistic transcriptional activation of the AdMLP by TIPT and TBP is a novel example for this previous finding. The fact that geminin can act on top of this must occur through protein-protein interactions. However, TIPT and geminin are enough to activate strongly AdMLP promoter. Thus, the following model derives from the experiment of the present study (Figure 28A). TIPT and TBP contact each other and the DNA, and interact with geminin constituting a complex which activates TATA-containing promoter genes.

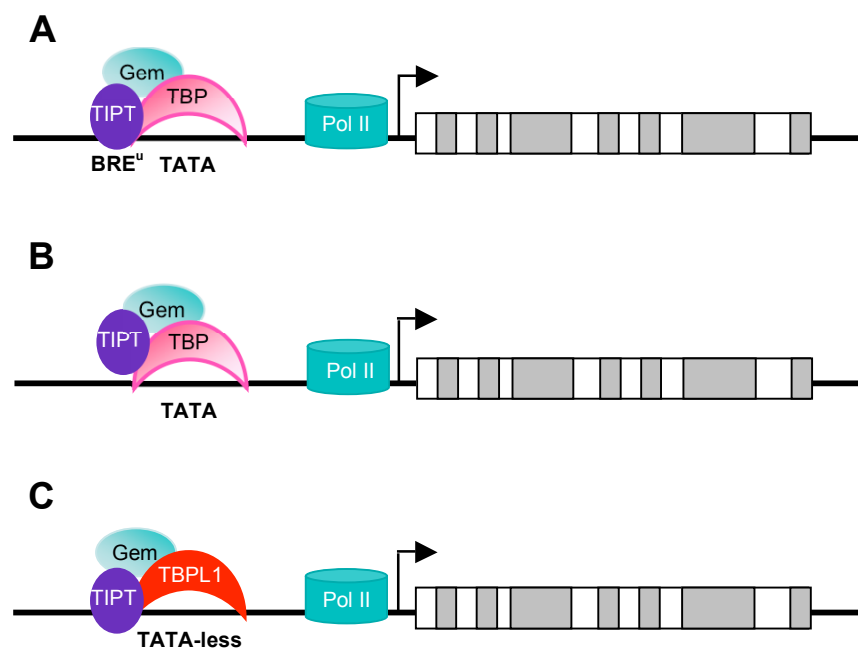


Figure 28. Model for effect of TIPT and geminin on TBP/TBPL1 Pol II driven transcription. (A) TIPT, geminin, and TBP activate synergistically the AdML promoter transcription. Geminin interacts with both TBP and TIPT, the later contacting the DNA on BRE^u element of AdML promoter. (B) TIPT, geminin and TBP activate synergistically HSVTK promoter. The binding of TIPT to DNA seems not to be required. (C) TIPT, geminin and TBPL1 activate synergistically the TATA-less NF1 promoter. Geminin contacts TBPL1 and TIPT, both contacting the NF1 promoter.

Unexpectedly, the same synergistic effect was obtained on the TATA box-containing herpes virus thymidine kinase reporter, even if no BRE^u element was found adjacent to TATA box. It means that TIPT-DNA interaction most probably is not necessary, and the strong stimulation

produced by co-expression of TIPT and geminin is realized through another mechanism, unidentified yet (Figure 28B).

The adenovirus E4 promoter, opposite to MLP, is a weak basal TATA box promoter, but is highly responsive to activators [15]. However, TIPT has no effect on TBP binding to the AdE4 promoter specific TATA sequence. Geminin does not bind directly to DNA, but represses the binding of TBP to AdE4 TATA box, probably due to its strong interaction to TBP. This effect is reversed partially by TIPT or anti-geminin antibodies. Geminin may repress TBP-TATA box binding in a similar way to other TBP inhibitors. NC2 binds TBP thus preventing TFIIB association and therefore preinitiation complex formation [154]. Mot1 binds TBP and releases it from DNA in an ATP-dependent manner [155]. TAF_{II}230 competes with TFIIA binding for TBP, as well inhibits TBP binding to DNA [156]. The structure of TAF_{II}230 resembles the distorted TBP-bound DNA, which binds directly to the DNA binding surface of TBP in a competitive manner [157].

5.2. TIPT and Geminin Effect on TATA-less Promoter

Ohbayashi et al. showed the alignment scores between TBPL1 and TBP for four domains in the DNA-binding region were quite low [54]. Another study suggested that both the N- and C-terminal repeats of TBPL1 contact DNA in a different way from TBP, suggesting that TBPL1 may not recognize the conserved TATA box [50]. Therefore, TBPL1 is not expected to bind the TATA box sequence. Mammalian TBPL1 does not stimulate transcription *in vitro* for TATA box-containing E4, AdML and Hsp70 promoters [53, 54, 56]. TBPL1 seems to repress TBP-dependent transcription by sequestering TFIIA factors [56, 57, 63]. Recently, it was shown that TBPL1-TFIIA complex binds *in vitro* to the neurofibromin promoter and TBPL1 could be found *in vivo* on the promoter [63]. The results from the present study revealed that TIPT binds the NF1 sequence as monomer, and probably also as dimer. The deletion of 12 bp containing a C/G tetramer abolished the independent binding of both TIPT and TBPL1 to DNA, which suggests that similar to AdML promoter, NF1 promoter is bound by TIPT on a G/C rich DNA region.

In vitro, TIPT, TBPL1 and NF1 promoter form a ternary complex. Geminin seems to enhance the rate of stable TIPT-TBPL1-DNA ternary complex formation, without affecting the mobility of the shift, suggesting a possible “hit and run” mechanism, previously shown in different contexts [158-160]. The synergistic transcriptional activation of the NF1 promoter

by TBPL1 and TIPT is similar to what was observed for the TATA box-containing promoters of major late and thymidine kinase viruses. Geminin enhances this effect strongly, most probably through protein-protein interactions. However, TIPT and geminin are enough to activate significantly the TATA-less NF1 promoter. From the present study the following model was derived for TATA-less promoters (Figure 28C). The model suggests that TBPL1 binds TIPT, both contacting DNA and geminin, together forming a complex, which activates TATA-less promoter genes.

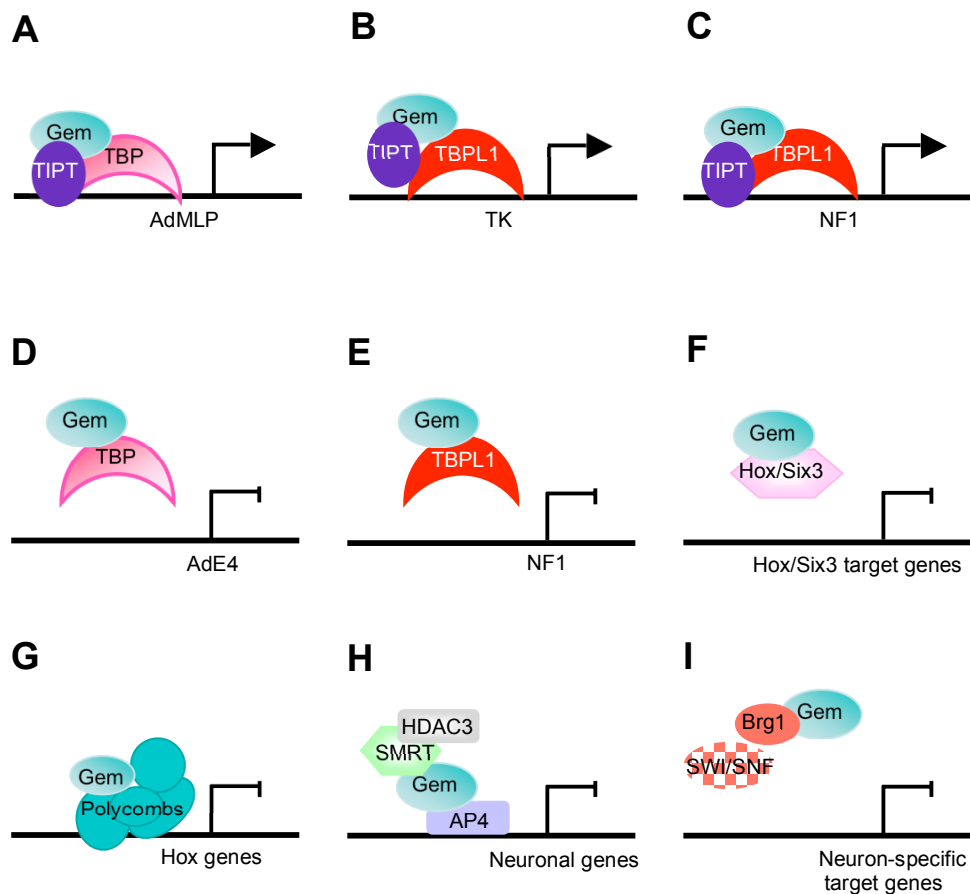


Figure 29. Transcriptional roles of geminin. (A) Geminin activates AdML promoter by interaction with TIPT and TBP (gene reporter assay). (B) Geminin activates HSV TK promoter by interaction with TIPT and TBP (gene reporter assay). (C) Geminin activates NF1 promoter by interaction with TIPT and TBPL1 (gene reporter assay). (D) Geminin represses TBP-AdE4 complex formation (gel shift assay). (E) Geminin represses TBPL1-NF1 complex formation (gel shift assay). (F) Geminin binds Hox/Six3 proteins repressing their target gene activation [87, 88]. (G) Geminin represses Hox genes activation by interaction with Polycomb group complex [87]. (H) Geminin represses neuronal genes activation in non-neuronal cells by interaction with AP4 repressor, SMRT and HDAC3 [94]. (I) Geminin sequesters Brg1 from SWI/SNF complex and inhibits neuronal genes activation [92].

Geminin seems to be involved in different transcription related complexes. From this study

came up several examples demonstrating an activatory role. From gene reporter assays was observed that geminin is a co-activator and modulates transcription from TATA box-containing and TATA-less promoters together with TIPT and TBP, respectively TBPL1 (Figure 29A-C). There are multiple evidences for a repressive role of geminin. In this study geminin represses *in vitro* the formation of TBP-AdE4 complex and TBPL1-NF1 complex (Figure 29D, E). The fact that geminin binds transcription factors preventing their activities is not new. Geminin binds Hox and Six3 proteins and impaires activation of their target genes (Figure 29F, [87, 88]). In addition, geminin represses gene transcription by associating with negative chromatin remodeling factors or blocking the recruitment of positive chromatin remodelers to target genes. Thus, geminin prevents transcription of *Hox* genes by directly binding to Polycomb group complex (Figure 29G, [87]). Geminin associates with AP4 transcriptional repressor to restrict neuron-specific target gene expression in non-neuronal cells by recruiting SMRT and histone deacetylase 3 (HDAC3) at the transcriptional level (Figure 29H, [94]). Geminin represses transcription of neuron-specific target genes by interacting with and sequestering Brg1, the catalytic subunit of SWI/SNF complex (Figure 29I, [92]).

Thus, geminin function as transcriptional activator is new and unexpected, adding to its function as repressor. This finding suggests that geminin is involved in many protein complexes with different functions, cell-type- or gene-specifics. Studies describe another chromatin remodeller, the SWI/SNF complex acting both as activator or repressor, depending on the gene [161, 162].

5.3. TIPT May be a Common Factor for TBP- and TBPL1-Dependent Transcriptional Activation

TBPL1 activates transcription from NF1 promoter and represses transcription from TATA box-containing c-fos promoter by competing with TBP for TFIIA factors [63]. This inhibition is rescued by TFIIA. TBP represses NF1 transcription however, addition of excess TFIIA could not overcome this effect, suggesting that TBP and TBPL1 compete also for another unknown activatory factor. TIPT binds TBP and TBPL1 transcription factors, contacts TATA box and NF1 TATA-less promoters, and activates transcription from both promoter types. Therefore, TIPT may play the role of this activator transcription factor, which is common for both TATA box-containing and TATA-less promoters (Figure 30).

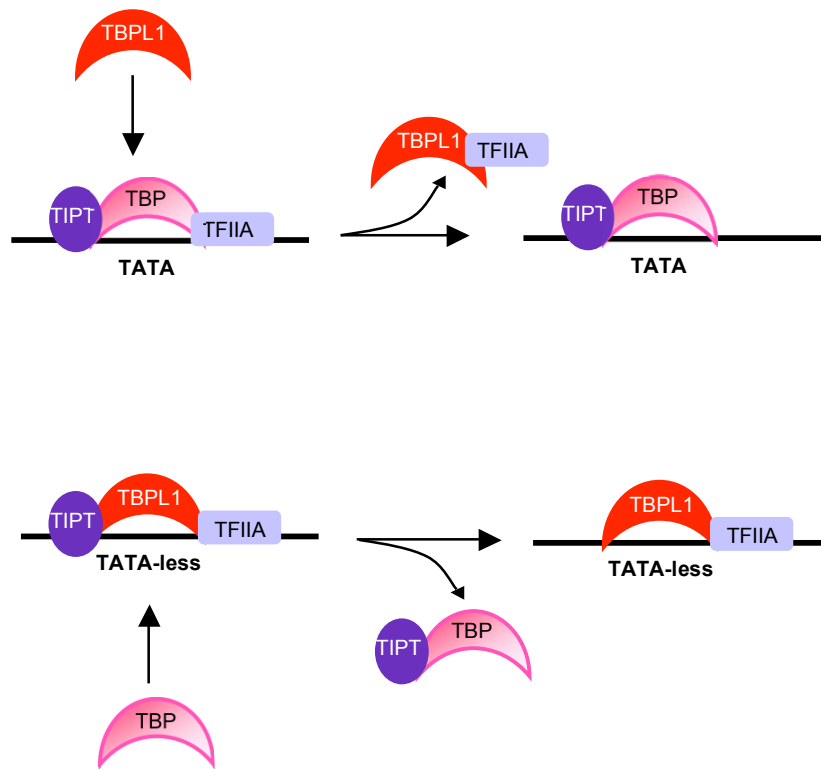


Figure 30. Model for TIPT-TBP/TBPL1 interaction on DNA. TBP and TBPL1 bind to the TATA (AdML) respectively TATA-less (NF1) promoters. TIPT binds DNA and contacts both TBP and TBPL1. In the model, TBPL1 competes with TBP for TFIIA, thus inhibiting TBP-responsive promoters [56, 57, 63]. TBP competes with TBPL1 for an undetermined general transcription factor/co-activator/activator to inhibit TBPL1-responsive promoters [63]. This factor can well be TIPT (adapted from Chong et al., 2005).

6. Conclusion

In this work a previously unidentified protein, named TIPT, which was found to interact with geminin in a two hybrid-screen, was characterized. TIPT is ubiquitous and highly expressed in embryonic and postnatal tissues, as well as in normal and cancer cell culture lines. It is enriched at the subcellular level in the nucleus, the cytoplasm and the centrosomes. Except for geminin, TIPT interaction with other chromatin-associated factors (Polycomb group complex and AF10), and with the basic transcription machinery (TBP and TBPL1) was observed. TIPT activated endogenous and reporter Pol I transcription. *In vitro*, TIPT was bound to the G/C rich DNA promoter regions and it formed complexes with TBPL1 or TBP, and DNA. It activated reporter Pol II-dependent transcription from both TATA-less and TATA box-containing promoters, and the binding to DNA seemed not to be necessary.

Geminin enhanced significantly this effect, most probably due to its direct interaction with TIPT, TBP and TBPL1. However, a geminin repressive role was also observed, inhibiting TBP or TBPL1 binding to DNA.

Materials and Methods

1. Isolation of Nucleic Acids

1.1. Plasmid DNA Isolation from *E. coli*

The plasmid DNA from *E.coli* was extracted using the QIAprep spin miniprep or maxiprep kits (Qiagen), according to the instructions of the manufacturer. Then, the plasmid DNA concentration was measured using a BioPhotometer (Eppendorf).

For cell transfection the maxiprep DNA was further extracted with 1 volume of phenol/chloroform/isoamylalcohol (PCIA) (25:24:1), followed by 13,500 rpm centrifugation using Centrifuge C5417 (Eppendorf) for 2 minutes. The supernatant was carefully collected and subjected to 1 volume of chloroform extraction once, followed again by centrifugation and supernatant collection. Then, the DNA was precipitated with 0.7 volume of isopropanol, 0.1 volumes of 3 M sodium acetate (NaAc), pH 5.2 and 1 µl 10 mg/ml glycogen at -20 °C for 15 minutes. Afterwards, the DNA was pelleted by centrifugation at 13,500 rpm for 15 minutes, washed with 300 µl 70% ethanol, centrifuged at 13,500 rpm for another 5 minutes, air dried, and dissolved in a proper volume of Millipore H₂O.

1.2. Genomic DNA Extraction from Mammalian Cells

The mammalian cells cultured in 24 wells were washed with PBS twice. Then, on the cells was applied 1 ml of lysis buffer (100 mM Tris, pH 8.0, 200 mM NaCl, 5 mM EDTA, 0.2% SDS) containing freshly added 10 µl of 100 µg/ml Proteinase K, and incubated in the 37 °C room for at least 8 hours. The lysis product was spun down at 13,000 rpm for 5 minutes and the supernatant was precipitated with 750 µl of isopropanol. The mixture was spun down again at 13,000 rpm for 15 minutes and the supernatant was discarded. The precipitated pellet was washed with 750 µl 70% ethanol, air dried, dissolved in 50 µl TE buffer, and incubated in a shaker at 55 °C for 30 minutes to allow the time to redissolve the DNA.

1.3. DNA Electrophoresis and Purification from Agarose Gel

0.5-2% agarose gel was prepared by melting agarose (Invitrogen) in 1×TBE Buffer (90 mM Tris-borate, 2 mM EDTA, pH 8.0) and subsequently adding ethidium bromide to a final concentration of 0.3 µg/ml. DNA sample was mixed with 5×DNA Loading Buffer (25%

Ficoll, 100 mM EDTA, 0.05% Bromophenol Blue), and electrophoresis was performed under 1-7 V/cm in 1×TBE buffer. For fragment purification, the band cut down was transferred into a small dialyse membrane pocket with 500 µl 0.5×TBE buffer. Then, the gel in the sealed pocket underwent electro-elution in 0.5×TBE buffer under 7.5 V/cm for 20 minutes, followed by 20 seconds with opposite polarity of electricity. After that, the eluted DNA solution from the pocket was collected and 500 µl 0.5×TBE buffer were used to wash the pocket and merged with 500 µl elution. This 1 ml solution was extracted by PCIA (25:24:1) once, precipitated with isopropanol plus 3 M NaAc and 1 µl 10 mg/ml glycogen for 20 minutes at -20 °C, followed by spinning at maximum speed in a microcentrifuge for 20 minutes. The pellet was washed with 70% ethanol and centrifuged at maximum speed for 5 minutes. The dried pellet was finally dissolved in 15 µl H₂O.

1.4. Total RNA Isolation from Eukaryotic Cells, Embryos, or Mouse Testis

Total RNA from cultured cells or mouse embryos was isolated using RNeasy Mini Kit (Qiagen) as described by the manufacturer. In addition, total RNA from testis was isolated using Trizol reagent (Invitrogen), which contains guanidine isothiocyanate and phenol. The testes were homogenized using the Polytron Power Homogenizer in 1 ml Trizol per 100 mg of tissue. The homogenate was incubated for 5 minutes at room temperature (RT) and then the phases were extracted using 0.2 ml chloroform per 1 ml Trizol used, shaken vigorously to mix everything well and then incubated at RT for 2-3 minutes. The mixture was centrifuged at 12,000 g for 15 minutes, at 4 °C. The upper aqueous phase including RNA was transferred into a fresh tube and the RNA was precipitated with 500 µl isopropyl alcohol per 1 ml Trizol used together with 1 µl of 10 mg/ml glycogen. The sample was incubated at RT for 10 minutes followed by spinning (10 min, 12,000 g, 4 °C). The supernatant was discarded and the residual RNA pellet was washed with 1 ml 75% ethanol/water before spinning again (5 min, 7,000 g, 4 °C). The ethanol was removed, the pellet got air-dried and the RNA was dissolved in 30 µl RNase-free water by pipetting, followed by 10 minutes incubation at 55 °C.

1.5. Purification of Linearized DNA or PCR Products

Linearized DNA by enzymatic digestion or PCR products were purified using QIAquick PCR Purification Kit (Qiagen) according to the instructions of the manufacturer.

2. Modifications and Manipulations of Nucleic Acids

2.1. DIG Labeled RNA Probe Preparation

5 µg plasmid DNA was linearized by incubating with 4 µl restriction enzyme at 37 °C for 2.5 hours, purified using QIAquick PCR purification kit and eluted in 25 µl H₂O. For linearization must be avoided restriction enzymes which leave 3' overhangs. 1 µl elution was loaded on an agarose gel to check the linearization efficiency. The transcription reaction was assembled at RT because spermidine present in the transcription buffer can co-precipitate the template DNA if the reaction is assembled on ice. DIG labeled antisense RNA probes were synthesized by incubating 1 µg linearized DNA, 2 µl 10×Transcription Buffer (Roche), 2 µl 10x DIG RNA labelling Mix (Roche), 1 µl RNasin (40U/µl) (Promega), 1 µl RNA polymerase (T3, T7 or SP6) (Roche), and 13 µl DEPC-H₂O in a total volume of 20 µl at 37 °C for 2 hours. Then, the transcription product was supplemented with 30 µl H₂O and purified with a G-50 Sephadex Micro Column (Amersham). 5 µl purified probe was checked on 1% agarose gel run for 30 minutes at 70 V.

2.2. Random Radioactively Labeled RNA Probe Preparation

The probe prepared in this way was used for the hybridization of the pre-made Northern blot (Ambion) in order to analyse TIPT expression. 1 µg linearized DNA template was incubated with 2 µl 10x transcription buffer (Roche), 10 mM of rATP, rGTP, rUTP, 0.25 mM rCTP, 5 µl of [α -³²P] rCTP (10 mCi/µl) (Amersham), 1 µl RNasin (40U/ul), 1 µl T3 RNA polymerase (Roche) and DEPC-H₂O to a total amount of 20 µl at 37 °C for 2.5 hours. The template DNA was removed by treating with 1.5 µl DNase (1 U/µl) (Promega). Then, the transcription product was supplemented with 30 µl H₂O and purified with a G-50 Sephadex Micro Column.

2.3. Purification of Labeled Nucleic Acids and Double Stranded DNA Oligos

The DIG, respectively [α -³²P] labeled nucleic acids were purified using ProbeQuant G-50 Sephadex Micro Column (Amersham). First, the resin was resuspended by vortexing the column, then the bottom closure of the column was snapped off and the cap loosen one-fourth turn. The column was placed in a 1.5 ml microcentrifuge tube for support, and spun at 770× g for 1 minute to generate the sample-loading surface. The tube was discarded, the column

placed in a new tube and 50 μ l of labeled sample (20 μ l labeling reaction plus 30 μ l H₂O) were slowly applied on the middle of the resin's loading surface. The column was spun at 770 \times g for 2 minutes, and the purified sample was collected in the support tube. The total amount was higher than 50 μ l (approximately 60 μ l).

2.4. DNA Digestion with Restriction Enzymes

10 μ g DNA was incubated with 20-40 U restriction enzymes at 37 °C for 3 hours. The reaction was incubated also O/N when enzyme was not reported to give a star activity. When the presence of the insert was checked, 200-500 ng DNA was digested with 2-3 U restriction enzymes by treating it with 800 W microwave for 12 seconds twice, then incubating at 37 °C for 20 minutes. For end cutting of the PCR product, it was purified either with QIAquick PCR Purification (Qiagen) or from the gel with QIAquick Gel Extraction Kit (Qiagen) and then incubated with 30-60 U restriction enzymes at 37 °C overnight.

2.5. Dephosphorylation of DNA Fragment

Always the digested plasmid further used in the ligation reaction was dephosphorylated. 5'-ends plasmid DNA dephosphorylation was performed by directly adding 1 μ l Alkaline Phosphatase (1U/ μ l, Roche) and 1 μ l Alkaline Phosphatase buffer into the restriction enzyme digestion mixture, followed by incubation at 37 °C for 1 hour.

2.6. Annealing of Complementary Single-Stranded DNAs

In a 0.5 ml PCR tube was prepared the annealing mixture which contains 5 μ l each of the complementary DNA single strand (0.1 nmol/ μ l, IBA), 2 μ l 10 \times Transcription Buffer (Roche), and 8 μ l H₂O in a total volume of 20 μ l. This annealing mixture was heated at 95 °C for 5 minutes and slowly cooled down to 25 °C in an incubator (Eppendorf). Then, the annealed double-stranded DNA fragment was directly used for ligation after a series of dilutions (1:1, 1:100, 1:1000).

2.7. Ligation

The ligation reactions were performed in a PCR tube by mixing 1 μ l 10 \times T4 DNA ligase buffer (MBI Fermentas), 25-100 ng purified vector fragment, 3-10 fold (molecular ratio) of purified insert fragment, 1 μ l 10 \times T4 DNA ligase buffer (MBI Fermentas), and 1 μ l T4 DNA ligase (3 U/ μ l, MBI Fermentas) in a total volume of 10 μ l. This ligation mixture was incubated at RT for 30 minutes-1 hour, or at 16 °C overnight.

3. Polymerase Chain Reaction (PCR)

3.1. Standard and Genomic PCRs

The TaKaRa LA Taq system (TaKaRa) was used for standard and genomic PCR. In this system, primers should be 22-26 nucleotides with T_m higher than 68 °C. The reaction mixture contained 1 μ l template DNA (10 pg-1 ng plasmid DNA, or 200 ng genomic DNA), 1 μ l 10 pmol/ μ l forward primer, 1 μ l 10 pmol/ μ l reverse primer, 5 μ l 10 \times LA PCR Buffer, 5 μ l 25 mM MgCl₂, 4-8 μ l 2.5 mM dNTPs, and 0.5 μ l LA Taq Polymerase (5U/ μ l) in a total volume of 50 μ l. The thermocycling program (Table 6) was carried out using Mastercycler Gradient (Eppendorf). If the PCR product was directly inserted into pGEM-T Easy T/A vector (Promega) or pDrive (Qiagen), 1 μ l Taq polymerase (Gene Craft) was added into the reaction mixture immediately after the Step 5 final elongation and incubated at 72 °C for 30 minutes.

<i>Step</i>	<i>Temperature</i>	<i>Duration</i>
1. Initial Denaturation	94 °C	1 minute
2. Denaturation	98 °C	10 seconds
3. Annealing and Elongation	68 °C	1-10 minutes (about 1 minute/kb)
4. Go to Step 2, Repeat 29 to 39 times (30-40 cycles)		
5. Final Elongation	72 °C	3-15 minutes

Table 6. The thermocycling program for genomic PCR using LA Taq system.

3.2. RT-PCR

The reaction was performed in two different ways, either using the One-Step RT-PCR Kit (Qiagen) according to the manufacturer instructions or using a two-step RT-PCR method. For the latter, a first strand cDNA was produced, which was further amplified in a PCR reaction.

The first strand cDNA was synthesized using the First-Strand cDNA Synthesis Kit (Amersham). The RNA was heated for 10 minutes at 65 °C to denature, and then chilled on ice. A master mix containing 11 µl of Bulk first-strand reaction mix, 1 µl of hexarandom primer pd(N)6, 1 µl of DTT was freshly prepared. 20 µl of RNA representing an amount of 5 µg were added to the mixture pipetting everything up and down several times and further followed by 1 hour incubation at 37 °C to allow the reverse-transcription reaction.

4. Transformation of *E. coli*

4.1. Preparation of Electrocompetent Cells

The electrocompetent cells, which were used for plasmid DNA transformation, were prepared from an *E. coli* DH5α strain (Invitrogen). Briefly, two single colonies of DH5α strain were inoculated in 2x10 ml Luria-Bertani medium (LB, autoclaved prior usage at 121 °C for 20 min, containing 10 g tryptone, 5 g yeast extract, 10 g NaCl and ddH₂O up to 1 liter) and grown overnight at 37 °C. with shaking 250 rpm. These overnight precultures were inoculated into 2x1 liter prewarmed LB medium and cultured then at 37 °C shaking to mid-log phase till O.D.₆₀₀ reached 0.6-0.8 (about 3 hours). The cells were chilled on ice for 10-30 minutes, and then spun at 5,000 rpm at 4 °C for 20 minutes. The supernatant was discarded and each pellet coming from 1 liter culture was washed with 1 liter prechilled water (1:1 wash) and then centrifuged at 5,000 rpm at 4 °C for 20 minutes. The supernatant was removed and each pellet was washed with 100 ml prechilled 10% glycerol (1:10 wash), and then centrifuged at 6,000 rpm (Sorvall HS-4 rotor) at 4 °C for 10 minutes. Again, the supernatant was discarded and each pellet was washed with 20 ml prechilled 10% glycerol (1:50 wash) and centrifuged at 6,000 rpm at 4 °C for 10 minutes. Next, each pellet remained after discarding supernatant was washed with 2 ml prechilled 10% glycerol (1:500 wash), and then centrifuged at 6,000 rpm at 4 °C for 5 minutes. The supernatant was carefully removed and each pellet was resuspended in 2-3 ml 10% glycerol. 50 µl or 100 µl resuspension was aliquoted into each tube on ice, frozen in liquid nitrogen, and stored at -80 °C.

4.2. Preparation of Competent Cells for Heat Shock Transformation

These cells were prepared from an *E. coli* DH5α or HB101 strain (Invitrogen) by calcium chloride treatment. Briefly, one colony was inoculated in 5 ml LB medium and grown

overnight at 37 °C. This pre-culture was inoculated in 50 ml LB medium. Cells were grown to mid-log phase (OD_{600} of 0.7). Next, they were harvested for 10 min at 2,000 rpm and resuspended in 25 ml of ice-cold 50 mM $CaCl_2$. After centrifugation for 10 min at 2,000 rpm, cells were treated with 3 ml of ice-cold 50 mM $CaCl_2$ supplemented with 10% glycerol, aliquoted (50 and 100 μ l), shock-frozen in liquid nitrogen and stored at -80 °C.

4.3. Transformation of *E. coli* by Electroporation

50 μ l competent cells were thawed on ice and transferred into a prechilled 0.1 cm electrode Gene Pulser Cuvette (Bio-Rad). 1 μ l DNA solution (1 ng/ μ l) or 1.5 μ l ligation product was added directly into the competent cells and mixed well by gently flicking. Then, the surface of the cuvette was completely dried and the electroporation was performed using Gene Pulser (Bio-Rad) under the condition of 1.8 kV for voltage, 200 Ω for resistance, 25 μ F for capacitance. Afterwards, 950 μ l prewarmed LB medium was immediately supplied to the electroporated *E. coli* for recovery. The cells were recovered at 37 °C rotating for 1 hour, followed by plating 100 μ l and 900 μ l (the 900 μ l are centrifuged for 2 minutes at 3000 rpm, and the pellet is resuspended in 100 μ l LB) on separate plates.

4.4. Transformation of *E. coli* by Heat Shock

50-100 μ l competent cells were thawed on ice and transferred into a Falcon 2059 polypropylene tube (BD Falcon). 10 ng pure DNA or 10 μ l ligation product were directly added into the competent cells and mixed well by gently flicking. The mixture was incubated on ice for 30 minutes, heat shocked at 42 °C for 1 minute, and incubated on ice for 1.5-2 minutes. Then, 900 μ l prewarmed LB or SOC medium (Invitrogen) were supplied to the heat shocked cells, and incubated at 37 °C rotating for 1 hour. The recovered cells were subsequently spun down at 3,000 rpm for 2 minutes, resuspended in 200 μ l medium and plated.

5. Protein Purification and Analysis

5.1. Protein Purification

5.1.1. GST-Fused Recombinant Protein Expression and Purification

For expression purpose, *E. coli* chimiocompetent cells were prepared from BL21DE3-RIL, BL21DE3 C41, XL-1Blue strains, and electrocompetent cells from Rosetta (DE3) strain. Full-length TIPT was inserted into pGEX-KT vector (Amersham) which contains a Thrombin cleavage site, between *Xho*I and *Hind*III sites in frame with GST. The mutated TIPT for geminin binding site was obtained by mutagenesis of this initial pGEX-KT-TIPT plasmid with the adequate primers. pGEX-KT-TIPT or pGEX-KT-TIPT mutated constructs were either heat shock transformed into BL21DE3-RIL, or transformed by electroporation into Rosetta (DE3) *E.coli* bacterial strains. Following transformation, the cells were used to inoculate a starter culture of 50 ml LB supplemented with the appropriate antibiotics for selection: ampicillin and chloramphenicol for Rosetta strain, and ampicillin for BL21DER-RIL. The antibiotics used in this study had the following concentrations: 25 µg/ml chloramphenicol (Boehringer) and 100 µg/ml ampicillin (Sigma). The culture was grown for 3-4 hours at 37 °C with shaking at 250 rpm. From the starter culture were inoculated 10 µl in 100 ml LB medium with required antibiotics and were grown overnight at 37 °C, with shaking at 150 rpm. Next, 150 µl from the overnight culture were inoculated in 1.5 l fresh LB medium supplemented with the required antibiotics. Cells were grown in 5 l shaking culture flasks at 37 °C and 150 rpm to reach OD₆₀₀ of 0.4. Then, the culture was transferred to 17 °C incubator, cultured to mid-log phase (OD₆₀₀ of 0.6-0.7), and induced by addition of 0.2 mM isopropyl-β-D-thiogalactopyranoside (Sigma). The cells were grown at 17 °C, with 140 rpm shaking overnight (15-16 hours) and harvested in 1l plastic flasks at 5,000 rpm at 4 °C for 25 minutes. The supernatant was discarded slowly, and the pellet with the remaining medium was resuspended and transferred into 50 ml Falcon tubes. The resuspension was centrifuged at 4,000 rpm, 4 °C, for 30 minutes and the supernatant obtained was discarded. The cell pellet was frozen at -80 °C overnight. The pellet from 1.5 l culture was resuspended in 40 ml protein lysis buffer (50 mM Tris, pH 7.5, 500 mM NaCl, 2 mM EDTA, 5 mM DTT, 10% glycerol, freshly added 1 mM PMSF and Complete-EDTA protease inhibitor tablet (Roche)) on ice. To the resuspension was added lysosyme 10 mg/10 ml resuspension solution and was incubated on ice for 30 minutes. This step was especially important for lysis of Rosetta strain

cells. The resuspension was then sonicated on ice for 6 x 20 pulses with 1-2 minutes break between each round of 20 pulses, with 1 cm tip using Cell Disruptor B15 (Branson Sonifier) under the condition of Output Option 5 and 50 % Duty Cycle. The lysate was centrifuged at 4 °C for 1 hour at 15,300 rpm. The supernatant was immediately removed after centrifugation has finished and incubated with 1.2 ml prewashed Glutathione Sepharose 4B (Amersham) at 4 °C on the rotating wheel for 2-5 hours. The mixture was centrifuged at 800 rpm at 4 °C for 5 minute and the supernatant was discarded. A 10 ml column (Pierce) was equilibrated with washing buffer 1 (50 mM Tris, pH 7.5, 200 mM NaCl, 2 mM EDTA, 5 mM DTT, 2% glycerol and freshly added protease inhibitors), in the 4 °C room. The beads were applied to the column and washed with 15 ml of wash buffer 1. Then the washing continued with 40 ml of wash buffer 2 containing 1 M NaCl without protease inhibitors. The elution was done 3 times, each time with 2 ml elution buffer (50 mM Tris, pH 8.0, 20 mM Glutathione 140 mM NaCl, 2 mM EDTA, 5 mM DTT, 2% glycerol supplemented with protease inhibitors) rotating end-over-end for 20 minutes at RT. The elutions were collected and the protein concentrations were measured by Bradford Assay (Bio-Rad), in which 10 µl of protein elution were mixed with 790 µl H₂O and 200 µl Bradford Reagent. For the blank were considered 10 µl of elution buffer. O.D.₅₉₅ of the sample was measured and the concentration of protein was determined according to the standard curve. The proteins were dialyzed in Slide-A-Lyzer dialysis cassettes (Pierce), in buffer without glutathione at 4 °C. The purified protein was aliquoted, shock-frozen in liquid nitrogen and stored at -80 °C.

5.1.2. Thrombin Cutting of GST-Fused Recombinant Protein

TIPT protein was obtained by cutting on the glutathione sepharose matrix the GST-TIPT bound protein with 50 U Thrombin in 1 ml thrombin cutting buffer (50 mM Tris, pH 7.5, 200 mM NaCl, 2 mM EDTA, 5 mM DTT, 2% glycerol) without PMSF because inhibits thrombin activity. The cutting was performed at 4 °C. The eluat was collected and 4 more elutions were performed, by washing the column with washing buffer described above. The elutions were passed over a column prepared with Benzamidine beads (Amersham) to remove the thrombin.

5.1.3. TIPT Protein for Rabbit Immunization

All the protein obtained after cutting with thrombin was loaded on a preparative 15% SDS-PAGE gel, stained with Coomassie blue. The presence of the protein was confirmed by mass spectrometry analysis. The appropriate band was removed from the gel, and the protein was

further electroeluted from the gel slices at 75 V overnight using Elutrap Electroelution system (Bio-Rad) and BT1 and BT2 filter membranes (Schleicher and Schuell).

5.2. Protein Extraction

5.2.1. Total Protein Extraction from Mouse Embryos

Day 8.5 p.c. mouse embryos from 4 mice were dissected out from the uterus in cold PBS, and solubilized in 600 μ l lysis buffer (20 mM Tris, pH 7.5, 100 mM KCl, 2 mM EDTA, 1% Triton X-100, 1 mM β -mercaptoethanol, and freshly added protease inhibitor) on ice, using glass homogenizer. The tissue was sonicated 5x8 pulses with 1-2 minutes break between each round of 8 pulses, with 1 cm tip using Cell Disruptor B15 (Branson Sonifier). The lysates were centrifuged at 13,000 rpm at 4 °C for 15 minutes, and the supernatant was collected. The protein concentration of the soluble extracts was measure at absorbance of 280 nm by BioPhotometer (Eppendorf) and normalized by BSA standards. The total protein extracts were aliquoted, frozen in liquid nitrogen, and stored at -80 °C.

5.2.2. Total Protein Extraction from Mouse Testis

Testis from mice different post partum days were dissected out in cold PBS. The testis were resuspended in 300 μ l lysis buffer (50 mM Tris, pH 7.5, 100 mM NaCl, 5 mM MgCl₂, 2% Triton X-100, 2% SDS, and protease inhibitors) for mice day 7 and 11 pp, 600 μ l for testis from mice day 15, 17, 19, 21 pp and 800 μ l lysis buffer for testis from mice day 23, 25, 30 pp and adult. The tissues were sonicated 3x 20 pulses with 1-2 minutes break between each round of 20 pulses, with 1 cm tip using Cell Disruptor B15 (Branson Sonifier) under the condition of Output Option 5 and 50% Duty Cycle. The supernatant was measured to determine the protein concentration, aliquoted, frozen in liquid nitrogen and stored at -70 °C.

5.2.3. Total Protein Extraction from Cells

The cells grown in 24 wells were washed with cold PBS and trypsinized. The cells coming from 2-3 wells were collected in a 2 ml Eppendorf tube and centrifuged at 1,000 rpm at 4 °C for 5 minutes. The pellet was washed twice with cold PBS, and boiled in 30 μ l 2xSDS-LB for 5 minutes and further stored at -20 °C.

Alternatively, the human or mouse cells untransfected, transiently or stable transfected, were grown in 10 or 15 cm dish. The cells were washed twice with 7 ml/10 cm dish or 15 ml/15 cm

dish cold PBS. The cells were scraped in ice cold PBS with a rubber policeman, collected into a 50 ml Falcon tube and were centrifuged at 1,500 rpm at 4 °C for 5 minutes. The supernatant was discarded and the pellet was resuspended in 1 ml cold PBS and transferred to 1.5 ml Eppendorf tube. The cells were centrifuged again at 1,500 rpm at 4 °C for 5 minutes and the pellet was resuspended in 1 ml lysis buffer (50 mM Tris, pH 7.4, 150 mM NaCl, 1% NP-40, 1 mM PMSF and Complete-EDTA protease inhibitor tablet (Roche)), passaged seven times through 20, 23 and 27 gauge needles followed by incubation on the rotating wheel at 4 °C for 30 minutes. The cell lysate was centrifuged at 14,000 g at 4 °C for 15 min and the supernatant was transferred into new Eppendorf tubes and protein concentration was measured by Bradford assay. The lysate must be diluted at least 1:10 in order to determine accurately the protein concentration. The extract was aliquoted and shock-frozen into liquid nitrogen and stored at -70 °C. This type of extract was further used for immunoprecipitations.

5.2.4. Nuclear and Cytoplasmic Protein Extraction from Cells

The cells grown on 10 or 15 cm dish were washed twice with 10 ml ice cold PBS, and then harvested with a rubber policeman in 10-15 ml ice cold PBS and collected to a 15 ml Falcon tube. The cells were centrifuged at 2,000 rpm without brake, for 5 minutes at 4 °C. The cell pellet was further resuspended in about 1 ml cold PBS, transferred to an Eppendorf tube and centrifuged at 2,000 rpm, at 4 °C for 5 minutes. The packed cell volume was determined (PCV is about 150-200 µl/ 15 cm dish). The packed cells were resuspended in 1 PCV of Roeder A buffer (10 mM Tris pH 7.9, 1.5 mM MgCl₂, 10 mM KCl, 0.5 mM DTT, 1 mM PMSF and Complete-EDTA free protease inhibitor cocktail (Roche)) and incubated on ice for 15 minutes to allow cells swelling. The cells were lysed by rapidly pushing them 7 times through 1 ml syringe with a narrow gauge needle (25 g). The nuclei were collected by centrifugation for 1 minute at 4 °C and 13,000 rpm. The supernatant representing the cytoplasmic fraction was transferred to a new tube and was supplemented with 0.11x volume of 10x cytoplasmic extract buffer (Roeder B) buffer (300 mM HEPES/KOH pH 7.9, 1.4 M KCl, 0.03 M MgCl₂ supplemented with 1 mM PMSF and protease inhibitor cocktail). This fraction was centrifuged at 30,000 g for 30 minutes at 4 °C and S30 supernatant extract was obtained. The nuclear pellet obtained in the previous step was resuspended in 2/3 of one PCV of Roeder C buffer (20 mM HEPES pH 7.9, 25% (v/v) glycerol, 420 mM NaCl, 1.5 mM MgCl₂, 0.2 mM EDTA, 0.5 mM DTT, 1 mM PMSF and Complete-EDTA free protease inhibitor cocktail (Roche)) and incubated for 30 minutes at 4 °C with stirring (200-300 rpm

range). The lysate was spun down at 13,000 rpm for 5 minutes at 4 °C to pellet the cell debris. The supernatant representing the nuclear extract was dialyzed against buffer D (20 mM HEPES pH 7.9, 10% (v/v) glycerol, 100 mM KCl, 1.5 mM MgCl₂, 0.2 mM EDTA, 0.5 mM DTT, 1 mM PMSF and Complete-EDTA free protease inhibitor cocktail (Roche)) for 2 hours at 4 °C in Slide-A-Lyzer Mini dialysis units (7,000 MWCO cut-off) (Pierce). The protein concentration was determined by Bradford assay and the extracts were shock-frozen in liquid nitrogen and stored at -80 °C.

5.2.5. Microsomal Extract for Protease Protection Assay

HeLa cells from 5x10 cm dish grown to 90% confluency were washed with PBS, trypsinized and pelleted at 1,000 rpm for 5 minutes at 4 °C. The cell pellet was resuspended in 1 ml cold PBS and was spun down again. The pellet obtained was washed in 1 ml microsomal buffer (3 mM Imidazole pH 7.4 and 250 mM sucrose without protease inhibitors), and spin down at 1,000 g for 5 minutes at 4 °C. The cells were disrupted by passage very slowly 10x 20 g, 10x 23 g and 10x 27 g needles in 1 ml microsomal buffer. The lysate was spun down at 3,000 g for 15 minutes and a large pellet was obtained. The pellet was resuspended in 920 µl microsomal buffer, 1290 µl 2xSDS-LB and 220 µl 1M DTT. The supernatant was split into two 500 µl samples. One sample was treated with protease inhibitor cocktail, and the other with trypsin (Trypsin PM, Serva). Before adding trypsin, the protein concentration was measured by Bradford assay (1.85 mg/ml). The sample was treated with trypsin and 0.07 mg trypsin/mg protein was added (10 mg/ml trypsin stock solution in microsomal buffer, pH adjusted with HEPES 0.1 M till pH 7.4). The sample was incubated for 30 minutes at RT. The reaction was stopped by addition of 64.8 µl trypsin inhibitor from soyabean (Sigma) (trypsin inhibitor: trypsin is 10:1). Both samples were ultracentrifuged in Beckman ultracentrifuge S150 AT rotor at 100,000 g for 1.5 hours, at 4 °C. The supernatants concentrations were measured (1 µg/µl for supernatant-proteinase inhibitor sample, and 1.6 µg/µl for supernatant-trypsin treated sample) and 10 µg of protein for each sample were taken and boiled with 2XSDS-LB. The pellets obtained were resuspended in 20 µl microsomal buffer, 30 µl 2XSDS-LB with 5 µl 1M DTT. The samples (3,000 g pellet-10 µl; 100,000 g supernatant proteinase inhibitor sample-20 µl; 100,000 g pellet proteinase inhibitor sample-15 µl; 100,000 g supernatant trypsin sample-20 µl; 100,000 g supernatant trypsin sample-20 µl) were loaded on a SDS-PAGE gel, Western blotted and TIPT distribution in cell was determined by using anti-TIPT antibodies.

5.3. *In vitro* Transcription/Translation

For *in vitro* transcription/translation, cDNA fragment with single ATG was cloned into pSP64 vector (Promega), maxiprep and further purified by phenol-chloroform. The assay was performed using TNT Reticulocyte Lysate System (Promega).

5.4. Protein Analysis

5.4.1. Protein Gel Electrophoresis

SDS-polyacrylamide gels were prepared using Protean II gel preparation system (Bio-Rad). The SDS-PAGE gel was usually prepared with 10% separating gel and 5 % stacking gels. For separating gel preparation was used 4X Separating gel buffer, pH 8.8 (1.5 M Tris, pH 8.8, 0.4% SDS), and for the stacking gel was used 4X stacking gel buffer, pH 6.8 (0.5 M Tris, pH 6.8, 0.4% SDS). A protein sample was mixed with the same volume of 2xSDS loading buffer (125 mM Tris, pH 6.8, 20% glycerol, 0.02% bromophenol blue, 2% β -mercaptoethanol, 4% SDS), and heated at 95 °C for 5 minutes or in boiling water for 3 minutes. Electrophoresis was performed in 1xSDS buffer (25 mM Tris-base, 0.1% SDS, 192 mM glycine, pH 8.75) under 20 mA/gel, following 30 minutes preelectrophoresis under the same condition. Then, the gel was either subjected to Western blotting directly, or fixed in fixation solution (45% methanol, 7.5% acetate) for 5 minutes and stained with Coomassie blue staining solution (0.25% Coomassie brilliant blue R 250, 45% methanol, 10% acetate; or 0.1% Serva R 250, 50% methanol, 10% acetate) at RT for 0.5-1 hour. The Coomassie stained gel was subsequently destained with 10% acetate for several hours or overnight.

<i>Separating gel (10%)-volume</i>	<i>30 ml</i>	<i>Stacking gel (5%) -volume</i>	<i>10 ml</i>
4X Separating buffer pH 8.8	7.5 ml	4X Stacking buffer pH 6.8	2.5 ml
30% Acrylamide-bisacrylamide solution (AA)	10 ml	30% AA	1.66 ml
dH ₂ O	12.3 ml	dH ₂ O	5.84 ml
APS 10%	0.1 ml	APS 10%	50 μ l
TEMED	0.1 ml	TEMED	25 μ l

Table 7. SDS-PAGE gel preparation.

5.4.2. Western Blotting

Western blotting and subsequent immunostaining were performed using primary antibodies presented in table 10 (appendix section). During the gel electrophoresis were cut a Protran Nitrocellulose Transfer Membrane (Schleicher & Schell BioScience) and 4 pieces of Whatman paper into a similar size to the gel, with the Whatman paper slightly larger. When the gel was stopped, the membrane and the papers were presoaked in blot buffer (48 mM Tris-base, 3.9 mM glycine, 0.037% SDS, 20% methanol). Between two double-layered presoaked Whatman papers, the SDS-polyacrylamide gel was placed tightly onto a presoaked nitrocellulose membrane avoiding any air bubble in between, with the membrane close to the anode and the gel close to the cathode. This sandwich including Whatman paper, gel, and membrane was tightly pressed together into a clamp. Wet electroblot transfer was performed in blot buffer using Western blotting system (Bio-Rad) under 15 V overnight or under 30 V for 2 hours with a cooling chamber. The membrane was removed from the transfer apparatus into a plastic tray containing Western buffer A (10 mM Tris, pH 7.4, 0.9% NaCl, 0.05% Tween 20). The transfer was checked by staining with 0.1% Ponceau S, followed by destaining with buffer A. Then the membrane was blocked in blocking solution (1-5% low fat milk powder in Western buffer A) at RT for 1 hour, rocking on a rocky machine (Biometra). The primary antibodies were applied in the right concentration, diluted in 1-5% blocking solution, and the membrane was further incubated at 4 °C with shaking overnight (preferred) or at RT rocking for 1-2 hours. The membrane was washed at RT by rocking with the buffers in the following sequence: buffer A, buffer B (0.9% NaCl, 0.5% Triton X-100, 0.1% SDS), buffer B, buffer A (10 minutes each washing step). The secondary HRP-conjugated antibodies were applied in the required concentrations, diluted in 5% blocking solution at RT rocking for 40 minutes. Then, the membrane was washed again in the same way as described before. The signal was detected using Pierce ECL Western Blotting Substrate Kit (Pierce). The substrate working solution was prepared by mixing equally 500 µl of Oxidizing Reagent and 500 µl Enhanced Luminol Reagent as the chemiluminescent substrate for HRP, and the mixture was distributed onto the membrane. The chemiluminescence was observed by exposing the membrane for 10 seconds to 20 minutes to a Lumi-Imager (Boehringer Mannheim) or to CL-XPosure films (Pierce) followed by developing with the Curix 60 developing machine (Agfa).

5.4.3. N-Terminal Coupling of Protein

GST-TIPT recombinant protein was N-terminally coupled to agarose matrix at 4 °C using AminoLink Plus Coupling Gel Kit (Pierce) according to the instructions of the manufacturer.

5.4.4. Antibody Purification from Crude Serum

The crude anti-TIPT rabbit antiserum was purified by chromatography at 4 °C using the affinity purification protocol described for SulfoLink Kit (Pierce). For this purpose, 5 mg of GST-TIPT recombinant protein were N-terminally coupled and used for antibodies purification from 25 ml of antiserum.

5.4.5. Antibody Purification Using Blotted Antigen

GST-TIPT protein was loaded onto several preparative gels (single well) SDS-PAGE gels. The protein was electroblotted onto Nitrocellulose membranes. The blots were transferred in water and further stained briefly with Ponceau S in order to visualize the protein. The protein bands were cut out and either stored dried between Whatman papers or washed with copious amount of water or Western buffer A until the Ponceau staining was gone. The membranes were blocked with 5% milk powder in Western buffer A for 30 minutes at RT, and then washed for 5-10 minutes with buffer A. The anti-TIPT crude serum was filtered through a 0.45 µm diameter filter and buffered with 1/10 PBS 10X, pH 8.0. The blots were transferred into a plastic tray with many slots, each slot having a volume of about 5 ml and incubated with serum (5-10 ml) at 4 °C for at least 4 hours, or at RT for 1-2 hours, with shaking. The serum was collected and the strips were washed one time with Western buffer A for 10 minutes. The washing continued one more time with buffer A for up to 30 minutes, and then with PBS, pH 8.0 for 5 minutes. An Eppendorf tube containing 40 µl of 1 M Tris HCl, pH 9.5 was prepared on ice. The PBS was soaked from the slots and all the strips were transferred into one slot. The bound antibodies were eluted with 500 µl 100 mM glycine, pH 2.5, for 1-2 minutes. The elution was immediately transferred into the Tris buffer to neutralize the antibody, preventing their denaturation. The elution was repeated 1-2 more times. The antibodies concentration was measured by Bradford assay, using as blank 30 µl of glycine in Tris buffer solution. Next, the antibodies were dialyzed in PBS, pH 8.0, O/N and the next day aliquoted and stored at -80 °C.

5.5. Casein Kinase II Assay

2 µg GST-TIPT and GST proteins were incubated with 30 µl (80%) glutathione beads in the same way as for the pull-down assay. The incubation was performed overnight, at 4 °C, end-over-end. The beads were washed with CKII kinase buffer (20 mM Tris, pH 7.5, 350 mM

NaCl, 1 mM EDTA, 2 mM DTT, 0.1% Triton X-100) three times. In 50 μ l reaction the beads were mixed with 5 μ l 10x CKII reaction buffer (200 mM tris, pH 7.5, 50 mM KCl and 10 mM MgCl_2), CKII (1-10-100 units), 2 μ l γ -[^{32}P]-dATP 10 $\mu\text{Ci}/\mu\text{l}$ and water. The reaction was incubated at 30 °C for 1 hour. Then, the beads were washed in association buffer (0.05% Triton X-100 in PBS) for three times. The proteins were eluted from the beads by boiling for 5 minutes in 20 μ l 2xSDS-LB. The samples were loaded on 10% SDS-PAGE gel. The gel was stained with Coomassie blue and immediately fixed in a developing cassette (wet, not dried), and exposed to a BioMax film (Kodak) at -80 °C overnight. The film was developed with Curix 60 developing machine.

6. Yeast Two-Hybrid Screen

The yeast two-hybrid screen was performed using ProQuest Two-Hybrid System (Gibco BRL) according to the instructions of the manufacturer. Briefly, the full-length TIPT was PCR out from pPC86-TIPT plasmid and cloned in frame with the Gal4 DNA binding domain in the pDBLeu vector, between *Sall* and *NotI* enzymatic restriction sites. Then, pDBLeu-TIPT construct used as bait was transformed into yeast strain MaV203 containing *HIS3* and *lacZ* reporter genes. After the self-activation was checked, was determined the concentration of 3-Amino-1, 2, 4- Triazole (3AT) required to titrate basal His3 expression level. The mouse 8.5 dpc cDNA library, cloned in frame with Gal4 DNA activation domain in pPC86 vector (Gibco BRL), was retransformed in *E.coli* bacteria due to the fact that the amount of DNA was insufficient for yeast transformation. Sequentially, the cDNA library was heat shocked in the pre-transformed pDBLeu-TIPT MaV203 yeast strain. About 6×10^6 clones were screened on plates lacking leucine, tryptophan and histidine, and supplemented with 50 mM 3AT. 428 independent colonies were selected out from the first round of screen. Then, all these clones were applied to the second round of screen in which beta-galactosidase activity was assayed for every clone, being selected according to their ability to activate the *lacZ* gene. From this step, 88 positive cDNA clones were identified: 51 strong interactors, 27 moderate, and 10 weak interactors. From all of them, yeast and bacterial DNA as well as glycerol stocks were prepared, and plasmids DNA were sequenced.

7. Analysis of Protein-Protein Interactions

7.1. GST Pull-Down Assay

The *in vitro* direct protein-protein interactions were studied using GST pull-down assays. 50 µl of Glutathione Sepharose 4B beads (40 µl bed volume) were prewashed with 500 µl protein lysis buffer (50 mM Tris, pH 7.5, 500 mM NaCl, 2 mM EDTA, 5 mM DTT, 10% glycerol, freshly added 1 mM PMSF and Complete-EDTA protease inhibitor tablet (Roche)). The beads were spun down by brief centrifugation at less than 4,000 rpm for several seconds, and the supernatants were carefully removed. Always about 50-100 µl were left above the beads bed. For coupling, the prewashed beads were incubated with 40 µg recombinant GST-TIPT or GST protein in 500 µl pull-down binding buffer (20 mM Tris, pH 7.5, 100 mM NaCl, 1 mM EDTA, 0.1% NP-40, freshly added 1 mM PMSF and protease inhibitor) at 4 °C rotating overnight. The beads were spun down by brief centrifugation and were washed twice for 10 minutes each with 500 µl pull-down binding buffer at 4 °C rotating, to get rid of the unbound proteins. The beads were spun down after each washing step and the supernatants were aspirated. GST-Geminin or GST coupled beads were incubated with 45 µl removed from 100 µl *in vitro* transcription/translation product, in 500 µl pull-down binding buffer at 4 °C rotating for 1-2 hours. The remaining 10 µl were removed as control, mixed with 2×SDS loading buffer and heated at 95 °C for 5 minutes. The beads were spun down and washed twice with pull-down binding buffer at 4°C rotating for 10 minutes each step. Two more washing steps were done in the same way with pull-down washing buffer (20 mM Tris, pH 7.5, 150 mM NaCl, 1 mM EDTA, 0.1% NP-40, freshly added 1 mM PMSF). The beads were spun down and the supernatant was aspirated completely. The protein from the beads was eluted with 20 µl 2×SDS loading buffer by heating at 95 °C for 5 minutes. After spinning down, the eluates were removed and the gel was loaded with 20 µl supernatants and 10 µl control. After electrophoresis, the gel was fixed for 3 minutes in 20% isopropanol and 10% acetic acid and washed with water. The gel was transferred on a wet Whatman paper and dried with a vacuum gel drier (Biometra) at 80 °C for 1 hour. The dried gel was fixed in a developing cassette, and exposed to a BioMax film at –80 °C overnight. The film was developed with Curix 60 developing machine.

7.2. Immunoprecipitation

The *in vivo* protein-protein interactions were studied using immunoprecipitations. The experiment was performed either by coupling the geminin antibodies to the Protein A Sepharose (PAS) beads, or using already coupled HA antibodies to protein sepharose beads (HA affinity matrix from Roche).

30 mg PAS CL-4B (Amersham) beads were hydrated with 500 μ l PBS, pH 8.0 (about 150 μ l bed volume), and the resuspended beads were washed with 1 ml PBS twice. 200 μ g purified anti-geminin antibodies (Santa-Cruz) (200 μ l) or 100 μ l pre-immune serum was incubated with up to 500 μ l PBS and washed beads at RT rotating overnight. The beads were washed 4 times with 500 μ l 0.2 M $\text{Na}_2\text{B}_4\text{O}_7$, pH 9.0 for 5 minutes each, and further resuspended in 600 μ l 0.2 M $\text{Na}_2\text{B}_4\text{O}_7$, pH 9.0. A 10 μ l aliquot was saved. 3.7 mg dimethylpimelimidate (about 20 mM) was added into the resuspensions and incubated at RT rotating for 30 minutes to crosslink the antibody with the beads. Another 10 μ l aliquot was saved, and the crosslinking reaction was stopped by washing the beads with 500 μ l 0.2 M ethanolamine, pH 8.0 at RT rotating for 2 hours, followed by washing with PBS three times for 5 minutes each.

0.6 ml mouse day 8.5 extract (2.5 mg/ml) was precleared by incubating with PAS resuspended beads for 30 minutes at 4 °C on the rotating wheel. The beads were spun down and the 275 μ l cleared supernatant was incubated with the coupled beads and up to 600 μ l protein lysis buffer (20 mM Tris, pH 7.5, 150 mM KCl, 1 mM EDTA, 0.1% Triton X-100, 1 mM β -mercaptoethanol, freshly added protease inhibitor) at 4 °C rotating for 2 hours. The beads were washed with 500 μ l IP washing buffer (20 mM Tris, pH 7.5, 150 mM KCl, 1 mM EDTA, 1 mM β -mercaptoethanol, 1 mM PMSF, 0.1% Triton X-100) three times at 4 °C rotating for 5 minutes each. The co-precipitated proteins were eluted in 60 μ l 2 \times SDS loading buffer by heating at 95 °C for 6 minutes. 20-30 μ l eluted co-precipitants were loaded on a 10% SDS-polyacrylamide gel, and Western blotting was performed using anti-geminin and anti-TIPT antibodies.

Another type of immunoprecipitation was performed using HA affinity matrix beads (Roche) (3.5 mg HA antibodies coupled to 1 ml beads, representing 25 nmol anti-HA/ml beads (25 μ M) antibodies concentration) and total or nuclear extract from HA-TIPT transiently or stable transfected human U2OS cells. As control, the beads were incubated with non-transfected U2OS cells. The PAS beads were resuspended and washed with PBS pH 8.0 as described

before. The extracts were precleared for 30 minutes-1 hour with PAS beads. An aliquot of the precleared extract was saved as control. 2-3 mg of cell extract were diluted in IPP150 buffer (20 mM HEPES/KOH pH 7.9, or 20 mM Tris, pH 7.9, 150 mM NaCl, 1.5 mM MgCl₂, 0.5 mM DTT, 0.05% NP-40, 1mM PMSF and Complete-EDTA free proteinase inhibitor) up to 1.5 ml and incubated for 4 hours with 50 µl HA beads, at 4 °C on the rotating wheel. The supernatant was removed after spinning down the beads by centrifugation for several seconds at 4,000 rpm. All the time the beads were let to settle for 2-3 minutes on ice before removing the supernatant. 5-6 washing steps with IPP150 were performed, 3 minutes each. The beads were spun down and the supernatant was removed completely. The elution was performed in two different ways: either by boiling the beads for 5 minutes with 50 µl 2xSDS-LB, or by elution with HA peptide. The HA peptide was diluted at 1mg/ml in Tris/HCl pH 7.5 or 7.9. The elution with HA must be performed with 60-fold excess of peptide over the antibodies. Thus, 50 µl beads were incubated with 75 µl peptide solution and 75 µl 2x elution buffer (40 mM HEPES/KOH, pH 7.9, 300 mM NaCl, 0.1% NP-40 and 1 mM DTT) (the final concentration of HA peptide should be 340 µM in 200 µl). The elution was performed at 4 °C for 1 hour with end-over-end rotation. After spinning down the beads, the supernatant was collected and boiled with 30 µl 6x SDS-LB for 5 minutes. A 10% gel was loaded with 20-30 µl eluted co-precipitants and Western blotting was performed using anti-HA, anti-geminin, anti-TBPL1, anti-TBP, anti-TFIIA and anti-NPM antibodies. Alternatively, 50 µl eluted co-precipitants were loaded on a 10% SDS-polyacrylamide gel, stained by Coomassie blue and send to mass spectrometry analysis.

7.3. Peptide Array Analysis

Dr. Lingfei Luo performed this experiment before the beginning of my PhD studies. TIPT peptide array membrane was blocked with 10 ml blocking solution (1.5% BSA in Western buffer A) at RT, rocking for 1 hour. Then, His-Geminin recombinant protein was added into the blocking solution to a final concentration of 1 µg/ml, and incubated at 4 °C with shaking overnight. Afterwards, the membrane was sequentially washed with 10 ml Western buffer A, Western buffer B, Western buffer B, and Western buffer A for 10 minutes each. The following steps from primary antibody staining are the same with the normal Western blotting, except the blocking solution.

8. Analysis of Protein-Nucleic Acids Associations

8.1. Gel Mobility Shift Assays

The *in vitro* protein-DNA interactions were studied using gel retardation assay. In this study were tested the interaction of human TBP, human TBPL1 complexed with TFIIA, recombinant GST-TIPT and His-geminin proteins with DNA. Oligonucleotides used were: adenovirus major late promoter oligo (-40 to -16), AdMLP mutated oligos (M1-M8), AdMLP mut (TATA box mutated), NF1 oligo (-288 to -252), adenovirus E4 oligo [57]. The sense strand was phosphorylated by mixing 1 μ l sense strand oligonucleotide (0.1 nmol) with 0.2 μ l polynucleotide kinase buffer (Roche), 3 μ l γ -[32 P]-dATP (30 mCi) and water up to 20 μ l. The reaction was incubated at 37 °C for 45 minutes. The volume was increased to 50 μ l H₂O and the labeling mixture was purified with a G-50 sephadex micro column. The approximately 60 μ l of flow through were mixed with 0.1 volume 1 M KCl and 1 μ l antisense strand oligonucleotides (0.1 nmol). The mixture was denatured at 95 °C for 10 minutes and the annealing was performed slowly by naturally cooling down for several hours. From 1 μ l labeled double-stranded oligo was counted the radioactivity with an LS1701 counter (Beckman). The labeled double-stranded oligo was always diluted 1:20 and approximately 0.7 ng of probe was used per binding reaction.

Different binding reactions were performed for TBP and TBPL1. The TBP binding reactions were performed in a volume of 15 μ l by mixing 3 μ l 5x binding buffer (60 mM HEPES/KOH, pH 7.6, 300 mM KCl, 15 mM DTT, 1 mM EDTA, 10% PEG-800 (w/v), 20 mM MgCl₂, 40% glycerol, 0.1% NP-40, 325 μ g/ml BSA) with 100 ng/ μ l poly(dG-dC), 3-15 ng TBP, 1 μ l hot oligo and water. For TBPL1 the binding reactions were performed also in 15 μ l by mixing 5 μ l 3x binding buffer (60 mM HEPES/KOH, pH 7.6, 180 mM KCl, 9 mM DTT, 60% glycerol, 60 μ g/ml BSA) with 200 ng BSA, 100 μ g poly(dG-dC), 10-20 ng TBPL1-TFIIA complex (purified by Prof. Dr. Martin Teichmann) [56] and water. The reactions were incubated at 30 °C for 45 minutes. The shift was performed on a 5% native gel. For 25 ml of gel were mixed 3.33 ml of 30% acrylamide-bisacrylamide 59:1, 1.25 ml glycerol, 1.25 ml 10xTBE, 25 μ l 1M DTT, 133.5 μ l 10% Ammonium persulphate freshly prepared, 13.35 μ l TEMED and 19 ml water. The gel was allowed to polymerize for 1 hour and then was prerun for 45 minutes at 200 V, at 4 °C in 0.5x TBE buffer for TBPL1 shifts, respectively 0.5 x TBE buffer supplemented with 5% glycerol and 0.05% NP-40 for TBP shifts. The samples were loaded

during running and the gels runned for 15 -20 minutes at 200 V (for TBP shifts), or 400 V (for TBPL1 shifts) at 4 °C. After running, one of the glass plates was removed and the gel together with the support glass were fixed in the cassette and exposed to a BioMax film at –80 °C for 20-40 hours. The film was developed with the Curix 60 developing machine.

8.2. Chromatin Immunoprecipitation (ChIP) Assay

Dr. Christine Mayer performed this experiment. To check whether TIPT interacts directly with rDNA promotor, ChIP experiments were performed. 293T cells were transfected with HA-TIPT or HA-CSB as positive control. Cells were cross-linked with formaldehyde at 60-80% of confluency. For each immunoprecipitation, pellets from two 10 cm dishes were used. The beads were prepared as following: HA-beads were washed twice in blocking buffer (10 mM Tris HCl pH 8.0, 2 mM EDTA, 1mg/ml BSA, 0.5 mg/ml salmon sperm), and 50% slurry was prepared and blocked in 4 °C over night. A/G beads were washed twice with blocking buffer, 30% of slurry was prepared and the beads were blocked in 4 °C for 40 min. Pellets from 2 dishes were combined and cells were lysed in 500 µl of cell lysis buffer (5 mM HEPES pH 8.0, 85 mM KCl, 0.5% NP-40, protease inhibitors). Then, nuclear lysates were prepared using 300 µl of nuclear lysis buffer (50 mM Tris HCl pH 8.0, 10 mM EDTA, 1% SDS, protease inhibitors). Sonication was performed twice for 20 min, 15 s on/off. For preclearing 150 µl of chromatin, 600 µl of IP dilution buffer (0.01% SDS, 1.1% Triton X-100, 1.2 mM EDTA, 16.7 mM Tris HCl pH 8.0, 167 mM NaCl) and 60 µl of 30% A/G beads slurry were used. Samples were incubated at 4 °C for 1h 20 min on the wheel. 35 µl of precleared chromatin was taken as input. For immunoprecipitation 350 µl of chromatin, 400 µl IP dilution buffer and 15-30 µl 50% HA-beads slurry were incubated 5.5 hours in 4°C on the wheel. Beads were washed twice with 800 µl of: low salt wash buffer (0.1% SDS, 1% Triton X 100, 2 mM EDTA, 20 mM Tris HCl pH 8.0, 150 mM NaCl), high salt wash buffer (0.1% SDS, 1% Triton X 100, 2 mM EDTA, 20 mM Tris HCl pH 8.0, 500 mM NaCl), LiCl wash buffer (10 mM Tris HCl pH 8.0, 2500 mM LiCl, 1% NP40, 1% deoxycholic acid, 1mM EDTA) and TE. After low salt wash buffer beads were transferred to fresh tubes. Samples were decross-linked over night. After that DNA was purified on the columns using QIAEX PCR purification kit (QIAGEN). DNA was eluted with 60 µl of 10 mM Tris HCl pH 8.0.

ChIP PCR reaction was made using 2xPCR master mix, DMSO and following primers:

- for rDNA human promoter: forward –150 bp, reverse +130 bp

- for human coding region: forward +8124 bp, reverse +8246 bp

DNA template was diluted 3 times and 3 or 9 μ l were used for PCR. Input DNA was diluted 100 times. PCR program: 94°C/5 min; 29 cycles (94°C/30 sec; 50°C/30 sec; 72°C/30 sec); 72°C/7 min; 4 °C/ ∞ . 12 μ l of each PCR product was loaded on the 2% agarose gel and electrophoresis was running for 20 min.

9. Cell Culture and Immunocytochemistry

9.1. Cell Revival

Cells from liquid nitrogen were revived in a 37 °C water bath as quickly as possible (3-4 minutes), then transferred gently into a 15 ml Falcon tube containing 5 ml proper culture medium, and centrifuged at 1,000 rpm for 5 minutes. The supernatant medium was aspirated, 3 ml fresh medium was added to the cell pellet and pipetted up and down for about 15 times to break cell aggregates. Then, the cell resuspension was distributed in a 10 cm petri dish containing 7 ml culture medium (10 ml in total). The dish was gently shaken left- right and backward- forward to achieve equally distribution of cells. Then, the cells were cultured in a BBD 6220 incubator (Heraeus) at 37 °C and 5% CO₂ concentration.

9.2. Cell Passage and Freeze

The cells cultured on 10 cm dish were passaged when reached 70- 95% confluency. First, the growth medium was aspirated and the cells were washed with 5 ml prewarmed PBS, which was then aspirated from the dish. 2.5 ml 1×Trypsin-EDTA solution (Gibco BRL) was equally distributed onto the washed cells, and cells were incubated at 37 °C for about 2 minutes. The dish was shaken until all the cells became floating. 7.5 ml culture medium was added to stop the trypsin digestion, pipetted up and down for several times to blow the cells, and then transferred into a 15 ml Falcon tube. Centrifugation was carried out at 1,000 rpm for 5 minutes to pellet the cells, followed by aspiration of the supernatant.

For passage, the cell pellet was resuspended in 6 ml culture medium by pipetting 15 to 20 times to break cell aggregates. 1 ml resuspension was finally equally distributed into a 10 cm dish containing 9 ml medium (1:6 dilution), gently shaken and incubated.

For freeze, the cell pellet was resuspended in 2 ml culture medium, and every 500 μ l cell resuspension was transferred into a cryotube (Nunc) containing 500 μ l of freezing medium (63.4% growth medium already supplemented with 10% FCS, 16.6% DMSO and 20% FCS),

mixed well by inverting, and sequentially frozen at -20°C overnight, at -80°C for a week to a month, and finally in liquid nitrogen.

9.3. HA-TIPT Human U2OS Stable Cell Line

To generate the HA-TIPT construct, TIPT was amplified in frame with the HA tag using the pPC86-TIPT construct, digested with *Bgl*III and *Not*I enzymes, and inserted into *Bam*HI and *Not*I sites of a modified pcDNA vector (Invitrogen) containing an intron and a HA epitope (kindly provided by R. Lührmann, Göttingen.). Human U2OS cells were stably transfected with pcDNA Ta2+i-TIPT plasmid that gives resistance to neomycin those cells that have it integrated in the genome. In order to find out the required amount of neomycin (G418) at which the untransfected cell are dead and the stably transfected are alive it was proceeded to a test. U2OS cells were passaged into several 6 well plate in duplicates, and different amounts of G418 were applied on cells: 100, 150, 200, 250, 300, 400, 450, 500, 550, 600 and 700 $\mu\text{g/ml}$ G418. The medium was changed every day and it was observed that after 5 days the cells transfected with the minimum amount of 500 $\mu\text{g/ml}$ G418 were completely dead. 100,000 U2OS cells were freshly added to 4 different 10 cm dish. The cells were transfected with a very low efficiency only with Eugene6 (Roche) for the control, or with HA-TIPT. The next day, 500 $\mu\text{g/ml}$ G418 in the McCoy's growth medium was applied for selection, and every second day the medium was changed. In the seventh day, the control cells were completely dead and the HA-TIPT transfected cells formed well-defined colonies. The clones were marked with diamond objective under the binocular microscope and were selected under the cell culture hood with the help of a stereomicroscope. 40 μl trypsin/well was added In 96 well plate, and gelatine was added in 24 well plate. The cells from the marked colonies were scraped with 20 μl pipette and transferred into the 96 well plate, and subsequently in 24 well plate after 2-3 minutes. The cells were incubated at 37°C in medium containing 250 $\mu\text{g/ml}$ G418. When the cells reached 80% confluency were trypsinized and passaged 1:3 into 3 new 24 wells for genomic DNA extraction, protein extraction and stock cells. Finally about half of the picked clones were obtained (17 clones, numbered from 1-17), the rest being arrested in growth and finally dead.

9.4. Cells Synchronization with Aphidicolin

The human U2OS cells were passaged at a concentration of 100,000 cells/6 well plate. After 20 hours the cells were transfected using Fugene6 with 1.5 µg pcDNA Ta2+i-TIPT, pcDNA Ta 2+i plasmids, or only Fugene6. After 19-20 hours the cells were blocked with 10 µg/ml Aphidicolin for other 19 hours. The cells were washed twice with PBS, once with growth medium and then released. The cells were collected at 0, 2, 4, 6, 8, 10 and 12 hours and samples were prepared for FACS analysis.

9.5. FACS Analysis of Human U2OS Cells

U2OS cells were harvested by trypsinization and the pellet was washed twice with 10 ml ice cold PBS. The cells were pelleted each time by 1,000 rpm centrifugation (Heraeus centrifuge) at 4 °C for 5 minutes. The supernatant was discarded and the pellet was resuspended in 1 ml ice cold PBS. The FACS tubes were already cooled on ice and filled with 3 ml 100% ethanol from -20 °C. The cells were aspirated into 1 ml syringe with a 27 gauge needle attached, and were injected into ethanol with pressure. The cells were incubated at least 1 hour on ice before FACS analysis, and stored for 24 hours to weeks at -20 °C.

The cells were spun down at 500 g (1,400 rpm) in Heraeus centrifuge for 5 minutes at 4 °C. The ethanol was carefully removed immediately after the centrifugation was stopped, and the pellet was let to dry by putting the tube over head on a tissue paper (2 to 5 minutes). The rest of the ethanol was removed from the walls of the tube with tissue paper. Depending on the amount of the pellet, the cells were either resuspended in 425 µl PBS when one 10 cm dish was used initially, or half of the amount if one 6 well plate of cell was the starting point. The following steps are presented for 425 µl PBS. The resuspended cells were vortexed on shaker step 3 (mild) to break cell clumps. RNase (Roche) dissolved in 10 mM Tris, pH 7.5 was inactivated for 15 minutes at 95 °C, aliquoted and frozen at -20 °C. 50 µl of 1 mg/ml RNase was added to the cell suspension, followed by 25 µl of 1 mg/ml propidium iodide (Sigma). The staining was performed for 30 minutes at RT in the dark. The cells were ready for Flow Cytometry Analysis using FACS Calibur Flow Cytometer (Beckton-Dickinson Biosciences, USA). The analysis was performed in the group of Prof. Dr. Detlef Doenecke (Göttingen) with the help of Dr. Nicole Happel. All the measurements must be performed within the next 3 hours upon staining. The FACS tubes were vortexed immediately before measurement. The collected data were analyzed using the Modifit LT software (Verify Software House Inc. ME,

USA). The program determined the control values and the indistinct peaks were located according to the control values. Auto-linearity was used for determining G2/G1 linearity.

9.6. Immunocytochemistry

9.6.1. Immunocytochemistry-PFA Fixation

The cells were passaged and cultured on coverslips arranged in 24 well dish in 0.5-1 ml medium under 5% CO₂ at 37 °C overnight. When cells reached the desired confluency (50-60%), the medium was aspirated and the cells were washed twice with PBS, and then fixed with 500 µl 4% PFA/PBS at RT for 20 minutes. Then, the cells were washed with 500 µl PBS three times for 5 minutes each, followed by permeabilization for 15 minutes at RT with 0.2% Triton X-100 in PBS. The cells were washed 4x PBS for a total time of 20 minutes and then incubated with 1% SDS in PBS for 10 minutes. After 4x PBS wash, the cells were blocked for 1 hour 10% FCS/PBS supplemented with 0.2% Triton X-1000 at RT. In a 10 cm petri dish were added several filter papers soaked in water and on the top of them was applied a sheet of parafilm. The coverslips with the cells facing up were transferred onto the parafilm and 25 µl of diluted primary antibody in blocking buffer was applied on the cells. The dish was further incubated at 4 °C overnight. The coverslips were transferred into the 24 wells and washed 4x PBS. The incubation with the diluted Alexa conjugated secondary antibodies in blocking solution was realized in the same way as described for primary antibodies, for 1-2 hours at RT. After the application of fluorescently labeled secondary antibody, all the following steps were done avoiding light. After four PBS washing steps, the coverslips were washed briefly in water and applied with the cells facing down on a slide on which was added a drop of Moviol mounting shield containing DAPI (Vector). After removing the excess of Moviol by gently pressing with a tissue paper, the coverslips were sealed with nail polish and let dry for at least 1 hour at RT. The sample was applied to a BX-60 fluorescence microscopy (Olympus).

9.6.2. Immunocytochemistry-Methanol Fixation

The cells were grown on coverslips as described above (section 9.6.1). The coverslips were washed with PBS buffer for 2-3 minutes, then the PBS was aspirated and methanol from -20 °C freezer was applied for 6 minutes on cells. The cells were rehydrated several times with PBS, for at least 10 minutes. The primary antibodies were diluted in 0.5% BSA in PBS. The

coverslips were applied on the parafilm and incubated with the primary antibodies as described before. All the following steps are as already described.

9.6.3. Immunohistochemistry on Cryosections

The mouse brain or testis cryosections were removed from -80 °C freezer and were allowed to come back to the RT for about 5-10 minutes. Around each tissue section was drawn a circle with the Dako fat pen (Dako). The freezing protecting medium was removed by dipping them 30 seconds in PBS and immediately blocking with PBS containing 5 % normal goat serum and 0.1% Triton X-100 for at least 1 hour at RT. The primary antibodies were diluted in blocking solutions and applied on the sections followed by incubation at 4 °C, overnight. The slides were washed three times with PBS, 20 minutes each washing step. Alexa-conjugated secondary antibodies were diluted in blocking solution and the slides were incubated for 40 minutes at RT in the dark. After the application of fluorescently labeled secondary antibody, all the following steps were done avoiding light. After three washing steps a small amount of Moviol mounting shield containing DAPI was applied and the coverslide was mounted on the slide and sealed with nail polish.

9.6.4. Smear Extract Preparation

The experiment was realised according to [100].

9.6.5. Testis Suspension Preparation

The experiment was realised according to [163].

9.6.7. Immunohistochemistry of Rat Hippocampal Cells

The experiment was realised with the help of Dr. Silvio Rizzolli. The rat hippocampal culture was prepared from newborn pups according to [164]. The cells were fixed with methanol followed by conventional immunostaining with anti-TIPT and anti-synaptotagmin 1 antibodies.

9.6.8. RNase A Experiment

In order to analyze how the RNA depletion affects protein localization, an RNase A experiment was performed. Human U2OS cells were grown on coverslips in 24 well plate. The medium was aspirated, and the cells were washed twice with PBS. To permeabilize the

cells 0.1 mg saponin in PBS was applied and the cells were transferred at 4 °C for 5 minutes. After washing with PBS twice, the RNase A at 1 mg/ml in PBS was added to the cells for 10 minutes at RT. As control, PBS alone was applied. Then cells were washed with 2x PBS and fixed with methanol. Further was proceeded as described before and cells were stained with anti-TIPT, anti-NPM and anti-TBPL1 to check the localization of these proteins after RNase A treatment.

9.6.9. Cycloheximide Treatment

To check the turnover of TIPT the protein synthesis was inhibited by cycloheximide (CHX) drug. The human U2OS cells were passaged in 6 well plates at a concentration of 100,000 cells/well. The next day 10 µg /ml CHX (CHX stock solution is 100 mg/ml in DMSO) was applied. The medium was aspirated at 0, 1, 2, 23 and 47 hours and the cells were harvested by trypsinization. The total cell extract was prepared by boiling in 20 µl 2xSDS-LB. 20 µl of extract was loaded on 10% SDS-polyacrylamide gel. TIPT and α -tubulin proteins were checked by Western blotting.

9.6.10. Drug Cell Treatment

The human U2OS and mouse 3T3 cells were treated with different drugs (actinomycin D, DRB, okadaic acid) according to table 8, then fixed and stained with anti-TIPT antibodies.

9.7. Cell Transfections with Plasmids or siRNAs

9.7.1. Cell Transfection with Plasmids

The DNA plasmid was introduced in cells either by lipofection using Fugene6(Roche), or electroporation (Amaxa). The transfections were performed according to the instructions of the manufacturer.

9.7.2. Cell Transfection with siRNAs

Several siRNAs, or short hairpin vectors were used to silence TIPT mouse or human expression. The siRNAs used were pre-designed sequences from Ambion (www.ambion.com), and Qiagen (www1.qiagen.com/Products/GeneSilencing/), which were created to silence mouse TIPT RNA. In addition, four shRNA vectors were constructed to silence human TIPT RNA, using the p*Silencer* 2.0-U6 Ambion vector. The design of the

hairpin siRNAs templates was done according to Ambion recommendation and using a web-based insert design tool (http://www.ambion.com/techlib/misc/psilencer_converter.html). Another approach was to use the predesigned siRNA *SMART* pool from Dharmacon (<http://www.dharmacon.com/siGENOME/Default.aspx>).

As transfection methods were used lipofection with Oligofectamine or Dharmafect1 reagents, and nucleofection using Amaxa nucleoporator machine and buffers. The experiments were realised according to the instructions of the manufacturer.

9.8. Luciferase Assay

The luciferase assay was performed using the Dual-Luciferase Reporter Assay sytem Kit (Promega). The experiment was performed according to the according to the instructions of the manufacturer.

References

1. Crick, F. (1970). Central dogma of molecular biology. *Nature* 227, 561-563.
2. Roeder, R.G., and Rutter, W.J. (1969). Multiple forms of DNA-dependent RNA polymerase in eukaryotic organisms. *Nature* 224, 234-237.
3. Hochheimer, A., and Tjian, R. (2003). Diversified transcription initiation complexes expand promoter selectivity and tissue-specific gene expression. *Genes Dev* 17, 1309-1320.
4. Roeder, R.G. (2005). Transcriptional regulation and the role of diverse coactivators in animal cells. *FEBS Lett* 579, 909-915.
5. Thiry, M., and Lafontaine, D.L. (2005). Birth of a nucleolus: the evolution of nucleolar compartments. *Trends Cell Biol* 15, 194-199.
6. Carmo-Fonseca, M., Mendes-Soares, L., and Campos, I. (2000). To be or not to be in the nucleolus. *Nat Cell Biol* 2, E107-112.
7. Gonzalez, I.L., and Sylvester, J.E. (1995). Complete sequence of the 43-kb human ribosomal DNA repeat: analysis of the intergenic spacer. *Genomics* 27, 320-328.
8. Russell, J., and Zomerdijk, J.C. (2005). RNA-polymerase-I-directed rDNA transcription, life and works. *Trends Biochem Sci* 30, 87-96.
9. Dundr, M., and Misteli, T. (2001). Functional architecture in the cell nucleus. *Biochem J* 356, 297-310.
10. Granneman, S., and Baserga, S.J. (2005). Crosstalk in gene expression: coupling and co-regulation of rDNA transcription, pre-ribosome assembly and pre-rRNA processing. *Curr Opin Cell Biol* 17, 281-286.
11. Kopp, K., Gasiorowski, J.Z., Chen, D., Gilmore, R., Norton, J.T., Wang, C., Leary, D.J., Chan, E.K., Dean, D.A., and Huang, S. (2006). Pol I Transcription and Pre-rRNA Processing Are Coordinated in a Transcription-dependent Manner in Mammalian Cells. *Mol Biol Cell*.
12. Levine, M., and Tjian, R. (2003). Transcription regulation and animal diversity. *Nature* 424, 147-151.
13. Lander, E.S., Linton, L.M., Birren, B., Nusbaum, C., Zody, M.C., Baldwin, J., Devon, K., Dewar, K., Doyle, M., FitzHugh, et al. (2001). Initial sequencing and analysis of the human genome. *Nature* 409, 860-921.
14. Smale, S.T., and Kadonaga, J.T. (2003). The RNA polymerase II core promoter. *Annu Rev Biochem* 72, 449-479.
15. Wolner, B.S., and Gralla, J.D. (2000). Roles for non-TATA core promoter sequences in transcription and factor binding. *Mol Cell Biol* 20, 3608-3615.
16. Thomas, M.C., and Chiang, C.M. (2006). The general transcription machinery and general cofactors. *Crit Rev Biochem Mol Biol* 41, 105-178.
17. Suzuki, Y., Tsunoda, T., Sese, J., Taira, H., Mizushima-Sugano, J., Hata, H., Ota, T., Isogai, T., Tanaka, T., Nakamura, Y., Suyama, A., Sakaki, Y., Morishita, S., Okubo, K., and Sugano, S. (2001). Identification and characterization of the potential promoter regions of 1031 kinds of human genes. *Genome Res* 11, 677-684.
18. Parker, C.S., and Topol, J. (1984). A *Drosophila* RNA polymerase II transcription factor contains a promoter-region-specific DNA-binding activity. *Cell* 36, 357-369.
19. Sawadogo, M., and Roeder, R.G. (1985). Interaction of a gene-specific transcription factor with the adenovirus major late promoter upstream of the TATA box region. *Cell* 43, 165-175.

20. Bucher, P. (1990). Weight matrix descriptions of four eukaryotic RNA polymerase II promoter elements derived from 502 unrelated promoter sequences. *J Mol Biol* *212*, 563-578.
21. Benoist, C., and Chambon, P. (1981). In vivo sequence requirements of the SV40 early promoter region. *Nature* *290*, 304-310.
22. Dynlacht, B.D., Hoey, T., and Tjian, R. (1991). Isolation of coactivators associated with the TATA-binding protein that mediate transcriptional activation. *Cell* *66*, 563-576.
23. Tanese, N., Pugh, B.F., and Tjian, R. (1991). Coactivators for a proline-rich activator purified from the multisubunit human TFIID complex. *Genes Dev* *5*, 2212-2224.
24. Burley, S.K., and Roeder, R.G. (1996). Biochemistry and structural biology of transcription factor IID (TFIID). *Annu Rev Biochem* *65*, 769-799.
25. Stargell, L.A., and Struhl, K. (1996). Mechanisms of transcriptional activation in vivo: two steps forward. *Trends Genet* *12*, 311-315.
26. Bondareva, A.A., and Schmidt, E.E. (2003). Early vertebrate evolution of the TATA-binding protein, TBP. *Mol Biol Evol* *20*, 1932-1939.
27. Tamura, T., Sumita, K., Fujino, I., Aoyama, A., Horikoshi, M., Hoffmann, A., Roeder, R.G., Muramatsu, M., and Mikoshiba, K. (1991). Striking homology of the 'variable' N-terminal as well as the 'conserved core' domains of the mouse and human TATA-factors (TFIID). *Nucleic Acids Res* *19*, 3861-3865.
28. Nikolov, D.B., and Burley, S.K. (1994). 2.1 Å resolution refined structure of a TATA box-binding protein (TBP). *Nat Struct Biol* *1*, 621-637.
29. Nikolov, D.B., Hu, S.H., Lin, J., Gasch, A., Hoffmann, A., Horikoshi, M., Chua, N.H., Roeder, R.G., and Burley, S.K. (1992). Crystal structure of TFIID TATA-box binding protein. *Nature* *360*, 40-46.
30. Chasman, D.I., Flaherty, K.M., Sharp, P.A., and Kornberg, R.D. (1993). Crystal structure of yeast TATA-binding protein and model for interaction with DNA. *Proc Natl Acad Sci U S A* *90*, 8174-8178.
31. Juo, Z.S., Chiu, T.K., Leiberman, P.M., Baikalov, I., Berk, A.J., and Dickerson, R.E. (1996). How proteins recognize the TATA box. *J Mol Biol* *261*, 239-254.
32. Nikolov, D.B., Chen, H., Halay, E.D., Hoffman, A., Roeder, R.G., and Burley, S.K. (1996). Crystal structure of a human TATA box-binding protein/TATA element complex. *Proc Natl Acad Sci U S A* *93*, 4862-4867.
33. Nikolov, D.B., and Burley, S.K. (1997). RNA polymerase II transcription initiation: a structural view. *Proc Natl Acad Sci U S A* *94*, 15-22.
34. Hahn, S. (2004). Structure and mechanism of the RNA polymerase II transcription machinery. *Nat Struct Mol Biol* *11*, 394-403.
35. Buratowski, S., Hahn, S., Guarente, L., and Sharp, P.A. (1989). Five intermediate complexes in transcription initiation by RNA polymerase II. *Cell* *56*, 549-561.
36. Nikolov, D.B., Chen, H., Halay, E.D., Usheva, A.A., Hisatake, K., Lee, D.K., Roeder, R.G., and Burley, S.K. (1995). Crystal structure of a TFIIB-TBP-TATA-element ternary complex. *Nature* *377*, 119-128.
37. Bushnell, D.A., Westover, K.D., Davis, R.E., and Kornberg, R.D. (2004). Structural basis of transcription: an RNA polymerase II-TFIIB cocrystal at 4.5 Å. *Science* *303*, 983-988.
38. Lagrange, T., Kapanidis, A.N., Tang, H., Reinberg, D., and Ebright, R.H. (1998). New core promoter element in RNA polymerase II-dependent transcription: sequence-specific DNA binding by transcription factor IIB. *Genes Dev* *12*, 34-44.

39. Tsai, F.T., and Sigler, P.B. (2000). Structural basis of preinitiation complex assembly on human pol II promoters. *Embo J* 19, 25-36.
40. Deng, W., and Roberts, S.G. (2005). A core promoter element downstream of the TATA box that is recognized by TFIIB. *Genes Dev* 19, 2418-2423.
41. Muller, F., Lakatos, L., Dantonel, J., Strahle, U., and Tora, L. (2001). TBP is not universally required for zygotic RNA polymerase II transcription in zebrafish. *Curr Biol* 11, 282-287.
42. Veenstra, G.J., Weeks, D.L., and Wolffe, A.P. (2000). Distinct roles for TBP and TBP-like factor in early embryonic gene transcription in *Xenopus*. *Science* 290, 2312-2315.
43. Martianov, I., Brancorsini, S., Gansmuller, A., Parvinen, M., Davidson, I., and Sassone-Corsi, P. (2002). Distinct functions of TBP and TLF/TRF2 during spermatogenesis: requirement of TLF for heterochromatic chromocenter formation in haploid round spermatids. *Development* 129, 945-955.
44. Crowley, T.E., Hoey, T., Liu, J.K., Jan, Y.N., Jan, L.Y., and Tjian, R. (1993). A new factor related to TATA-binding protein has highly restricted expression patterns in *Drosophila*. *Nature* 361, 557-561.
45. Hansen, S.K., Takada, S., Jacobson, R.H., Lis, J.T., and Tjian, R. (1997). Transcription properties of a cell type-specific TATA-binding protein, TRF. *Cell* 91, 71-83.
46. Persengiev, S.P., Zhu, X., Dixit, B.L., Maston, G.A., Kittler, E.L., and Green, M.R. (2003). TRF3, a TATA-box-binding protein-related factor, is vertebrate-specific and widely expressed. *Proc Natl Acad Sci U S A* 100, 14887-14891.
47. Bartfai, R., Balduf, C., Hilton, T., Rathmann, Y., Hadzhiev, Y., Tora, L., Orban, L., and Muller, F. (2004). TBP2, a vertebrate-specific member of the TBP family, is required in embryonic development of zebrafish. *Curr Biol* 14, 593-598.
48. Jallow, Z., Jacobi, U.G., Weeks, D.L., Dawid, I.B., and Veenstra, G.J. (2004). Specialized and redundant roles of TBP and a vertebrate-specific TBP paralog in embryonic gene regulation in *Xenopus*. *Proc Natl Acad Sci U S A* 101, 13525-13530.
49. Yang, Y., Cao, J., Huang, L., Fang, H.Y., and Sheng, H.Z. (2006). Regulated expression of TATA-binding protein-related factor 3 (TRF3) during early embryogenesis. *Cell Res* 16, 610-621.
50. Dantonel, J.C., Wurtz, J.M., Poch, O., Moras, D., and Tora, L. (1999). The TBP-like factor: an alternative transcription factor in metazoa? *Trends Biochem Sci* 24, 335-339.
51. Dantonel, J.C., Quintin, S., Lakatos, L., Labouesse, M., and Tora, L. (2000). TBP-like factor is required for embryonic RNA polymerase II transcription in *C. elegans*. *Mol Cell* 6, 715-722.
52. Kaltenbach, L., Horner, M.A., Rothman, J.H., and Mango, S.E. (2000). The TBP-like factor CeTLF is required to activate RNA polymerase II transcription during *C. elegans* embryogenesis. *Mol Cell* 6, 705-713.
53. Ohbayashi, T., Kishimoto, T., Makino, Y., Shimada, M., Nakadai, T., Aoki, T., Kawata, T., Niwa, S., and Tamura, T. (1999). Isolation of cDNA, chromosome mapping, and expression of the human TBP-like protein. *Biochem Biophys Res Commun* 255, 137-142.
54. Ohbayashi, T., Makino, Y., and Tamura, T.A. (1999). Identification of a mouse TBP-like protein (TLP) distantly related to the drosophila TBP-related factor. *Nucleic Acids Res* 27, 750-755.

55. Rabenstein, M.D., Zhou, S., Lis, J.T., and Tjian, R. (1999). TATA box-binding protein (TBP)-related factor 2 (TRF2), a third member of the TBP family. *Proc Natl Acad Sci U S A* *96*, 4791-4796.
56. Teichmann, M., Wang, Z., Martinez, E., Tjernberg, A., Zhang, D., Vollmer, F., Chait, B.T., and Roeder, R.G. (1999). Human TATA-binding protein-related factor-2 (hTRF2) stably associates with hTFIIA in HeLa cells. *Proc Natl Acad Sci U S A* *96*, 13720-13725.
57. Moore, P.A., Ozer, J., Salunek, M., Jan, G., Zerby, D., Campbell, S., and Lieberman, P.M. (1999). A human TATA binding protein-related protein with altered DNA binding specificity inhibits transcription from multiple promoters and activators. *Mol Cell Biol* *19*, 7610-7620.
58. Guillebault, D., Sasorith, S., Derelle, E., Wurtz, J.M., Lozano, J.C., Bingham, S., Tora, L., and Moreau, H. (2002). A new class of transcription initiation factors, intermediate between TATA box-binding proteins (TBPs) and TBP-like factors (TLFs), is present in the marine unicellular organism, the dinoflagellate *Cryptothecodinium cohnii*. *J Biol Chem* *277*, 40881-40886.
59. Hochheimer, A., Zhou, S., Zheng, S., Holmes, M.C., and Tjian, R. (2002). TRF2 associates with DREF and directs promoter-selective gene expression in *Drosophila*. *Nature* *420*, 439-445.
60. Shimada, M., Nakadai, T., and Tamura, T.A. (2003). TATA-binding protein-like protein (TLP/TRF2/TLF) negatively regulates cell cycle progression and is required for the stress-mediated G(2) checkpoint. *Mol Cell Biol* *23*, 4107-4120.
61. Kopytova, D.V., Krasnov, A.N., Kopantceva, M.R., Nabirochkina, E.N., Nikolenko, J.V., Maksimenko, O., Kurshakova, M.M., Lebedeva, L.A., Yerokhin, M.M., Simonova, O.B., Korochkin, L.I., Tora, L., Georgiev, P.G., and Georgieva, S.G. (2006). Two isoforms of *Drosophila* TRF2 are involved in embryonic development, premeiotic chromatin condensation, and proper differentiation of germ cells of both sexes. *Mol Cell Biol* *26*, 7492-7505.
62. Ohbayashi, T., Shimada, M., Nakadai, T., Wada, T., Handa, H., and Tamura, T. (2003). Vertebrate TBP-like protein (TLP/TRF2/TLF) stimulates TATA-less terminal deoxynucleotidyl transferase promoters in a transient reporter assay, and TFIIA-binding capacity of TLP is required for this function. *Nucleic Acids Res* *31*, 2127-2133.
63. Chong, J.A., Moran, M.M., Teichmann, M., Kaczmarek, J.S., Roeder, R., and Clapham, D.E. (2005). TATA-binding protein (TBP)-like factor (TLF) is a functional regulator of transcription: reciprocal regulation of the neurofibromatosis type 1 and c-fos genes by TLF/TRF2 and TBP. *Mol Cell Biol* *25*, 2632-2643.
64. Nakadai, T., Shimada, M., Shima, D., Handa, H., and Tamura, T.A. (2004). Specific interaction with transcription factor IIA and localization of the mammalian TATA-binding protein-like protein (TLP/TRF2/TLF). *J Biol Chem* *279*, 7447-7455.
65. Kieffer-Kwon, P., Martianov, I., and Davidson, I. (2004). Cell-specific nucleolar localization of TBP-related factor 2. *Mol Biol Cell* *15*, 4356-4368.
66. Tanaka, Y., Nanba, Y.A., Park, K.A., Mabuchi, T., Suenaga, Y., Shiraishi, S., Shimada, M., Nakadai, T., and Tamura, T.A. (2006). Transcriptional repression of the mouse *wee1* gene by TBP-related factor 2. *Biochem Biophys Res Commun*.
67. Martianov, I., Fimia, G.M., Dierich, A., Parvinen, M., Sassone-Corsi, P., and Davidson, I. (2001). Late arrest of spermiogenesis and germ cell apoptosis in mice lacking the TBP-like TLF/TRF2 gene. *Mol Cell* *7*, 509-515.

68. Zhang, D., Penttilä, T.L., Morris, P.L., and Roeder, R.G. (2001). Cell- and stage-specific high-level expression of TBP-related factor 2 (TRF2) during mouse spermatogenesis. *Mech Dev* 106, 203-205.
69. Nebel, B.R., Amarose, A.P., and Hackett, E.M. (1961). Calendar of gametogenic development in the prepuberal male mouse. *Science* 134, 832-833.
70. Bellve, A.R., Cavicchia, J.C., Millette, C.F., O'Brien, D.A., Bhatnagar, Y.M., and Dym, M. (1977). Spermatogenic cells of the prepuberal mouse. Isolation and morphological characterization. *J Cell Biol* 74, 68-85.
71. Kimmins, S., and Sassone-Corsi, P. (2005). Chromatin remodelling and epigenetic features of germ cells. *Nature* 434, 583-589.
72. Sassone-Corsi, P. (2002). Unique chromatin remodeling and transcriptional regulation in spermatogenesis. *Science* 296, 2176-2178.
73. Pirrotta, V. (1997). PcG complexes and chromatin silencing. *Curr Opin Genet Dev* 7, 249-258.
74. Francis, N.J., Saurin, A.J., Shao, Z., and Kingston, R.E. (2001). Reconstitution of a functional core polycomb repressive complex. *Mol Cell* 8, 545-556.
75. Shao, Z., Raible, F., Mollaaghababa, R., Guyon, J.R., Wu, C.T., Bender, W., and Kingston, R.E. (1999). Stabilization of chromatin structure by PRC1, a Polycomb complex. *Cell* 98, 37-46.
76. Kuzmichev, A., Nishioka, K., Erdjument-Bromage, H., Tempst, P., and Reinberg, D. (2002). Histone methyltransferase activity associated with a human multiprotein complex containing the Enhancer of Zeste protein. *Genes Dev* 16, 2893-2905.
77. Muller, J., Hart, C.M., Francis, N.J., Vargas, M.L., Sengupta, A., Wild, B., Miller, E.L., O'Connor, M.B., Kingston, R.E., and Simon, J.A. (2002). Histone methyltransferase activity of a Drosophila Polycomb group repressor complex. *Cell* 111, 197-208.
78. Cao, R., Wang, L., Wang, H., Xia, L., Erdjument-Bromage, H., Tempst, P., Jones, R.S., and Zhang, Y. (2002). Role of histone H3 lysine 27 methylation in Polycomb-group silencing. *Science* 298, 1039-1043.
79. Wang, H., Wang, L., Erdjument-Bromage, H., Vidal, M., Tempst, P., Jones, R.S., and Zhang, Y. (2004). Role of histone H2A ubiquitination in Polycomb silencing. *Nature* 431, 873-878.
80. Lee, T.I., Jenner, R.G., Boyer, L.A., Guenther, M.G., Levine, S.S., Kumar, R.M., Chevalier, B., Johnstone, S.E., Cole, M.F., Isono, K., Koseki, H., Fuchikami, T., Abe, K., Murray, H.L., Zucker, J.P., Yuan, B., Bell, G.W., Herbolzheimer, E., Hannett, N.M., Sun, K., Odom, D.T., Otte, A.P., Volkert, T.L., Bartel, D.P., Melton, D.A., Gifford, D.K., Jaenisch, R., and Young, R.A. (2006). Control of developmental regulators by Polycomb in human embryonic stem cells. *Cell* 125, 301-313.
81. Boyer, L.A., Plath, K., Zeitlinger, J., Brambrink, T., Medeiros, L.A., Lee, T.I., Levine, S.S., Wernig, M., Tajonar, A., Ray, M.K., Bell, G.W., Otte, A.P., Vidal, M., Gifford, D.K., Young, R.A., and Jaenisch, R. (2006). Polycomb complexes repress developmental regulators in murine embryonic stem cells. *Nature* 441, 349-353.
82. Bracken, A.P., Dietrich, N., Pasini, D., Hansen, K.H., and Helin, K. (2006). Genome-wide mapping of Polycomb target genes unravels their roles in cell fate transitions. *Genes Dev* 20, 1123-1136.
83. Saurin, A.J., Shao, Z., Erdjument-Bromage, H., Tempst, P., and Kingston, R.E. (2001). A Drosophila Polycomb group complex includes Zeste and dTAFII proteins. *Nature* 412, 655-660.

84. Breiling, A., Turner, B.M., Bianchi, M.E., and Orlando, V. (2001). General transcription factors bind promoters repressed by Polycomb group proteins. *Nature* 412, 651-655.
85. Dellino, G.I., Schwartz, Y.B., Farkas, G., McCabe, D., Elgin, S.C., and Pirrotta, V. (2004). Polycomb silencing blocks transcription initiation. *Mol Cell* 13, 887-893.
86. Luo, L., and Kessel, M. (2004). Geminin coordinates cell cycle and developmental control. *Cell Cycle* 3, 711-714.
87. Luo, L., Yang, X., Takihara, Y., Knoetgen, H., and Kessel, M. (2004). The cell-cycle regulator geminin inhibits Hox function through direct and polycomb-mediated interactions. *Nature* 427, 749-753.
88. Del Bene, F., Tessmar-Raible, K., and Wittbrodt, J. (2004). Direct interaction of geminin and Six3 in eye development. *Nature* 427, 745-749.
89. McGarry, T.J., and Kirschner, M.W. (1998). Geminin, an inhibitor of DNA replication, is degraded during mitosis. *Cell* 93, 1043-1053.
90. Wohlschlegel, J.A., Dwyer, B.T., Dhar, S.K., Cvetic, C., Walter, J.C., and Dutta, A. (2000). Inhibition of eukaryotic DNA replication by geminin binding to Cdt1. *Science* 290, 2309-2312.
91. Tachibana, K.E., Gonzalez, M.A., Guarguaglini, G., Nigg, E.A., and Laskey, R.A. (2005). Depletion of licensing inhibitor geminin causes centrosome overduplication and mitotic defects. *EMBO Rep* 6, 1052-1057.
92. Seo, S., Herr, A., Lim, J.W., Richardson, G.A., Richardson, H., and Kroll, K.L. (2005). Geminin regulates neuronal differentiation by antagonizing Brg1 activity. *Genes Dev* 19, 1723-1734.
93. Kroll, K.L., Salic, A.N., Evans, L.M., and Kirschner, M.W. (1998). Geminin, a neuralizing molecule that demarcates the future neural plate at the onset of gastrulation. *Development* 125, 3247-3258.
94. Kim, M.Y., Jeong, B.C., Lee, J.H., Kee, H.J., Kook, H., Kim, N.S., Kim, Y.H., Kim, J.K., Ahn, K.Y., and Kim, K.K. (2006). A repressor complex, AP4 transcription factor and geminin, negatively regulates expression of target genes in nonneuronal cells. *Proc Natl Acad Sci U S A* 103, 13074-13079.
95. Zandomeni, R., Zandomeni, M.C., Shugar, D., and Weinmann, R. (1986). Casein kinase type II is involved in the inhibition by 5,6-dichloro-1-beta-D-ribofuranosylbenzimidazole of specific RNA polymerase II transcription. *J Biol Chem* 261, 3414-3419.
96. Zimmerman, S., Steding, G., Emmen, J.M., Brinkmann, A.O., Nayernia, K., Holstein, A.F., Engel, W., Adham, I.M. (1999). Targeted disruption of the *Insl3* gene causes bilateral cryptorchidism. *Mol Endocrinol* 13, 681-691.
97. Loveland, K.L., and Schlatt, S. (1997). Stem cell factor and c-kit in the mammalian testis: lessons originating from Mother Nature's gene knockouts. *J Endocrinol* 153, 337-344.
98. Cebra-Thomas, J.A., Decker, C.L., Snyder, L.C., Pilder, S.H., and Silver, L.M. (1991). Allele- and haploid-specific product generated by alternative splicing from a mouse t complex responder locus candidate. *Nature* 349, 239-241.
99. Huynh, T., Mollard, R., and Trounson, A. (2002). Selected genetic factors associated with male infertility. *Hum Reprod Update* 8, 183-198.
100. Nayernia, K., Diaconu, M., Aumuller, G., Wennemuth, G., Schwandt, I., Kleene, K., Kuehn, H., and Engel, W. (2004). Phospholipid hydroperoxide glutathione peroxidase: expression pattern during testicular development in mouse and evolutionary conservation in spermatozoa. *Mol Reprod Dev* 67, 458-464.

101. Eward, K.L., Obermann, E.C., Shreeram, S., Loddo, M., Fanshawe, T., Williams, C., Jung, H.I., Prevost, A.T., Blow, J.J., Stoeber, K., and Williams, G.H. (2004). DNA replication licensing in somatic and germ cells. *J Cell Sci* 117, 5875-5886.
102. Linder, B., Jones, L.K., Chaplin, T., Mohd-Sarip, A., Heinlein, U.A., Young, B.D., and Saha, V. (1998). Expression pattern and cellular distribution of the murine homologue of AF10. *Biochim Biophys Acta* 1443, 285-296.
103. Zhao, M., Shirley, C.R., Yu, Y.E., Mohapatra, B., Zhang, Y., Unni, E., Deng, J.M., Arango, N.A., Terry, N.H., Weil, M.M., Russell, L.D., Behringer, R.R., and Meistrich, M.L. (2001). Targeted disruption of the transition protein 2 gene affects sperm chromatin structure and reduces fertility in mice. *Mol Cell Biol* 21, 7243-7255.
104. Schiebel, E. (2000). gamma-tubulin complexes: binding to the centrosome, regulation and microtubule nucleation. *Curr Opin Cell Biol* 12, 113-118.
105. Brinkley, B.R., Cox, S.M., Pepper, D.A., Wible, L., Brenner, S.L., and Pardue, R.L. (1981). Tubulin assembly sites and the organization of cytoplasmic microtubules in cultured mammalian cells. *J Cell Biol* 90, 554-562.
106. Serebriiskii, I.G., and Golemis, E.A. (2001). Two-hybrid system and false positives. Approaches to detection and elimination. *Methods Mol Biol* 177, 123-134.
107. Chaplin, T., Bernard, O., Beverloo, H.B., Saha, V., Hagemeijer, A., Berger, R., and Young, B.D. (1995). The t(10;11) translocation in acute myeloid leukemia (M5) consistently fuses the leucine zipper motif of AF10 onto the HRX gene. *Blood* 86, 2073-2076.
108. Dreyling, M.H., Martinez-Climent, J.A., Zheng, M., Mao, J., Rowley, J.D., and Bohlander, S.K. (1996). The t(10;11)(p13;q14) in the U937 cell line results in the fusion of the AF10 gene and CALM, encoding a new member of the AP-3 clathrin assembly protein family. *Proc Natl Acad Sci U S A* 93, 4804-4809.
109. Okada, Y., Feng, Q., Lin, Y., Jiang, Q., Li, Y., Coffield, V.M., Su, L., Xu, G., and Zhang, Y. (2005). hDOT1L links histone methylation to leukemogenesis. *Cell* 121, 167-178.
110. de Bruijn, D.R., dos Santos, N.R., Thijssen, J., Balemans, M., Debernardi, S., Linder, B., Young, B.D., and Geurts van Kessel, A. (2001). The synovial sarcoma associated protein SYT interacts with the acute leukemia associated protein AF10. *Oncogene* 20, 3281-3289.
111. Herrera, J.E., Savkur, R., and Olson, M.O. (1995). The ribonuclease activity of nucleolar protein B23. *Nucleic Acids Res* 23, 3974-3979.
112. Zhang, S., Kohler, C., Hemmerich, P., and Grosse, F. (2004). Nuclear DNA helicase II (RNA helicase A) binds to an F-actin containing shell that surrounds the nucleolus. *Exp Cell Res* 293, 248-258.
113. Blangy, A., Lane, H.A., d'Herin, P., Harper, M., Kress, M., and Nigg, E.A. (1995). Phosphorylation by p34cdc2 regulates spindle association of human Eg5, a kinesin-related motor essential for bipolar spindle formation in vivo. *Cell* 83, 1159-1169.
114. Okuda, M., Horn, H.F., Tarapore, P., Tokuyama, Y., Smulian, A.G., Chan, P.K., Knudsen, E.S., Hofmann, I.A., Snyder, J.D., Bove, K.E., and Fukasawa, K. (2000). Nucleophosmin/B23 is a target of CDK2/cyclin E in centrosome duplication. *Cell* 103, 127-140.
115. Montanari, M., Boninsegna, A., Faraglia, B., Coco, C., Giordano, A., Cittadini, A., and Sgambato, A. (2005). Increased expression of geminin stimulates the growth of mammary epithelial cells and is a frequent event in human tumors. *J Cell Physiol* 202, 215-222.

116. Um, M., Yamauchi, J., Kato, S., and Manley, J.L. (2001). Heterozygous disruption of the TATA-binding protein gene in DT40 cells causes reduced cdc25B phosphatase expression and delayed mitosis. *Mol Cell Biol* 21, 2435-2448.
117. Perry, R.P. (1962). The Cellular Sites of Synthesis of Ribosomal and 4s Rna. *Proc Natl Acad Sci U S A* 48, 2179-2186.
118. Liu, X., and Berk, A.J. (1995). Reversal of in vitro p53 sequestration by both TFIIB and TFIID. *Mol Cell Biol* 15, 6474-6478.
119. Bleichenbacher, M., Tan, S., and Richmond, T.J. (2003). Novel interactions between the components of human and yeast TFIIA/TBP/DNA complexes. *J Mol Biol* 332, 783-793.
120. Hajra, A., Martin-Gallardo, A., Tarle, S.A., Freedman, M., Wilson-Gunn, S., Bernards, A., and Collins, F.S. (1994). DNA sequences in the promoter region of the NF1 gene are highly conserved between human and mouse. *Genomics* 21, 649-652.
121. Estivill-Torrus, G., Pearson, H., van Heyningen, V., Price, D.J., and Rashbass, P. (2002). Pax6 is required to regulate the cell cycle and the rate of progression from symmetrical to asymmetrical division in mammalian cortical progenitors. *Development* 129, 455-466.
122. Frederiksen, K., and McKay, R.D. (1988). Proliferation and differentiation of rat neuroepithelial precursor cells in vivo. *J Neurosci* 8, 1144-1151.
123. Geschwind, D.H., and Hockfield, S. (1989). Identification of proteins that are developmentally regulated during early cerebral corticogenesis in the rat. *J Neurosci* 9, 4303-4317.
124. Lendahl, U., Zimmerman, L.B., and McKay, R.D. (1990). CNS stem cells express a new class of intermediate filament protein. *Cell* 60, 585-595.
125. Nishitani, H., Taraviras, S., Lygerou, Z., and Nishimoto, T. (2001). The human licensing factor for DNA replication Cdt1 accumulates in G1 and is destabilized after initiation of S-phase. *J Biol Chem* 276, 44905-44911.
126. Hiller, M.A., Lin, T.Y., Wood, C., and Fuller, M.T. (2001). Developmental regulation of transcription by a tissue-specific TAF homolog. *Genes Dev* 15, 1021-1030.
127. Chen, X., Hiller, M., Sancak, Y., and Fuller, M.T. (2005). Tissue-specific TAFs counteract Polycomb to turn on terminal differentiation. *Science* 310, 869-872.
128. Hiller, M., Chen, X., Pringle, M.J., Suchorolski, M., Sancak, Y., Viswanathan, S., Bolival, B., Lin, T.Y., Marino, S., and Fuller, M.T. (2004). Testis-specific TAF homologs collaborate to control a tissue-specific transcription program. *Development* 131, 5297-5308.
129. Muller, F., and Tora, L. (2004). The multicoloured world of promoter recognition complexes. *Embo J* 23, 2-8.
130. Xiao, L., Kim, M., and DeJong, J. (2006). Developmental and cell type-specific regulation of core promoter transcription factors in germ cells of frogs and mice. *Gene Expr Patterns* 6, 409-419.
131. Catena, R., Argentini, M., Martianov, I., Parello, C., Brancorsini, S., Parvinen, M., Sassone-Corsi, P., and Davidson, I. (2005). Proteolytic cleavage of ALF into alpha- and beta-subunits that form homologous and heterologous complexes with somatic TFIIA and TRF2 in male germ cells. *FEBS Lett* 579, 3401-3410.
132. Coute, Y., Burgess, J.A., Diaz, J.J., Chichester, C., Lisacek, F., Greco, A., and Sanchez, J.C. (2006). Deciphering the human nucleolar proteome. *Mass Spectrom Rev* 25, 215-234.

133. Andersen, J.S., Lyon, C.E., Fox, A.H., Leung, A.K., Lam, Y.W., Steen, H., Mann, M., and Lamond, A.I. (2002). Directed proteomic analysis of the human nucleolus. *Curr Biol* 12, 1-11.
134. Andersen, J.S., Lam, Y.W., Leung, A.K., Ong, S.E., Lyon, C.E., Lamond, A.I., and Mann, M. (2005). Nucleolar proteome dynamics. *Nature* 433, 77-83.
135. Scherl, A., Coute, Y., Deon, C., Calle, A., Kindbeiter, K., Sanchez, J.C., Greco, A., Hochstrasser, D., and Diaz, J.J. (2002). Functional proteomic analysis of human nucleolus. *Mol Biol Cell* 13, 4100-4109.
136. Corsetti, M.T., Levi, G., Lancia, F., Sanseverino, L., Ferrini, S., Boncinelli, E., and Corte, G. (1995). Nucleolar localisation of three Hox homeoproteins. *J Cell Sci* 108 (Pt 1), 187-193.
137. Andersen, J.S., Wilkinson, C.J., Mayor, T., Mortensen, P., Nigg, E.A., and Mann, M. (2003). Proteomic characterization of the human centrosome by protein correlation profiling. *Nature* 426, 570-574.
138. Wong, C., and Stearns, T. (2003). Centrosome number is controlled by a centrosome-intrinsic block to reduplication. *Nat Cell Biol* 5, 539-544.
139. Tachibana, K.E., and Nigg, E.A. (2006). Geminin regulates multiple steps of the chromosome inheritance cycle. *Cell Cycle* 5, 151-154.
140. Le Guellec, R., Paris, J., Couturier, A., Roghi, C., and Philippe, M. (1991). Cloning by differential screening of a *Xenopus* cDNA that encodes a kinesin-related protein. *Mol Cell Biol* 11, 3395-3398.
141. Sawin, K.E., and Mitchison, T.J. (1995). Mutations in the kinesin-like protein Eg5 disrupting localization to the mitotic spindle. *Proc Natl Acad Sci U S A* 92, 4289-4293.
142. Debernardi, S., Bassini, A., Jones, L.K., Chaplin, T., Linder, B., de Bruijn, D.R., Meese, E., and Young, B.D. (2002). The MLL fusion partner AF10 binds GAS41, a protein that interacts with the human SWI/SNF complex. *Blood* 99, 275-281.
143. Thaete, C., Brett, D., Monaghan, P., Whitehouse, S., Rennie, G., Rayner, E., Cooper, C.S., and Goodwin, G. (1999). Functional domains of the SYT and SYT-SSX synovial sarcoma translocation proteins and co-localization with the SNF protein BRM in the nucleus. *Hum Mol Genet* 8, 585-591.
144. King, I.F., Francis, N.J., and Kingston, R.E. (2002). Native and recombinant polycomb group complexes establish a selective block to template accessibility to repress transcription in vitro. *Mol Cell Biol* 22, 7919-7928.
145. Zhou, B.B., and Elledge, S.J. (2000). The DNA damage response: putting checkpoints in perspective. *Nature* 408, 433-439.
146. Zatsepina, O.V., Voit, R., Grummt, I., Spring, H., Semenov, M.V., and Trendelenburg, M.F. (1993). The RNA polymerase I-specific transcription initiation factor UBF is associated with transcriptionally active and inactive ribosomal genes. *Chromosoma* 102, 599-611.
147. Jordan, M.A., Wendell, K., Gardiner, S., Derry, W.B., Copp, H., and Wilson, L. (1996). Mitotic block induced in HeLa cells by low concentrations of paclitaxel (Taxol) results in abnormal mitotic exit and apoptotic cell death. *Cancer Res* 56, 816-825.
148. Gebrane-Younes, J., Fomproix, N., and Hernandez-Verdun, D. (1997). When rDNA transcription is arrested during mitosis, UBF is still associated with non-condensed rDNA. *J Cell Sci* 110 (Pt 19), 2429-2440.

149. Lee, M.S., Henry, M., and Silver, P.A. (1996). A protein that shuttles between the nucleus and the cytoplasm is an important mediator of RNA export. *Genes Dev* 10, 1233-1246.
150. Hayano, T., Yanagida, M., Yamauchi, Y., Shinkawa, T., Isobe, T., and Takahashi, N. (2003). Proteomic analysis of human Nop56p-associated pre-ribosomal ribonucleoprotein complexes. Possible link between Nop56p and the nucleolar protein treacle responsible for Treacher Collins syndrome. *J Biol Chem* 278, 34309-34319.
151. Yanagida, M., Shimamoto, A., Nishikawa, K., Furuichi, Y., Isobe, T., and Takahashi, N. (2001). Isolation and proteomic characterization of the major proteins of the nucleolin-binding ribonucleoprotein complexes. *Proteomics* 1, 1390-1404.
152. Waslylyk, B., Kedinger, C., Corden, J., Brison, O., and Chambon, P. (1980). Specific in vitro initiation of transcription on conalbumin and ovalbumin genes and comparison with adenovirus-2 early and late genes. *Nature* 285, 367-373.
153. Bensimhon, M., Gabarro-Arpa, J., Ehrlich, R., and Reiss, C. (1983). Physical characteristics in eucaryotic promoters. *Nucleic Acids Res* 11, 4521-4540.
154. Inostroza, J.A., Mermelstein, F.H., Ha, I., Lane, W.S., and Reinberg, D. (1992). Dr1, a TATA-binding protein-associated phosphoprotein and inhibitor of class II gene transcription. *Cell* 70, 477-489.
155. Auble, D.T., Hansen, K.E., Mueller, C.G., Lane, W.S., Thorner, J., and Hahn, S. (1994). Mot1, a global repressor of RNA polymerase II transcription, inhibits TBP binding to DNA by an ATP-dependent mechanism. *Genes Dev* 8, 1920-1934.
156. Kokubo, T., Yamashita, S., Horikoshi, M., Roeder, R.G., and Nakatani, Y. (1994). Interaction between the N-terminal domain of the 230-kDa subunit and the TATA box-binding subunit of TFIID negatively regulates TATA-box binding. *Proc Natl Acad Sci U S A* 91, 3520-3524.
157. Liu, D., Ishima, R., Tong, K.I., Bagby, S., Kokubo, T., Muhandiram, D.R., Kay, L.E., Nakatani, Y., and Ikura, M. (1998). Solution structure of a TBP-TAF(II)230 complex: protein mimicry of the minor groove surface of the TATA box unwound by TBP. *Cell* 94, 573-583.
158. Campillos, M., Garcia, M.A., Valdivieso, F., and Vazquez, J. (2003). Transcriptional activation by AP-2alpha is modulated by the oncogene DEK. *Nucleic Acids Res* 31, 1571-1575.
159. Wu, L., Wu, H., Ma, L., Sangiorgi, F., Wu, N., Bell, J.R., Lyons, G.E., and Maxson, R. (1997). Miz1, a novel zinc finger transcription factor that interacts with Msx2 and enhances its affinity for DNA. *Mech Dev* 65, 3-17.
160. Grueneberg, D.A., Natesan, S., Alexandre, C., and Gilman, M.Z. (1992). Human and Drosophila homeodomain proteins that enhance the DNA-binding activity of serum response factor. *Science* 257, 1089-1095.
161. Murphy, D.J., Hardy, S., and Engel, D.A. (1999). Human SWI-SNF component BRG1 represses transcription of the c-fos gene. *Mol Cell Biol* 19, 2724-2733.
162. Trouche, D., Le Chalony, C., Muchardt, C., Yaniv, M., and Kouzarides, T. (1997). RB and hbrm cooperate to repress the activation functions of E2F1. *Proc Natl Acad Sci U S A* 94, 11268-11273.
163. Nayernia, K., Vauti, F., Meinhardt, A., Cadenas, C., Schweyer, S., Meyer, B.I., Schwandt, I., Chowdhury, K., Engel, W., and Arnold, H.H. (2003). Inactivation of a testis-specific Lis1 transcript in mice prevents spermatid differentiation and causes male infertility. *J Biol Chem* 278, 48377-48385.

164. Rizzoli, S.O., Bethani, I., Zwillig, D., Wenzel, D., Siddiqui, T.J., Brandhorst, D., and Jahn, R. (2006). Evidence for early endosome-like fusion of recently endocytosed synaptic vesicles. *Traffic* 7, 1163-1176.

Appendices

1. Chemicals

<i>Product name</i>	<i>Description</i>	<i>Stock concentration</i>	<i>Working concentration</i>	<i>Time</i>
DRB	Inhibits protein kinase (CKII inhibitor; Pol II transcription inhibitor)	25 mg/ml	50 µg/ml	1 h
			5 mM	15 min
Okadaic acid	Inhibits Ser/Thr protein phosphatase 1	10 µM	10 nM	6 h/24h
Actinomycin D	Inhibits rRNA synthesis	1 mg/ml	0.04 µg/ml	30 min
	Inhibits total RNA synthesis		0.04 µg/ml	17 h
RNase A	Degrades single-stranded RNA	10 mg/ml	10 µg/ml	10 min
Cycloheximide	Inhibits protein synthesis	100 mg/ml	10 µg/ml	0-47 h
Aphidicolin	Blocks G1/S phase transition	10 mg/ml	10 µg/ml	19 h

Table 8. The drugs applied to cells.

2. Cell lines

<i>Cell line name</i>	<i>Description</i>	<i>Specie</i>	<i>Cell culture medium (Gibco BRL)</i>
U2OS	Osteosarcoma cells	Human	McCoy's +1.5 mM L-glutamine + 10% FCS
HA-TIPT (clones 1-17)	Osteosarcoma cells overexpressing mouse HA-TIPT	Human	McCoy's +1.5 mM L-glutamine + 10% FCS + 250 µg/ml G418
HeLa	Cervical cancer cells	Human	DMEM+ 2 mM L-glutamine+ 4.5 mg/ml glucose +10 % FCS
HEK 293T	Adenotransformed embryonic kidney cells	Human	DMEM+ 10 % FCS +1% L-glutamine
NIH3T3; SNL	Fibroblasts	Mouse	DMEM+ 4 mM L-glutamine+ 4.5 mg/ml glucose +10 % FCS
Cos-7	SV40-transformed fibroblasts	Monkey	DMEM+ 4 mM L-glutamine+ 4.5 mg/ml glucose +10 % FCS

Table 9. The cell lines used in the study.

3. Primary antibodies

<i>Name</i>	<i>Host and antibody type</i>	<i>Working dilution- WB</i>	<i>Working dilution- IHC</i>	<i>Company/source</i>
Anti-AF10	Mouse monoclonal	1:500		Abcam
Anti-Flag	Rabbit polyclonal	1:500	1:1000	Sigma
Anti-GAL4 DNA-BD	Mouse monoclonal	1:4000		BD Bioscience
Anti-GAL4 DNA-AD	Mouse monoclonal	1:4000		BD Bioscience
Anti-geminin (FL-209)	Rabbit polyclonal	1:500-1:1000		Santa-Cruz
Anti-geminin	Rabbit polyclonal	1:500-1:1000		Lingfei Luo
Anti-GFP	Mouse monoclonal	1:1000		Chemicon
Anti-GFP	Mouse monoclonal	1:1000		MoBiTec
Anti-GFP	Mouse monoclonal	1:1000		Roche
Anti-GST	Mouse monoclonal	1:10000		Novagen
Anti-HA (3F10)	Rat monoclonal	1:500	1:250	Roche
Anti-NPM	Mouse monoclonal	1:500	1:200	Abcam
Anti-TBP (3G3)	Mouse monoclonal	1:5000		Irwin Davidson
Anti-TBP	Mouse monoclonal	1:5000		Martin Teichmann
Anti-TBPL1 (2A1)	Mouse monoclonal	1:500	1:100	Irwin Davidson
Anti-TFIIA	Mouse monoclonal	1:3000		Martin Teichmann
Anti-TIPT	Rabbit polyclonal	1:500-1:1000	1:100-1:1000	Mara Pitulescu
Anti- α -tubulin	Mouse monoclonal	1:4000		Sigma
Anti- γ -tubulin (GTU-88)	Mouse monoclonal		1:100-1:200	Abcam

Table 10. The primary antibodies used in this study.

Abbreviations

AA: acrylamide-bisacrylamide
3AT: 3-amino-1, 2, 4-triazole
ActD: actinomycin D
AdE4: adenovirus E4 promoter
AdMLP: adenovirus major late promoter
APS: ammonium persulphate
ATM: ataxia telangectasia mutated
bHLH: basic helix-loop-helix
bp: base pair
BRE: TFIIB binding element
BRE^d: BRE downstream
BRE^u: BRE upstream
C: cytoplasmic fraction
ChIP: chromatin immunoprecipitation
CHX: cycloheximide
CKII: casein kinase II
cpm: counts per minute
DAPI: 4,6-diamidino-2-phenylindol
DEPC: diethyl pyrocarbonate
DIG: digoxigenin
DMEM: Dulbecco's modified Eagle's medium
DMSO: dimethylsulfoxide
DPE: downstream promoter element
dpp: days post-partum
DRB: 5,6-dichloro-1-beta-D-ribofuranosylbenzimidazole
EDTA: ethylenediaminetetraacetic acid
EGFP: enhanced green fluorescence protein
FACS: Fluorescence-activated cell sorting
FCS: fetal calf serum
GFP: green fluorescent protein
Gmn: geminin

GSK3: glycogen synthase kinase 3
GST: glutathione sulfur transferase
HRP: horseradish peroxidase
HSV TK: herpes simplex virus thymidine kinase
INR: initiator element
IPTG: isopropylthio- β -D-galactoside
kDa: kilo Daltons
LB: Luria-Bertani medium
Mk: marker
N: nuclear fraction
NF1: neurofibromin 1
Ngn2: neurogenin 2
NPM: nucleophosmin
O.D.: optical density
oligo: oligonucleotides
ORF: open reading frame
P: pellet
PBS: phosphate buffered saline
PC: Polycomb
p.c.: post coitum
PcG: Polycomb group
PCR: polymerase chain reaction
PCV: packed cell volume
PFA: paraformaldehyde
PHGPx: phospholipids hydroperoxide glutathione peroxidase
PMSF: phenylmethylsulfonyl fluoride
Pol I: RNA polymerase I
Pol II: RNA polymerase II
Pol III: RNA polymerase III
pp: post partum
PRC1: polycomb repressive complex 1
PRC1L: polycomb repressive complex 1-like
Prm: protamines

PSC: posterior sex combs

RNase A: ribonuclease A

rpm: round per minute

rRNA: ribosomal RNA

RT: room temperature

RT-PCR: reverse transcription-polymerase chain reaction

S: supernatant

SAM/SPM: sterile alpha motif domain

Scmh1: Sex comb on midleg homolog 1

SDS: sodium dodecyl sulfate

siRNA: small interference RNA

SLI: selectivity factor I

SRB: suppressors of RNA polymerase B mutations

SVZ: subventricular zone

Syt I: synaptotagmin I

TAFs: TBP-associated proteins

TBE: Tris-borate-EDTA

TBP: TATA box binding protein

TBPL1: TATA binding protein-like factor

TEMED: N,N,N',N'-tetramethyl-ethylenediamine

TFII: Transcription factors II

TIPT: TATA binding protein-like factor-interacting protein

T_m: melting temperature

Tpn: transition proteins

TRF: TBP-related factors

tTAFs: testis specific TAFs

Tuj1: neuronal tubulin

U: units

UBF: upstream binding factor

UCE: upstream control element

V: volts

VZ: ventricular zone

Acknowledgements

In the first place I would like to express my most sincere thanks to my supervisor Prof. Dr. Michael Kessel, first of all for giving me the chance to do my PhD in his laboratory. I am really grateful for all the patience and the time he invested in opening my eyes on what it means the real science. I own him a lot of gratitude for teaching me a new way to think. I would never forget his advices, which will follow me constantly wherever the future drives me.

I am grateful to Prof. Dr. Ernst Wimmer for accepting to be my referee and also to all the members of my PhD committee, Prof. Dr. Ralf Ficner, Prof. Dr. Robert Gradstein, Prof. Dr. Jörg Stülke and to Prof. Dr. Rüdiger Hardeland.

I want to thank to my excellent collaborators Dr. Christine Mayer, Prof. Dr. Ingrid Grummt, Prof. Dr. Martin Teichmann and Dr. Reinhard Klement for their great help and always precious advices concerning my work.

My special thanks to Priv. Doz. Dr. Anastassia Stoykova for lightening my neuronal connections and supporting me constantly. I want to address a “Merci beaucoup” to the French speakers from my department, Prof. Dr. Ahmed Mansouri and Dr. Patrick Collombat for all their support and encouragements during the difficult times. As they always told me, “Alles wird Gut!”. I would like to thank to Dr. Kamal Chowdhury, Dr. Jan Schindehutte, Dr. Silvio Rizzoli, Dr. Hans Dieter Schmitt, Tran Cong Tuoc for interesting discussions and suggestions.

To the head of the Mass Spectrometry Department, Dr. Henning Urlaub, and to Uwe Pleßmann and Monika Raabe, I thank for the many protein sequencing, which constituted valuable information for my work. Besides I would like to express gratitude to Prof. Dr. Wolfgang Engel and Prof. Dr. Karim Nayernia for their considerable help. I am grateful to Prof. Dr. Detlef Doenecke and Dr. Nicole Happel for important help for FACS analysis. I would like to acknowledge Dr. Olga and Dr. Genia Makarov for guiding my steps into biochemistry field and for their friendship.

I have a special thank to Sharif Mahsur and Petra Rus for their technical help and happy atmosphere created in the lab. I am very thankful to my actual and former lab mates, Dr.

Lingfei Luo, Dr. Lars Wittler, Dr. Hyun-Jin Kim, Dr. Derek Spieler, Sven Pilarski, Naisana Asli, Yvonne Uerlings and Wiebke Behrens for sharing good and bad times. I also want to thank them for nice discussions, especially to my friend Naisana for the good jokes. Besides I would like to express gratitude to all the members of the Gruss department for the friendly atmosphere and their continuous help during the past few years. I will miss you all!

I am indebted to DFG-Graduiertenkolleg “Molekulare Genetik der Entwicklung“ for giving me the opportunity to be a member of a scientific community and for the generously financial support. I would like to express my special thanks to Prof. Dr. Thomas Pieler, Prof. Dr. Ernst Wimmer and Manuela Manafas for all the seminars and workshops organized.

For providing experimental material I would like to acknowledge Prof. Dr. Martin Teichmann, Prof. Dr. Irwin Davidson, Dr. Jayhong Chong, Prof. Dr. Mary Osborn for their generosity.

Many warm thanks to the Romanian friends from Göttingen, especially to Eva and Toni Kreiter, Alexandra Andrei, Mihaela Diaconu, Dana and Ovidiu Ioan, Vlad and Rodica Pena, Silvio Rizzoli for the nice time we shared together and their support.

Special thanks to Prof. Dr. Andrei Anghel, who allowed me to join the Biochemistry team in Romania and to Dr. Ovidiu Sirbu for giving me the impulse to follow science. Also I want to thank to the all members of the Biochemistry Department from UMF Timisoara for the nice time we had together.

From all my heart, a truely “Thank you!” to my parents, Gheorghe-Sava and Tudorita Manescu, for their love, sacrifice and permanent support. I also want to thank to my grandmother Mandita for her precious help during my years of study and for all the prayers. I have special thanks full of regrets to my grandmother Mara, my “Mami”, which passed away before time, for all the care and love. To the best sister one can ever have, Mihaela, and to my soul mate, Marian, I thank you deeply for being next to me, always. Thank you Marian for being my best friend all over the years, and for your unconditional love.

Mii de multumiri celor din tara care au facut posibil acest vis, Mica, Diana, Draga Miscov, Victor si Marcela Vanturici. Va multumesc!

Scumpii mei parinti, va multumesc pentru tot ceea ce ati facut pentru mine!

Curriculum Vitae

Personal Data

Surname: Pitulescu
Forename: Mara-Elena
Nationality: Romanian
Birth: May 20th 1976 in Resita, Romania
Marital Status: Married
Private Address: Stiegel 7
37077 Göttingen, Germany
Work Address: Research Group Developmental Biology
Department of Molecular Cell Biology
Max Planck Institute for Biophysical Chemistry
Am Fassberg 11
37077 Göttingen, Germany
E-mail: mpitule@gwdg.de

Scientific Education:

Oct. 2002-Present PhD student
Research Group Developmental Biology
Department of Molecular Cell Biology
Max Planck Institute for Biophysical Chemistry, Göttingen
Ian. 2002-Oct. 2002 Research Assistant
Department of Biochemistry
“Victor Babes” University of Medicine and Pharmacy,
Timisoara, Romania
Ian. 2001-Ian. 2002 Medical Internship
County Hospital Timisoara, Romania
Sept. 2000 MD degree
Oct. 1994-Sept. 2000 MD student
General Medicine Specialization
“Victor Babes” University of Medicine and Pharmacy,
Timisoara, Romania

Publications:

Bart JM, Morariu S, Knapp J, Ilie MS, **Pitulescu M**, Anghel A, Cosoroaba I and Piarroux R. Genetic typing of *Echinococcus granulosus* in Romania. *Parasitol Res.* (2006), 98: 130-7.

Pitulescu M, Kessel M, and Luo L. The regulation of embryonic patterning and DNA replication by geminin. *Cell Mol Life Sci.* (2005), 82:1425-33.

Anghel A, Marian C, **Pitulescu M**, Daba A, Sirbu IO, Rusu V, Budowle B. Population genetic study of eight short tandem repeat loci CSF1PO, TPOX, TH01, F1A301, FESFPS, vWA, F13B and LPL in the Western Romanian population. *Forensics Sci Int.* (2003), 28; 218-9.